

Durham E-Theses

Functional analysis of inositol phosphoryl ceramide synthase isoforms from arabidopsis thaliana

Yoko Okada

How to cite:

Okada, Yoko (2008) Functional analysis of inositol phosphoryl ceramide synthase isoforms from arabidopsis thaliana. Unspecified thesis, Durham University.

Use policy

The full-text may be used and/or reproduced, and given to third parties in any format or medium, without prior permission or charge, for personal research or study, educational, or not-for-profit purposes provided that:

- a full bibliographic reference is made to the original source
- a <https://etheses.durham.ac.uk/id/eprint/2293/> is made to the metadata record in Durham E-Theses
- the full-text is not changed in any way

The full-text must not be sold in any format or medium without the formal permission of the copyright holders.

Please consult the [full Durham E-Theses policy](#) for further details.

**Functional Analysis of
Inositol Phosphoryl Ceramide Synthase
Isoforms from *Arabidopsis thaliana***

The copyright of this thesis rests with the author or the university to which it was submitted. No quotation from it, or information derived from it may be published without the prior written consent of the author or university, and any information derived from it should be acknowledged.

YOKO OKADA

Supervised by Dr. Tony Fawcett

18 DEC 2008



Contents

List of Figures.....	iv
List of Tables.....	v
List of Tables.....	v
Abbreviations	vi
Acknowledgements	viii
Abstract.....	ix
1. Introduction	1
1.1 What are Sphingolipids?.....	1
1.2 Sphingolipid Biosynthesis in Yeast.....	2
1.3 Sphingolipids in Plants	4
1.3.1 Metabolism of Sphingolipid	4
1.3.2 Function of Sphingolipids in Plants	7
1.5 Sphingolipids and Diseases	9
1.6 What is known about IPC synthase	9
1.7 Aim of Study	11
2. Materials and Methods	12
2.1 Growing Arabidopsis thaliana.....	12
2.2 Planting Arabidopsis	12
2.3 Purification of RNA from Plant Material.....	13
2.4 RNA Precipitation	13
2.5 Reverse Transcriptase (RT) Reaction.....	13
2.6 DNase Treatment.....	14
2.7 Polymerase Chain Reaction (PCR) amplification of DNA	14
2.7.1 PXE 0.5 Thermal Cycler	14
2.7.2 Robocycler Gradient 96 PCR.....	14
2.7.3 Colony PCR.....	15
2.7.4 Quantitative PCR.....	15
2.8 Gel Electrophoresis.....	15
2.9 Purifying DNA form Agarose Gel	16
2.10 Ligation and Transformation.....	16
2.11 Purifying Plasmid from E. coli cells.....	17
2.12 Restriction Enzyme Digestion.....	17

2.13 Sequencing	17
2.14 NanoDrop ND-1000 Spectrophotometer.....	18
2.15 Preparation of Yeast Competent Cells for Transformation.....	18
2.16 Spotting Yeast on Plates.....	18
2.17 Agar Diffusion Assay.....	18
2.18 Fluorescence Labelling.....	19
2.18.1 Fluorescence Labelling for AUR1.....	19
2.18.2 Fluorescence Labelling for ISC1.....	19
2.19 Preparation of Membranes for ISC1 Assay.....	20
2.20 Preparation of STE Buffer and Storage Buffer	21
2.21 Labelling Prepared Microsomes for NBD-C ₆ -Sphingomyelin Fluorescence Assay.....	21
2.22 Measuring fluorescence.....	22
2.23 Scanning TLC plates	22
3. Results - Identifying, Cloning and Characterisation of IPCS.....	23
3.1 Identification and Cloning of IPCS	23
3.1.1 Designing Primer Pairs.....	24
3.1.2 Optimising Primers for Cloning Full Length IPCS Genes	24
3.1.3 Cloning Full Length IPCS cDNAs into pGEM-TEasy	27
3.1.4 Cloning into pRS426 MET Plasmid.....	29
3.2 Characterizing the Function of IPCS.....	34
3.2.1 AUR1 Mutant Cells Complemented with <i>Arabidopsis thaliana</i> IPCS Genes....	34
3.2.1.1 Transforming pRS426 MET plasmids into AUR1 Yeast Cells.....	34
3.2.1.2 <i>In vitro</i> Complementation Assay / Functional Assay of IPCS Activity.....	36
3.2.1.3 Biochemical Assay of Metabolic Labelling	37
3.2.1.4 Sensitivity of <i>At</i> IPCS to Aureobasidin A	39
3.2.2 Testing Phospholipase Activity in <i>Arabidopsis thaliana</i> IPCS Genes.....	41
3.2.2.1 Transforming pRS426 MET plasmids into ISC1 Yeast Cells.....	41
3.2.2.2 <i>In vivo</i> Complementation of ISC1 - Salt Tolerance Test.....	41
3.2.2.3 Biochemical Assay of IPC-PLC Activity by Metabolic Labelling	46
4. Results - Expression of IPCS Genes in <i>Arabidopsis thaliana</i>	48
4.1 Gene Specific Primers for Real Time PCR.....	48
4.2 Optimising Primers for 150bp IPCS Amplicons	51
4.3 Confirming specificity of 150bp Primers	53
4.4 Expression of IPCS genes in <i>Arabidopsis</i> tissues (QPCR)	55

4.5 Preparing Samples	55
4.6 RT-PCR.....	56
4.7 Primer Optimization	56
4.8 Creating Standard Curve	59
4.9 Quantitative PCR.....	61
4.10 Quantification of IPCS Gene Expressed	61
5. Discussion.....	65
5.1 Function of At IPCS	65
5.2 Expression of At IPCS.....	73
6. Future Work.....	74
7. References	75
Appendix I - Preparation of Media.....	81

List of Figures

Figure 1 Yeast Sphingolipid Metabolism.....	3
Figure 2 Sphingolipid Metabolism in Plants	6
Figure 3 Reaction Catalyzed by IPC Synthase.....	10
Figure 4 Map of Plasmid pRS426 MET	17
Figure 5 Model of IPCS3 and IPCS4 Protein Coding Gene	23
Figure 6 Amplification of Full Length IPCS ORFs	25
Figure 7 Restriction Digest of IPCS3	28
Figure 8 Restriction Enzyme of pRS426.....	30
Figure 9 Colony PCR of IPCS-pRS426	30
Figure 10 Alignment of Cloned IPCS Genes and Sequence of each Gene	33
Figure 11 Results of Colony PCR of IPCS transformants to AUR1	35
Figure 12 Functional Complementation of AUR1 Mutant Cells	36
Figure 13 Functional Complementation of AUR1 Mutant Cells	36
Figure 14 <i>At</i> IPCS genes complement AUR1	38
Figure 15 <i>At</i> IPCS is resistant to AbA.....	40
Figure 16 <i>In vivo</i> Complementation Assay of ISC1 on YPD Media	43
Figure 17 <i>In vivo</i> Complementation Assay of ISC1	45
Figure 18 TLC of ISC1 complemented by <i>At</i> IPCS genes - Metabolic labelling	47
Figure 19 Alignment of IPCS Genes and Designed Primer Pairs.....	50
Figure 20 PCR Product of IPCS Amplicons from <i>A. thaliana</i> cDNA	52
Figure 21 PCR Results of IPCS Amplicons - RNA with and without DNase Treatment..	52
Figure 22 Confirming Specificity of IPCS Primer Sets	54
Figure 23 Primer Optimization.....	57
Figure 24 Further Primer Optimization.....	58
Figure 25 Standard Curve.....	60
Figure 26 Quantification of IPCS transcripts per microgram of total RNA.....	63
Figure 27 Alignment of <i>A. thaliana</i> IPCS and <i>S. cerevisiae</i> IPCS (AUR1)	67
Figure 28 Motif Scan of IPCS Genes	68
Figure 29 Alignment of Motif D3 and D4.....	70
Figure 30 Alignment with Various Species.....	71

List of Tables

Table 1 Fungal toxins that target sphingolipid metabolism	4
Table 2 Selected Media for Yeast Cells	20
Table 3 Primer Pairs Designed for each IPCS Gene	24
Table 4 Optimal Primer Pair Conditions	26
Table 5 Quantity of Purified IPCS	26
Table 6 Gene Specific Primer Pairs.....	50
Table 7 Optimised Primer Set Conditions.....	53
Table 8 Extracted RNA Samples.....	55
Table 9 Values of Standard Curve.....	59
Table 10 EST and cDNA in each IPCS Gene	62
Table 11 Microarray Data for IPCS2	62
Table 12 Properties of Amino Acids Found at the <i>Sc</i> 158bp Position	72

Abbreviations

½ MS	Murashige and skoog basal salt mixture
AbA	Aureobasidin A
ACD	Accelerated cell death
<i>At</i>	<i>Arabidopsis thaliana</i>
Cer	Ceramide
CERase	Ceramidase
DHS	Dihydrosphingosine
DMSO	Dimethyl sulfoxide
DTT	Dithiothreitol
EDTA	Ethylenediaminetetraacetic acid
Gal	Galactose
GCase	Glucosylceramidase
GCS	Glucosylceramide synthase
GDP mannose	Guanosine diphosphate mannose
GLD	Globoid cell leukodystrophy
Glu	Glucose
GPCR	G protein-coupled receptor
GPI	Glycosylphosphatidylinositol
HFA	Hydroxylated fatty acids
His	Histidine
HPTLC	High-performance thin layer chromatography
IPC	Inositolphosphorylceramide
IPC-PLC	Inositol phosphoceramide phospholipase C
IPCS	Inositolphosphorylceramide synthase
IPS-PLC	Inositol phosphosphingolipid phospholipase C
KSR	3-ketosphinganine reductase
LB	Luria-bertani broth
LCB	Long chain base
LCBK	Long-chain base kinase
LCBPL	Long-chain base-phosphate lyase
LCBPP	Long-chain base-phosphate phosphatase
LPP	Lipid phosphate phosphatase

MET	Methionine
MIPC	Mannosylinositolphosphorylceramide
M(IP)₂C	Mannosyldiinositolphosphorylceramide
MQ	Milli Q water
MYR	Myriocin
NADPH	Nicotinamide adenine dinucleotide phosphate
NBD	Nitro-2-1, 3-BenzoxaDiazol-4-yl
NHFA	Nonhydroxylated fatty acids
N-SMase	NBD-SMase
ORF	Open reading frame
PAP	Phosphatidic acid phosphatase
PCD	Programme cell death
PCR	Poly chain reaction
PGA	Poly-gamma-glutamate
PLC	Phospholipase C
Q-PCR	Quantitative PCR
Raf	Raffinose
RT-PCR	Real time PCR
SAT	Sphinganine acyltransferase
<i>Sc</i>	<i>Saccharomyces cerevisiae</i>
SD	Scientifically Defined
SH	Sphinganine hydroxylase
SM	Sphingomyelin
SMase	Sphingomyelin phosphodiesterase
SPT	Serine palmitoyltransferase
S1P	Sphingosine 1-phosphate
TLC	Thin layer chromatography
UV	Ultraviolet
Ura	Uracil
YPD	Yeast peptone dextrose
YPGR	Yeast peptone galactose and raffinose

Acknowledgements

First of all, I would like to thank my supervisor Dr. Tony Fawcett for giving me an opportunity to carry out an MSc and guiding me through the process. And many thanks to Dr. Paul Denny for supporting me through the biochemical assays and J. G. Mina for providing me important information in Figure 11 and Rf values in Figure 14.

I would also like to thank all the lab members, especially Adrian and Johan for helping me out at difficult times, and John Rowland for helping me with the computer.

I cannot show enough appreciation to all my department friends and college friends and other friends (you know who you are), who supported me and made me laugh through difficult and stressful times. It wouldn't have been the same without you.

Finally but not the least, I would like to thank my family and grandparents for supporting me financially and emotionally throughout the year to accomplish my goal.

All I can say is thank you!

Abstract

Sphingolipids are ubiquitous and essential components of eukaryotic cells. They are major components of the membrane, and have also been identified to be important in signalling. Until recently, very little has been known about IPCS in plants. The activity has been characterized in bean microsomes in 2003 by Bromley *et al.*, but until now no genes encoding IPCS have been identified. Here the three *Arabidopsis thaliana* genes potentially encoding IPCS, which is responsible for a step in sphingolipid synthesis have been characterized and the expression level has been identified. Genes have been cloned and transformed into the yeast-*E. coli* shuttle vector pRS426 MET for investigating the encoded activity. *In vivo* and metabolic labelling *in vitro* studies of the complementation studies of AUR1 of these IPCS genes demonstrated that IPCS function as *AUR1*. Although salt tolerance *in vivo* studies and metabolic labelling *in vitro* studies of *ISC1* complementation studies showed that IPCS did not function as *ISC1*, *IPC-PLC*. By designing gene specific primer sets, tissue-specific expression patterns for these genes have been identified for the first time and suggest that the expression of particular IPCS genes are regulated in a tissue-specific and developmental-stage manner. Furthermore, *A. thaliana* IPCS was found to be resistant to the anti-fungal agent aureobasidin A (AbA). This may provide important aspects to future management and prevention of fungal diseases in plants. Identifying the functions and characteristics of *A. thaliana* IPCS provides important aspects of sphingolipid synthesis and signalling in plants.

1. Introduction

1.1 What are Sphingolipids?

Sphingolipids are ubiquitous constituents of eukaryotic cells, and are present in almost all eukaryotes as well as a few prokaryotes (Lynch and Dunn 2004). They are major components of the plasma membrane, tonoplast, and other endomembranes. The name “sphingolipid” was given due to its enigmatic (sphinx-like) chemical structure (Hakomori 1983). Over 300 different sphingolipids have been characterized structurally (A. H. Jr. Merrill 1996), and when variations in the LCB and acyl chain are also considered, the possible molecular species number in the thousands (Vesper *et al.* 1999).

Sphingolipids are based on long-chain sphingoid bases and constituents of phospholipids and glycolipids (Huwiler *et al.* 2000b; Huwiler *et al.* 2000a). In mammals the predominant sphingolipid classes are sphingomyelin and many neutral and acidic glycolipids (Hakomori 1983; A. H. Jr. Merrill 1996).

In fungi, sphingolipids consist of glucosylceramides and inositolphosphorylceramides (IPCs) (Sakaki *et al.* 2001), but in *Saccharomyces cerevisiae* they are exclusively IPCs (Lester and Dickson 1993).

However in plants, the major long-chain bases (LCBs), trihydroxy 18:1(18E/Z isoforms) and dihydroxy 18:2(4E/(E/Z)) in plants are not found in animals and yeast (Markham *et al.* 2006). In plants, the predominant complex sphingolipid is glucosylceramide (Warnecke and Heinz 2003). Complex (polar) glyco-phosphosphingolipids (glycosylated IPC species) have been isolated as well (Lester and Dickson 1993). Further research in *A. thaliana* has revealed only one major anionic sphingolipid class, hexose-hexuronic-inositolphosphoceramide. This was identified using hydrolysis of sphingolipids, high performance liquid chromatography analysis and mass spectrometry (Markham *et al.* 2006).

By developing a single solvent system with reversed-phase high performance liquid chromatography coupled to electrospray ionization tandem mass spectrometry detection, 168 sphingolipids from crude *A. thaliana* samples were separated and measured (Markham and Jaworski 2007). Major sphingolipid classes, glycosylinositolphosphoceramides, glucosylceramides, hydroxyceramides and ceramides and other minor but potentially important free long-chain bases sphingolipids and their phosphorylated derivatives were identified.



At first sphingolipids were thought to serve primarily as inert structural compounds, contributing to mechanical stabilisation and chemical resistance of the outer leaflet of the plasma membrane (Karlsson 1970). Since 1986 however, it has been established that sphingolipids function as bioactive molecules in animal cells (Hannun *et al.* 1986). In neuronal tissue, sphingolipids and their anabolic compounds are also important components and are closely associated with nerve function. The sphingolipids, sphingomyelin and gangliosides are important components of nerve myelin sheaths and play a crucial role in the development of the neuronal tissue and its function and stability in the mature organism (Milstien *et al.* 2007).

1.2 Sphingolipid Biosynthesis in Yeast

A diagram of the sphingolipid biosynthesis in yeast is shown below Figure 1. In yeast, as in mammalian cells, the first step in sphingolipid metabolism involves the condensation of serine and palmitoyl-CoA in the endoplasmic reticulum (ER) by serine palmitoyl transferase (SPT) (Dickson and Lester 1999). For this activity, two LCBs, *LCB1* and *LCB2*, found in all organisms that make sphingolipids, are required (Nagiec *et al.* 1994). After the initial condensation of serine and palmitoyl-CoA into 3-keto dihydrosphingosine, the enzyme 3-keto reductase (TSC gene) converts it into dihydrosphingosine which is also carried out in the ER (Beeler *et al.* 1998).

The next step in yeast, which is different to that of the mammalian reaction, is that either dihydrosphingosine or dihydroceramide are hydroxylated by the ceramide synthase, *SUR2/SYR2* into phytosphingosine or phytoceramide, respectively (Haak *et al.* 1997, Grilley *et al.* 1998). Then the LCB, phytosphingosine is acylated to phytoceramide. This step is also different to mammalian cells, which involves very long-chain fatty acids. This enzyme is encoded by *LAG1* and its homologue *LAC1* (Guillas *et al.* 2001). Finally ceramides in yeast are incorporated into complex sphingolipids such as inositolphosphorylceramide (IPC). The enzyme involved in this step is encoded by *AUR1* which is an essential yeast gene (Nagiec *et al.* 1997). This enzyme, which is not present in mammalian cells, is a target for aureobasidin, a fungal toxin (Zhong *et al.* 2000). Therefore, it has a potential importance for anti-fungal drugs. IPC is further mannosylated to *MIPC* and *MIP₂C* in the Golgi by GDP mannose.

ISC1 (YER019w), an enzyme involved in the breakdown of sphingolipids have been identified. This enzyme hydrolyses IPC back to ceramide (Sawai *et al.* 2000b).

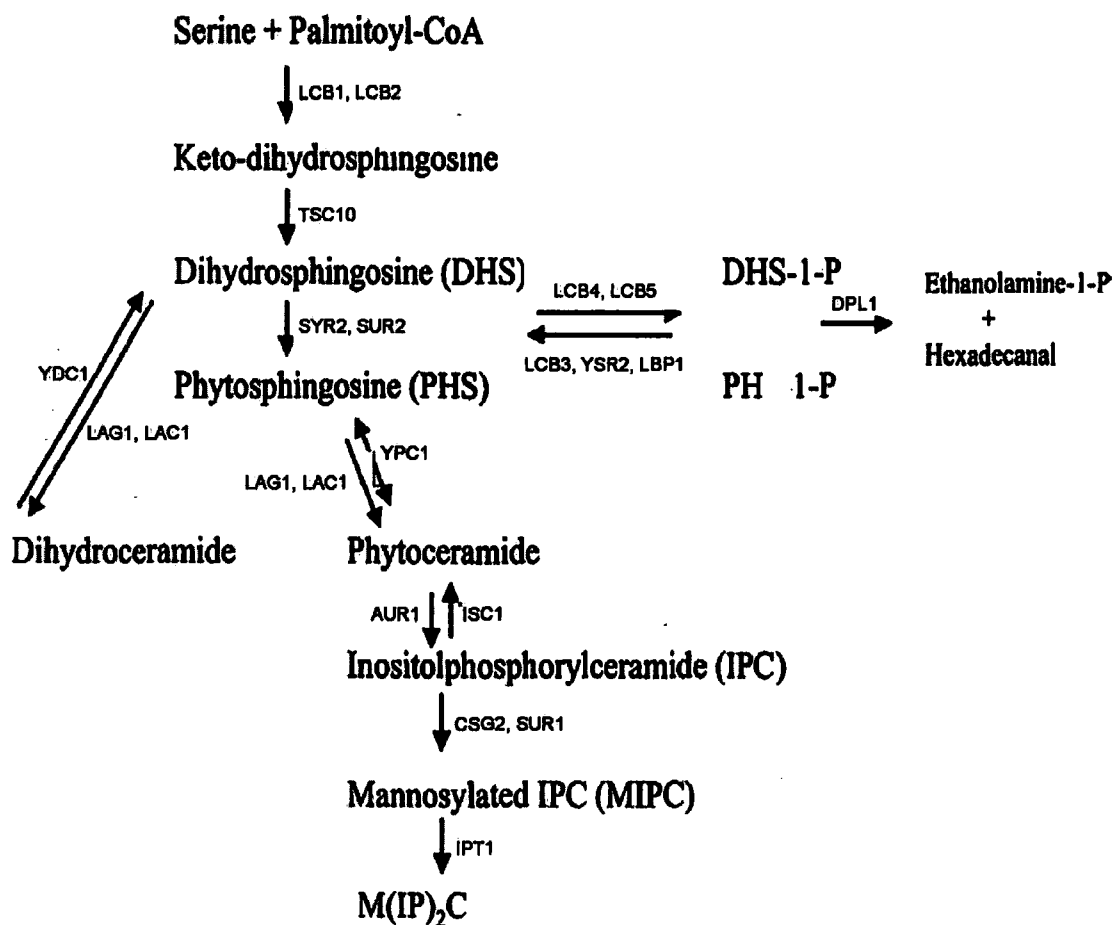


Figure 1 Yeast Sphingolipid Metabolism

The first step in sphingolipid metabolism involves the condensation of serine and palmitoyl-CoA in the endoplasmic reticulum by SPT, which is encoded by two LCB, *lcb1* and *lcb2*. After the initial condensation of serine and palmitoyl-CoA into 3-keto dihydrospingosine, the enzyme 3-keto reductase (*tsc*) converts it into DHS, which is also carried out in the ER. Next step is either dihydrospingosine or dihydroceramide are hydroxylated by the ceramide synthase, SUR2/SYR2 into phytospingosine or phytoceramide, respectively. This is different to the reaction of that in mammals. Then the LCB, phytospingosine is acylated to phytoceramide. This enzyme is encoded by *lag1* and its homologue *lac1*. Finally ceramides are incorporated into complex sphingolipids such as IPC encoded by *aur1* which is an essential yeast gene. ISC1 encodes inositolphosphosphingolipids phospholipase C. IPC is further mannosylated to MIPC and MIP₂C in the Golgi by GDP mannose. Figure adapted from (Obeid *et al.* 2002a)

Sphingolipid LCBs are known as signalling molecules for regulating growth (Sun *et al.* 2000), response to stress (Aerts *et al.* 2006) and cell wall synthesis and repair (Schmelzle *et al.* 2002).

Other roles have recently been discovered such as protein trafficking/exocytosis (Skrzypek *et al.* 1997), lipid rafts or microdomains, which constitutes cholesterol and sphingolipids. (Hearn *et al.* 2003), calcium homeostasis (Futerman 2005), longevity and cellular aging (Jiang *et al.* 2004), nutrient uptake (Chung *et al.* 2001), cross talk with sterols (Kihara and Igarashi 2004) and the action of some antifungal agents (Nagiec *et al.* 2003a).

Fungal toxins that target sphingolipid metabolism are shown in Table 1 (Obeid *et al.* 2002a).

Table 1 Fungal toxins that target sphingolipid metabolism

Toxin	Enzyme target
Myriocin	Serine palmitoyltransferase (Lcb1p)
Syringomycin E	Dihydrosphingosine hydroxylase (Sur2p/Syr2p)
Fumonisin B	Ceramide synthase
Australifungin	Ceramide synthase
Aureobasidin	Inositol phosphoceramide synthase (Aur1p)

1.3 Sphingolipids in Plants

1.3.1 Metabolism of Sphingolipid

A diagram of the sphingolipid metabolism pathways in plants is shown below (Figure 2). The metabolic pathway is constructed of three parts which is synthesis and fates of sphinganine, conversion of ceramide to complex sphingolipids, and LCB and acyl-chain modification.

As in yeast, sphingolipid biosynthesis starts with the condensation of palmitoyl-CoA and serine to yield 3-ketosphinganine, catalyzed by SPT. Plants have one homolog of the yeast *LCB1* and two homologs of *LCB2*. *A. thaliana LCB1* encodes a genuine subunit of SPT that rescues the sphingolipid LCB auxotrophy of *Saccharomyces cerevisiae* SPT mutants when coexpressed with *Arabidopsis LCB2*. Non lethal reduction of *At LCB1* expression results in profound alterations in the growth and development of *Arabidopsis* and in the

LCB composition of complex sphingolipids which show that sphingolipids are essential in *Arabidopsis* (Chen *et al.* 2006).

In the next step, 3-ketosphinganine is reduced with NADPH by KSR to yield sphinganine. Two homologs of the yeast gene TSC10 are found in *A. thaliana*, but their functions have not been demonstrated.

In the next step, the amino group of sphinganine is acylated to yield ceramide. The activity of sphinganine N-acyltransferases in *A. thaliana* has been demonstrated in microsomal membrane (Sessler *et al.* 1993).

Following the acylation of sphinganine, the resulting ceramide serves as substrate for the formation of glucosylceramide and IPC. Activity of IPC synthase has been demonstrated by monitoring the incorporation of fluorescent NBD-C₆ ceramide or [³H]inositolphosphate from radiolabeled phosphatidylinositol (PI) into product identified by TLC. Also, two fungal IPC inhibitors, AbA and rustmicin have been shown to inhibit the enzyme activity in bean microsomes (Bromley *et al.* 2003).

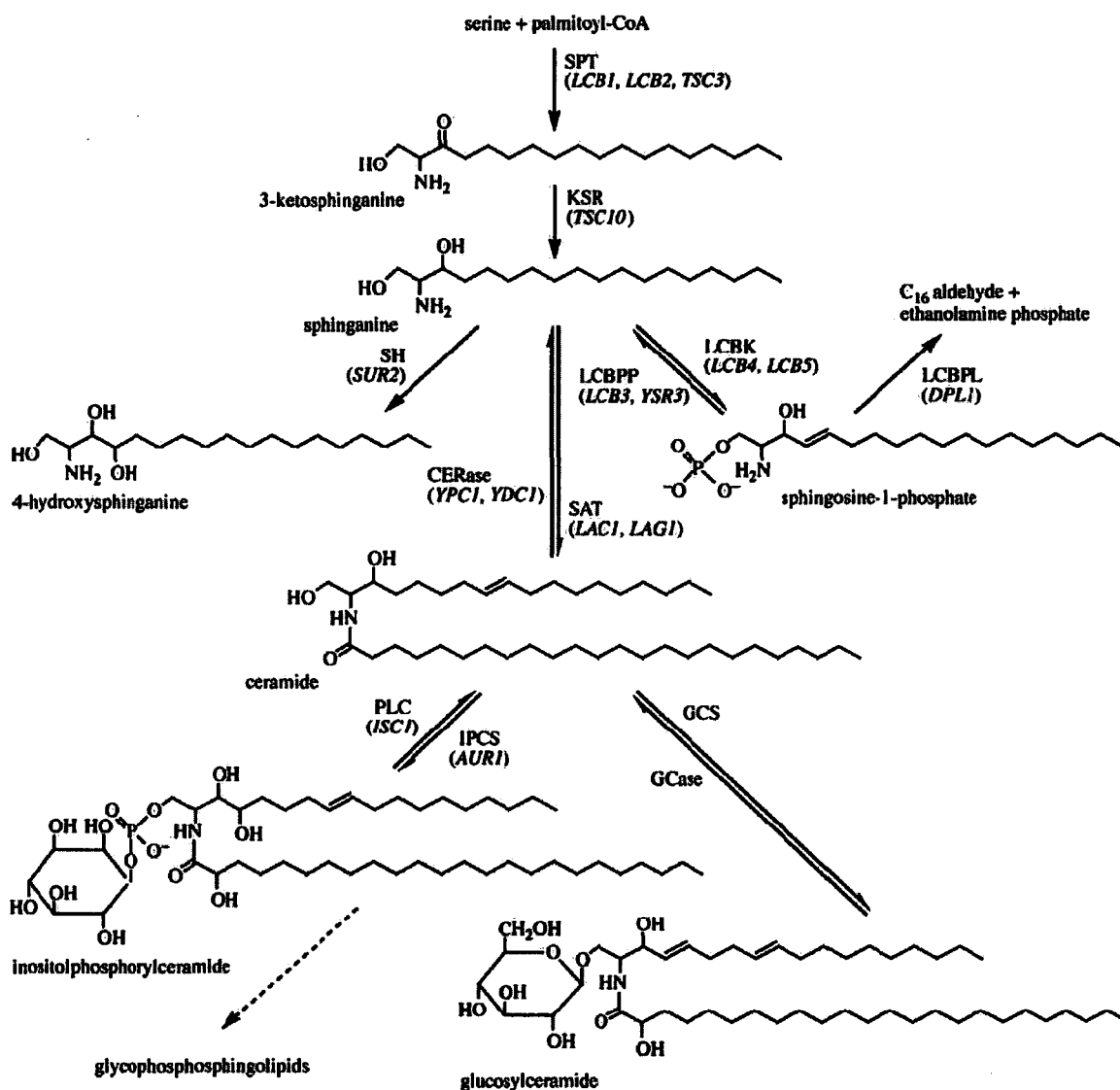


Figure 2 Spingolipid Metabolism in Plants

Plant sphingolipid biosynthesis starts with the condensation of palmitoyl-CoA and serine to yield 3-ketosphinganine as in yeast. Plants have one homolog of the yeast LCB1 and two homologs of LCB2. Next, 3-ketosphinganine is reduced with NADPH by KSR to yield sphinganine. Then the amino group of sphinganine is acylated to yield ceramide. Following the acylation of sphinganine, the resulting ceramide serves as substrate for the formation of glucosylceramide and IPC. Known yeast gene orthologues are listed in brackets. Abbreviations: CERase, ceramidase; GCase, glucosylceramidase; GCS, glucosylceramide synthase; IPCS, inositolphosphorylceramide synthase; KSR, 3-ketosphinganine reductase; LCBK, long-chain base kinase; LCBPL; long-chain base-phosphate lyase; LCBPP, long-chain base-phosphate phosphatase; PLC, phospholipase C; SAT, sphinganine acyltransferase; SH, sphinganine hydroxylase; SPT, serine palmitoyltransferase. Figure adapted from (Dunn *et al.* 2004)

1.3.2 Function of Sphingolipids in Plants

Roles of sphingolipids in plants include membrane structural components (Borner *et al.* 2005), cell signaling (Bille *et al.* 1992; Wang *et al.* 1996), stress response (Borner *et al.* 2002), pathogenesis (Birch *et al.* 1999) and apoptosis (Wang *et al.* 1996).

In *A. thaliana*, glycosylinositolphosphoceramides are the most abundant sphingolipid class with the major species being hexose-hexuronic-inositolphosphoceramide, and then monohexosylceramides, and ceramides accounted for 69%, 31%, and 2% of the total sphingolipids, respectively, suggesting there is an important role for the anionic sphingolipids in plant membranes (Markham *et al.* 2006).

In membranes, sphingolipids are known to serve as structural components. They are synthesized in the endoplasmic reticulum and the Golgi but are enriched in plasma membrane and endosomes which would indicate they travel between organelles where they perform many of their functions. This is how the function of rafts and translocators were proposed (van Meer and Lisman 2002).

In mammals and fungi, sphingolipids associate with cholesterol or ergosterol, respectively, and form clusters of raft-like domains. These domains, which are enriched in GPI-linked proteins have been found to facilitate lateral sorting of proteins, membrane trafficking and signal transduction (van Meer and Lisman 2002). Such domains exist in plants as well though in plants they contain sterols in addition to cholesterol (Peskan *et al.* 2000). Plant sterols are known to stabilize raft structure effectively (Xu *et al.* 2001). As detergent-resistant sphingolipid- and sterol-rich membrane domains are associated with the trafficking and function of cell surface proteins in eukaryotic cells, evidence of lipid domains in plant membranes were researched (Borner *et al.* 2005). Using proteomic approaches, in *A. thaliana*, eight GPI-anchored proteins, several plasma membrane ATPases, multidrug resistance proteins, and proteins of the stomatin/prohibitin/hypersensitive response family were found in detergent-resistant-membranes (Borner *et al.* 2005).

Sphingolipids also play a role in cell signalling. Sphingolipid signalling is thought to be a complex multifactorial signal derived from the interaction of several different sphingolipids, making the examination of all sphingolipids a critical factor in the dissection of sphingolipid function (Markham *et al.* 2006).

The important signalling molecules in eukaryotic organisms are sphingoid LCBs and their phosphorylated derivatives (LCB-*Ps*). In plants, S1P is a key sphingolipid second messenger. The knock-out of an *A. thaliana* gene coding for a protein accelerating *in vitro* (*E*)-sphing-4-*enine* transfer between membranes caused activation of cell death and defense (Brodersen *et al.* 2002). Also S1P has been shown to be a Ca²⁺-mobilizing messenger active in stomatal guard cell in drought and abscisic acid signalling in *Commelina communis* (Ng *et al.* 2001). In animals, the action of S1P is mediated largely through G protein-coupled receptors (GPCRs) of the S1P receptor family (Kluk and Hla 2001). In *A. thaliana*, the enzyme responsible for S1P production, sphingosine kinase (SphK), is activated by abscisic acid, and is involved in both abscisic acid inhibition of stomatal opening and promotion of stomatal closure (Coursol *et al.* 2003).

Glycophosphosphingolipids and their metabolites in plants may also be involved in cell signalling or cell-cell recognition as there is a similarity to animal complex sphingolipids (Hetherington and Drobak 1992), though at present, no direct evidence have been shown that these sphingolipids are signalling molecules (Worrall *et al.* 2003).

Recent evidence suggests that mycotoxin-induced and PCD results from alterations in sphingolipid metabolism and that PCD is associated with accumulation of free sphingoid bases, dihydrosphingosine and 3-ketodihydrosphingosine. Interestingly, mycotoxin-induced PCD can be rescued by ceramide (Brandwagt *et al.* 2000), suggesting that cellular levels of ceramide and sphingoid bases can function as a rheostat to determine PCD or survival, similar to the S1P-ceramide rheostat proposed in mammalian cells (Maceyka *et al.* 2002).

Sphinganine-analogous mycotoxins are known to induce necrosis, DNA fragmentation and accumulation of free long chain unsaturated bases in different plant tissues (Moore *et al.* 1999). This could be attributed to a competitive inhibition of the sphinganine N-acyltransferase (ceramide synthase) activity (Gable *et al.* 2000).

In plants, sphingolipids are essential for the establishment and maintenance of cell polarity by controlling actin cytoskeleton. Accumulation of ceramide is likely to be responsible for arresting the first step of the cell cycle, G1, in which the genes are expressed and proteins are synthesised (Cheng *et al.* 2001).

1.5 Sphingolipids and Diseases

Sphingolipids are involved in disorders and diseases such as globoid cell leukodystrophy (GLD) and Krabbe's disease (Clementi *et al.* 2003). The multinuclear cells associated with GLD are called globoid cells, from which the name derives from. It is found that GLD is a neurological disease characterized by severe myelin loss, and mental and motor deterioration in infants (Suzuki 1998). The primary defect of GLD is a deficiency of galactosylceramidase, which is the lysosomal enzyme that catalyzes the hydrolysis of GalCer to Gal and ceramide (Mitsuo *et al.* 1989). The GalCer deficiency leads to disruption of the metabolism of GalCer-related sphingolipids and therefore results in the accumulation of lysosphingolipid psychosine. Disturbances of the fragile balance in myelin components are directly linked with various disorders of central nervous system (CNS) (Kinney *et al.* 1994).

Sphingolipids may be used for the development of therapeutic approaches which is based on the role of ceramide in processes for cancer, ischemia-reperfusion injury, and diseases of the immune system (Kester and Kolesnick 2003). They also may play a key role in transmission of HIV infection (Ono and Freed 2001).

In plants, sphingolipids and its phosphorylated derivatives, synthesised in plants through ceramide biosynthetic pathway, were the signal molecules that trigger the endogenous PCD during susceptible disease response (Khurana *et al.* 2005).

A disease resistant gene Asc-1 is known to prevent the disruption of sphingolipid metabolism during AAL (a necrotrophic fungus *Alternaria alternata f.sp. lycopersici*)-toxin-induced programmed cell death. The interaction between or a sensing of the levels of ceramide and free LCBs trigger apoptosis (Spassieva *et al.* 2002). The presence of Asc-1 is able to relieve an AAL-toxin-induced block on sphingolipid synthesis which would otherwise lead to PCD. In *Arabidopsis*, mutant Accelerated Cell Death 11 (ACD11) is deficient in putative sphingolipid LCB transfer protein (Brodersen *et al.* 2002). And *ACD5* gene has been identified as a lipid kinase with specificity for short-chain fatty acyl ceramides (Liang *et al.* 2003).

1.6 What is known about IPC synthase

Inositol-containing sphingolipids are present in fungi, protozoa and plants. IPCS (phosphatidylinositol ceramide inositolphosphate transferase), is an enzyme which

catalyzes the reaction between phosphatidylinositol and ceramide, such as nonhydroxy fatty acid-containing ceramide, hydroxy fatty acid-containing ceramide, and NBD-C₆ ceramide, to complex sphingolipids producing diacylglycerol (Figure 3).

Many complex IPC derivatives have been found in plant tissues which show a large structural diversity (Kondo and Nakano 1987). These derivatives are components of plant cell membranes, especially the plasma membrane and tonoplast. In *S. cerevisiae*, M(IP)₂C is the major sphingolipid and is prevalent in the plasma membrane, while MIPC and IPC are minor sphingolipids and are enriched in the Golgi and tonoplast (Obeid *et al.* 2002b).

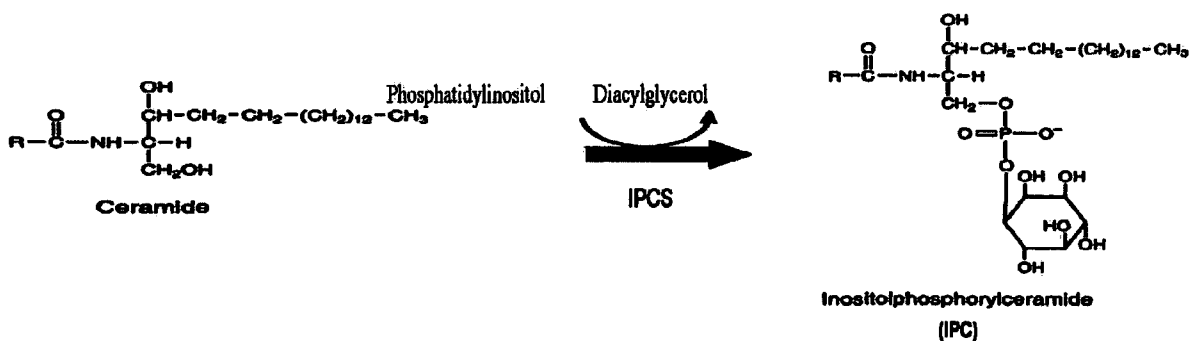


Figure 3 Reaction Catalyzed by IPC Synthase

IPC synthase catalyzes the transfer of inositolphosphate from phosphatidylinositol to ceramide producing diacylglycerol and IPC. Figure adapted from (Lynch and Dunn 2004)

IPCS is encoded by the AUR1 gene, and when IPC synthesis was inhibited, it led to lethality which would suggest that it is vital in *S. cerevisiae* (Mandala *et al.* 1998). Not much has been known about IPCS in plants, but it is thought to be similar to its yeast counterpart in many respects (Bromley *et al.* 2003). In animal cells, ceramide is a substrate for SM which is catalyzed by SM synthase. As these IPC derivatives are absent in animals and required in various fungi, this gives IPCS a great potential for antifungal agents. AbA, a fungal inhibitor, is known to inhibit IPCS in yeast (Zhong *et al.* 1999) and bean microsomes (Bromley *et al.* 2003), but is resistant to *Leishmania donovani* IPCS (J. G. Mina Unpublished).

Research by Bromley *et al.*, suggests that light does not affect the enzyme levels in the tissue as the IPC detected in 4 day old bean hypocotyl and 3 weeks old leaf were the same. Also the enzyme may be less active in monocots than dicots as corn and onion produce less IPC compared to bean, red bell pepper fruit and spinach respects (Bromley *et al.* 2003). Also it was demonstrated that IPCS does not exhibit any strict substrate specificity as all three types of ceramides (HFA-Cer, NHFA-Cer, and NBD-C₆) served as substrate.

A. thaliana IPCS was identified with the predicted protein sequence of *Leishmania* IPCS using the Arabidopsis genome database (<http://www.tigr.org/tdb/e2k1/ath1/>). Four open reading frames encoding three highly related sequence orthologues, *At* IPCS1, *At* IPCS2, *At* IPCS3 and *At* IPCS4 were identified J. G. Mina Unpublished. The AGI numbers of these genes were, *At* IPCS1 (*At*3g54020), *At* IPCS2 (*At*2g37940), *At* IPCS3 (*At*2g29525.1) and *At* IPCS4 (*At*2g29525.2).

1.7 Aim of Study

The aim of this study was to clone plant orthologues of yeast AUR1 gene to test whether plant IPCS can functionally complement yeast AUR1 mutant and to see if plant IPCS have activity of PLC (ISC1). To quantify the expression of these IPCS genes in plant tissue, gene specific PCR primer sets for IPCS 1, 2, and 3 were developed.

2. Materials and Methods

2.1 Growing *Arabidopsis thaliana*

Arabidopsis thaliana seeds were sterilised before planting; seeds were placed in a 7.5ml plastic bijou bottle and immersed in 70% ethanol for 30 seconds. The ethanol was removed with a pasteur pipette, and the pipette was kept in the tube for subsequent changes of solutions and for spreading the seeds on the petri dish. The tubes were then filled with 10% commercial bleach and 1 drop of tween 20 (a surfactant) and left for 20 minutes. Then the bleach was removed with the pasteur pipette and the seeds were rinsed twice with sterile distilled water. Enough water was left to spread out the seeds using the pasteur pipette onto the surface of growth media ½ MS 10 agar plates. The formulation of this media is described in the appendix, Preparing Media.

Once spread, plates were sealed with micropore tape and incubated for one week in the dark at 4°C. This was to facilitate the stratification of the seeds. Then plates were transferred into the tissue culture room which was set at 22°C with intensive light for 24 hours to germinate.

2.2 Planting *Arabidopsis*

Plants were transferred into soil after they had grown to approximately 1cm on tissue culture media. One part sand was added to four parts of sieved soil then the soil was transferred into containers and was soaked in water. 0.2g/l of intercept70WG (Levington) per batch was poured on top of the soil to avoid insects and then plants were carefully planted from the growth media into the soil.

After the rosette leaves had developed, araconbases and aracontubes (Arasystem) were put around individual plants to avoid cross fertilisation of the plants and to aid seed collection.

Water was provided regularly and the plants were growing in a regulated green house; 16 hours of day light, 6 hours of auxiliary lights. Day temperature was regulated at 23°C and night temperature was 18°C.

2.3 Purification of RNA from Plant Material

RNA from plants was purified using an RNeasy Plant Mini Kit (Qiagen). Plant tissue was immediately placed in liquid nitrogen and was ground thoroughly with an autoclaved mortar and pestle. The tissue powder was decanted into an RNase-free 2ml microcentrifuge tube.

The extraction of RNA from plant material was carried out according to the manufacture's protocol. Buffer RLT was used for *A. thaliana*. Buffer RLT contains guanidine thiocyanate and it disrupts cells and denatures properties.

To elute RNA, RNeasy spin column was placed in a new 1.5 ml collection tube. 30 μ l of RNase-free water was added directly to the spin column membrane and centrifuged for 1 min at $\geq 10,000$ rpm twice. Then RNA was quantified by NanoDrop ND-1000 Spectrophotometer (Labtech International) to check the purity and quantity and samples were stored at -20°C .

2.4 RNA Precipitation

RNA precipitation was carried out for subsequent use where RNA yield was low.

Milli Q water (MQ) was added to DNase treated RNA (described below) to make a volume of 100 μ l. Equal amount of phenol: chloroform: isoamyl alcohol (25: 24: 1 v/v) was added and vortexed and briefly centrifuged. The aqueous phase was transferred into a new eppendorf tube and RNA was re-extracted from sample. 4M LiCl was added to the extracted RNA to make a final concentration of 0.5M LiCl and left on ice for 30 min. Samples were centrifuged at 4°C for 20 min at 16kg. Pellet was washed with 80% EtOH and air dried for 2 min. The pellet was re-suspended in smaller volume of MQ. Purity and quantity of RNA was checked by looking at the A260/280 and A260/230 value using NanoDrop ND-1000 Spectrophotometer. See 2.14 for further details.

2.5 Reverse Transcriptase (RT) Reaction

RT-reactions were carried out to prepare cDNA from extracted RNA. 1.0 μ l of 500 μ g/ml oligo dT (Invitrogen), $\sim 1.0\mu$ g of total plant RNA (2 μ g for QPCR) and MQ were added to a final volume of 11 μ l. Samples were incubated at 65°C for 5 min and then quenched on ice for 5 min. 4.0 μ l of RT buffer, 2.0 μ l of 0.1M DTT (Invitrogen), 1.0 μ l of 10mM dNTPs, 1.0 μ l of RNasin (40u/ μ l, Promega) and 1.0 μ l of superscriptIII (200u/ μ l, Invitrogen) were

added, which made a final concentration of 10mM DTT and 0.5mM dNTPs, and samples were incubated at 42 °C for 90min, and then 72 °C for 15min.

If there was genomic DNA contamination in the cDNA, DNase treatment of the RNA samples were carried out during the extraction.

2.6 DNase Treatment

DNase treatment using RQ1 RNase-Free DNase (Promega) was carried out according to the manufacture's protocol. All procedures were done in RNase free condition.

An on-column DNase digest was carried for Q-PCR RNA samples, according to the manufacturers protocol (QIAGEN).

2.7 Polymerase Chain Reaction (PCR) amplification of DNA

2.7.1 PXE 0.5 Thermal Cycler

PCR was carried out using BIOTAQ DNA polymerase (Bioline) and a PXE 0.5 Thermal Cycler (Thermo Electron Corporation) PCR machine. As a general reaction mixture, 5 μ l of 10 x NH₄ reaction buffer, 1.5 μ l of 50mM MgCl₂, 1 μ l of 10mM dNTPs, 1 μ l of DNA, 1 μ l of forward primer, 1 μ l of reverse primer, 0.2 μ l of TAQ, and MQ to make up to 50 μ l. This gave a final concentration of 1.5mM MgCl₂, 0.2mM dNTPs and 0.4 μ M primer. The amount of MgCl₂, Primers and DNA were altered to obtain the strongest band. The general programme was, 1 cycle of 5 min of 95°C, 30 cycles of 30 sec of 95 °C, 30 sec of annealing temperature and 90 sec of 72 °C, and 1 cycle of 72 °C for 5 min. The annealing temperature was calculated from the sequence of the primer sets.

2.7.2 Robocycler Gradient 96 PCR

A robocycler gradient 96 (Stratagene) was used to optimise the annealing temperature of primer sets. The general solutions used were the same as a thermal cycler. The general programme used was, 1 cycle of 95 °C for 6 min, 30 cycles of 50 sec of 95 °C, 70 sec of 44-66 °C, 90 sec of 72 °C, and 1 cycle of 5min of 72 °C. MgCl₂ was optimised for each primer sets.

2.7.3 Colony PCR

Colony PCR was carried out to confirm successful yeast transformation with recombinant plasmids.

A standard PCR solution (stated above) was prepared with 1 μ l of water instead of 1 μ l of DNA. 20 μ l of solution was placed into eppendorf tubes, and cells from the colonies with no prior heat treatment were added with an autoclaved tooth pick.

A normal PCR programme was used and colonies with insertion were determined by agarose gel electrophoresis of the PCR product.

2.7.4 Quantitative PCR

To quantify the steady-state levels of RNA for each IPCS gene in plant material, a real time quantitative PCR was carried out using Rotor-Gene RG-3000 (CORBETT RESEARCH).

For the general reaction solution, 2 μ l of 10 x NH_4 reaction buffer, 0.6 μ l of 50mM MgCl_2 , 0.4 μ l of 10mM dNTPs, 4 μ l of appropriately diluted DNA, 0.4 μ l of forward primer, 0.4 μ l of reverse primer, 0.08 μ l of TAQ, 0.2 μ l of SYBR Green and MQ to make up to 20 μ l. SYBR Green I nucleic acid gel stain (Invitrogen) was diluted 600 fold). Final concentration of each solution was, 1.5mM MgCl_2 , 0.2mM dNTPs and 0.4 μ M primer. The amount of MgCl_2 used with each primer pair was based on the end point PCR, and primer sets and DNA were optimised to obtain the best results. The general programme was, 1 cycle of 10 min of 95°C, 30 cycles of 10 sec of 95 °C, 15 sec of annealing temperature and 20 sec of 72 °C, melt analysis was 1 cycle of 72 °C to 95 °C rising 1 °C each step and waiting for 45sec on first step and then waiting for 5sec for each step onwards. The annealing temperature was set from end point PCR results for each primer pair concentration.

2.8 Gel Electrophoresis

After PCR, products were generally electrophoresed through a 0.8% agarose gel to check band size. Gels were made from agarose multi-purpose (Bioline) and 1xTAE (4.84g Tris, 1.142ml glacial acetic acid and 2ml 0.5M of pH8.0 EDTA in a litre). The solution was heated and dissolved in the microwave, and once it had cooled, 0.07 μ l/ml of 10mg/ml ethidium bromide was added and poured into the plates to give a final concentration of 0.7 μ g/ml. 1x TAE was used for buffer.

10 μ l of PCR product was mixed with 1 μ l of 10-times orange G loading buffer (4g sucrose, 20mg orange G dye topped up to 10ml MQ) and was carefully loaded into wells. An appropriate marker was chosen, and the gel electrophoresis was run at 120V for 30 to 40 min. The gel was then examined under UV light to determine the band size in comparison to the appropriate size molecular markers (Φ X x HAEIII, Lamda x HinDIII and Hyperladder V - Bioline).

2.9 Purifying DNA from Agarose Gel

DNA was purified from agarose gels using a Perfectprep Gel Cleanup Kit (Eppendorf) following the manufacturer's protocol. DNA was eluted in 30 μ l elution buffer, and quantified using NanoDrop ND-1000 Spectrophotometer and stored at -20°C.

2.10 Ligation and Transformation

Ligations of PCR products were set using pGEM-TEasy vectors (Promega) according to the manufacturer's protocol. Samples were incubated at 4°C overnight and transformation was carried out using *E. coli* XL1-blue made competent by calcium chloride treatment (Hanahan 1983). Competent *E. coli* XL1-blue cells were thawed on ice for 5 min. 5 μ l of ligation was carefully added to 50 μ l of competent *E. coli* XL1-blue cells and placed on ice for 30 min. Using a heat-shock method, eppendorf tubes were placed in a 42 °C water bath to allow the plasmid to transform competent *E. coli* XL1-blue cells. Then tubes were placed on ice for 2 min and 900 μ l of LB broth was added to tubes and were incubated at 37 °C for 1 hour with shaking.

After incubation, cells were centrifuged at 10,000xg and gently re-suspended with 300 μ l of the incubated LB broth. Then 100 μ l of sample was plated on to ampicillin, IPTG and X-Gal containing LB plates (50mg/ml ampicillin, 200 μ M IPTG and 20mg/ml X-Gal), and incubated at 37 °C overnight.

White and light blue cells were selected and inoculated into ampicillin containing LB media and on LB plates. Media/ plates were incubated at 37 °C overnight with shaking.

2.11 Purifying Plasmid from *E. coli* cells

After the cells have grown in ampicillin containing LB broth, plasmid was purified using Wizard Plus SV Minipreps DNA Purification System (Promega). DNA was eluted in 30 μ l x 3 of water, quantified by NanoDrop ND-1000 Spectrophotometer and stored at -20°C.

2.12 Restriction Enzyme Digestion

To confirm the success of ligation/transformation, restriction enzyme digestion was carried out. 1.2 μ l of the appropriate buffer, 2 μ l of the plasmid, 1 μ l of appropriate restriction enzyme and 7.8 μ l of water was added. Digestion was incubated at 37°C for 2 to 3 hours.

2.13 Sequencing

Sequencing was sent to an internal sequencing lab, and was carried out using pUC/M13 forward and reverse primers. Specific primers were designed to confirm the sequence in pRS426 MET (Figure 4) prior to cloning into yeast mutant cells (Details in Results). Sequence was checked using NCBI-Blast to confirm the correct sequence. An alignment was carried out with the forward and reverse primer results, and sequences were determined.

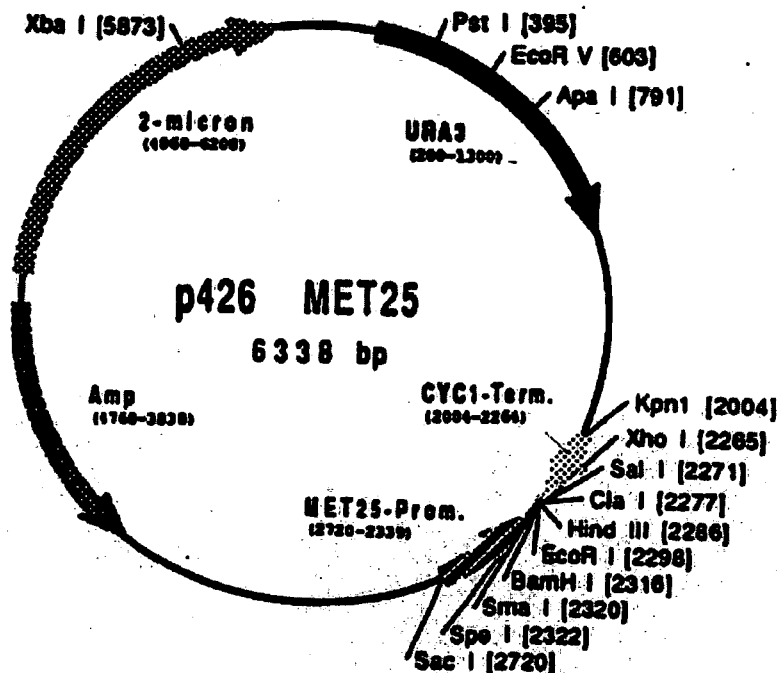


Figure 4 Map of Plasmid pRS426 MET

EcoRI and SalI sites were used to clone IPCS. Figure adapted from Mumberg 1994.

2.14 NanoDrop ND-1000 Spectrophotometer

To determine the quantity of RNA or DNA, a NanoDrop ND-1000 Spectrophotometer (Labtech International) was used.

The surface of the NanoDrop was cleaned and initialized with water prior to use. Using 2 μ l of the eluted solution, a blank was measured, and samples were measured placing 2 μ l on the spectrophotometer. Each time before measuring a new sample, the spectrophotometer was cleaned with water.

2.15 Preparation of Yeast Competent Cells for Transformation

Yeast cells, strain YPH499-HIS-GAL-AUR1 *S. cerevisiae* and YER019w were made competent by following the small-scale yeast transformation protocol from Invitrogen (pYD1 Yeast Display Vector Kit).

Cells were grown in 50ml of media (YPD for ISC1 and YPGR for AUR1) overnight and the culture was diluted to an OD₆₀₀ of 0.4 in 50ml of medium and was grown for an additional 2 hours. Cells were plated on selective plates (SD-Ura for ISC1 and SD-His-Ura/ Gal Raf for AUR1) and incubated at 30°C until colonies formed.

2.16 Spotting Yeast on Plates

For testing the function of IPCS in yeast mutant cells (AUR1 or ISC1), were grown to log-phase and spotted onto agar plates of various compositions. The OD₆₀₀ of the grown yeast cells were measured and all yeast samples were adjusted to the same OD₆₀₀ so the yeast density will be equal. A dilution series was carried out using 0.9% NaCl (filter sterilised), and 10 μ l of the yeast cells were spotted onto each plate.

2.17 Agar Diffusion Assay

The conditional AUR1 mutant strain YPH499-HIS-GAL-AUR1 complemented with *ScAUR1* or *At IPCS* were assayed for susceptibility to AbA (Takara Bio Inc.) (Denny *et al.* 2006) and myriocin (MYR) (Sigma) as previously described (Nagiec *et al.* 2003b). 2.4×10^7 logarithmically dividing cells were embedded in 15 ml of SD-His-Ura/Glc cooled to 42°C on 100-mm² square petri dishes (Sarstedt). Inhibitors were applied in DMSO and the

dishes incubated at 30 °C for 3 to 4 days. Inhibitors applied were volumes of 1, 2, and 3 μ l of 25 μ M *AbA*, 1mM *MYR* and DMSO (control).

2.18 Fluorescence Labelling

2.18.1 Fluorescence Labelling for AUR1

For metabolic labelling experiments AUR1 cells were grown in 10ml SD-His-Ura/Glu media for 72 hours with shaking. The OD₆₀₀ was measured and at OD₆₀₀ 2.5 cells were pelleted. The pellet was re-suspended in 250 μ l SD-His-Ura/Glu and 2.5 μ l of 5mM (6-((N-(7-nitrobenz-2-oxa-1,3-diazol-4-yl)amino)hexanoyl)sphingosine) (NBD-C₆-Ceramide) was added. Samples were incubated at 30 °C for 2 hours. Cells were then transferred into a 1.5ml eppendorf tube and pelleted and washed with water three times. 250 μ l of chloroform: methanol: water (C/M/W) 10:10:3 (v/v/v) was added to the pellet and then sonicated for 15min in the sonic bath.

Samples were centrifuged and the solvent phase was transferred into a new tube. The organic extracts were dried in a Concentrator 5301 (Eppendorf) and re-suspended in 20 μ l of C/M/W 10:10:3 (v/v/v). Fluorescence was measured using Fusion[®] α plate reader at excitation 466nm and emission 536nm.

Equal amounts of fluorescent reaction products were spotted on HPTLC silica plates (Merck) after equilibration. The TLC plate was run using eluent system chloroform/methanol/aqueous 0.25% KCl 55:45:10 (v/v/v).

2.18.2 Fluorescence Labelling for ISC1

Cells were inoculated into 10 ml SD-Ura media and incubated with shaking overnight at 30°C. The OD₆₀₀ was measured and the cell density was adjusted to approximately 2×10^7 cells in 400 μ l SD-Ura. 2.0 μ l of 2.5 μ M NBD-C₆-SM (BODIPY[®] FLC₁₂-sphingomyelin, (Molecular Probes) was added and cells were incubated at 30°C for 1 hour with shaking.

Cells were pelleted and washed with SD-Ura three times, then re-suspended in 400 μ l of 1:1 chloroform: methanol (v/v). Approximately 100 μ l of 0.5mm glass beads (BioSpec) were added and 10 cycles of 10sec vortexing and 10sec on ice was carried out to break the cell wall to increase the lipid extraction. 100 μ l of MQ was added to separate the phases and the solvent phase (bottom phase) was extracted into a new tube. The mixture was re-extracted

with another 400µl of 1:1 C: M (v/v). To clean the solution, 100µl of MQ was added and the solvent phase was removed into a new tube.

Solvent was dried using a Concentrator 5301 (Eppendorf) at 45°C for 10 min and the pellet was re-suspended in 30µl of 10:10:3 C: M: W (v/v/v).

The fluorescence was measured using Fusion® α plate reader and equal amount of the reaction products were spotted onto HPTLC silica plates (Merck) after equilibration. The TLC plate was run using eluent system chloroform/methanol/15mM CaCl₂ 60:35:8 (v/v/v).

2.19 Preparation of Membranes for ISC1 Assay

Media was prepared for growing yeast cells to prepare membranes for assay.

Table 2 Selected Media for Yeast Cells

Type of Cell	Selected Media
Wild Type (JS91)	YPD
Mutant (DZY1)	YPD
Mutant + Arabidopsis IPCS1	SD-Ura
Mutant + Arabidopsis IPCS2	SD-Ura
Mutant + Arabidopsis IPCS3	SD-Ura

To determine if IPCS in *A. thaliana* also encodes for an ISC1 function, crude membranes of ISC1 mutant cells complemented with *A. thaliana* IPCS1, 2 and 3 were prepared in appropriate media. A single colony was inoculated into 200 ml liquid media, and was incubated at 30°C for 24 hours with shaking.

Crude membranes were prepared by carrying out various speed of centrifugation after cell breakage. 200ml of culture was harvested by centrifugation (Beckman Avanti 30 Centrifuge, F0650) at 5000 x g, 4°C for 10min. The pellets obtained were washed with cold PBS (2 × 4 ml). The sediment was suspended in 0.5 ml STE buffer (25mM Tris/HCl, 250mM sucrose and 1mM EDTA) and the cells were disrupted with 0.5 g of chilled 0.5mm glass beads (BioSpec) using a vortex mixer for 10 cycles (1 min vortex followed by 1 min rest on ice). The mixture was centrifuged (Beckman Avanti 30 Centrifuge, F2402) at 2,800 x g at 4°C for 15 min and the supernatant was collected. The pellet was re-extracted with another 0.5 ml of STE buffer for another 10 cycles followed by centrifugation (Beckman Avanti 30 Centrifuge, F2402) at 2,800 x g at 4°C for 15 min. The supernatant was extracted and combined with the first extraction and were centrifuged as follows.

An initial centrifugation (Beckman Optima TLX Ultracentrifuge, F2402) of 27,000 x g at 4°C for 30min removed large granular fraction of cell components. The supernatant was then centrifuged (Beckman Optima TLX Ultracentrifuge, F2402) at 150,000 x g at 4°C for 90 min to sediment the small granular fraction enriched in microsomal membranes. The obtained pellets were then suspended in storage buffer (50mM Tris/HCl, 10%w/v glycerol and 5mM MgCl₂) and protein contents were prepared for quantification using RC DC Protein Assay (BIO RAD). The membranes were flash frozen in liquid nitrogen and stored at -80 °C until use.

2.20 Preparation of STE Buffer and Storage Buffer

STE buffer was prepared using 1.25ml of 1M Tris/HCl, 12.5g of 1M sucrose, 100 µl of 0.5M EDTA and 1 tab of complete® protease inhibitor cocktail (Roche Applied Science) and distilled water was added to make 50ml. The final concentration was 25mM Tris/HCl, 250mM sucrose and 1mM EDTA.

Storage buffer was prepared using 2.5ml of 1M Tris/HCl, 6.25ml of 80%w/v glycerol, 0.25ml of 1M MgCl₂ and 1 tab of complete® protease inhibitor cocktail and distilled water was added to make 50ml. The final concentration was 50mM Tris/HCl, 10%w/v glycerol and 5mM MgCl₂.

2.21 Labelling Prepared Microsomes for NBD-C₆-Sphingomyelin Fluorescence Assay

Microsomes were labelled with NBD-C₆-sphingomyelin (Molecular Probes) to examine the ISC1 function of IPCS. NBD-C₆-sphingomyelin; (6-((N-(7-nitrobenz-2-oxa-1,3-diazol-4-yl)amino)hexanoyl)sphingosyl phosphocholine) is used for following sphingolipid metabolism in cells.

1 µl of 50mM PI was evaporated into each reaction tube. 20 µl of Tris/EDTA/BSA buffer was added to the dried PI. The solution was sonicated for 2 min in a sonicating water bath then rested on ice for 1min. 20 µg of the microsomal preparation was added and distilled water was added to finalize the volume to 49 µl. The reaction was started by the addition of 1µl of 5mM NBD-C₆-sphingomyelin. The assay final volume was 50 µL and final concentrations were 1 mM PI, 100 mM Tris/HCl buffer and 100 µM NBD-C₆-

sphingomyelin. The reaction mixture was incubated at 30 °C for 60 min. The reaction was quenched by the addition of 150 μ l of chloroform/methanol/water 10:10:3 (v/v/v).

The resultant mixture was vortexed and then centrifuged to separate phases. The organic layer was collected and the aqueous phase was re-extracted with 50 μ l of chloroform. Combined organic extracts were dried in a Concentrator 5301 (Eppendorf) and re-suspended in 20 μ l of the C/M/W 10:10:3. Reaction products were spotted on HPTLC silica plates (Merck) after equilibration. The TLC plate was run using the solvent system chloroform/methanol/aqueous 0.25% KCl 55:45:10 (v/v/v). The plate was scanned using a Typhoon 9400 Variable Mode Imager (GE Healthcare). The excitation and emission of NBD- C₆-sphingomyelin is 466nm and 536nm respectively. The R_f values for the excess NBD-C₆-sphingomyelin and NBD-C₆-IPC were 0.93, 0.37 respectively.

2.22 Measuring fluorescence

The amount of fluorescence in each sample was measured using Fusion[®] \square plate reader (Packard Bioscience) using a black plate (OptiPlate-96 F from Perkin Elmer). 2.0 μ l of sample was added to 100 μ l of methanol.

2.23 Scanning TLC plates

TLC plates were scanned on Typhoon 9400 Variable Mode Imager (GE Healthcare). 520BP40/ Blue2 (488nm) was selected for the laser, platen was selected for focal plane and the plate was pressed. Sensitivity was adjusted for each sample by changing the pixel size and resolution so none of the data was saturated.

3. Results - Identifying, Cloning and Characterisation of IPCS

3.1 Identification and Cloning of IPCS

IPCS in plant has only been characterized recently in bean microsomes (Bromley *et al.* 2003), but until now no genes encoding IPCS have been identified. From unpublished data by P. W. Denny, 3 highly related sequence orthologues of *Leishmania* in *A. thaliana*, *At* IPCS1, *At* IPCS2 and *At* IPCS3 were identified (J. G. Mina Unpublished). These *A. thaliana* genes potentially encode IPCS, responsible for a step in sphingolipid synthesis. Although a fourth IPCS ORF, At2g29525.2 was identified, as the gene does not recognise the splicing site and the transcript ends due to a stop codon (Figure 5), it was expected that the protein was not functional. Therefore for these experiments, IPCS4 was excluded and the 3 genes IPCS1, IPCS2 and IPCS3 were used.

In this chapter, primers were designed to clone these potential IPCS genes from *A. thaliana* and cDNA was prepared from total leaf RNA by RT-PCR and PCR was carried out.



Figure 5 Model of IPCS3 and IPCS4 Protein Coding Gene

The protein coding gene model was extracted from TAIR. At2g29525 is located in chromosome 2 in position 12,645,431 to 12,647,897. The blue line depicts the gene model and the blue boxes are the peptides of the corresponding gene model.

This shows the splicing region of IPCS4 (At2g29525.2) is missing and the transcript is ended due to a stop codon.

3.1.1 Designing Primer Pairs

After identifying the three possible IPCS genes, primer sets were designed to clone the full length ORF of each. As the pRS426 MET plasmid has *EcoRI* and *SalI* site, *EcoRI* site was attached to the 5' prime end of the forward primers, and *SalI* site was attached to the 3' prime end of the reverse primers to allow directional cloning into the appropriately digested vector (Table 3).

Table 3 Primer Paris Designed for each IPCS Gene

IPCS 1	Forward: <u>GAATTC</u> ATGACGCTTTATATTCGCCGCG Reverse: <u>GTCGAC</u> GAGCAGAGATCTCATGTGCC
IPCS 2	Forward: <u>GAATTC</u> ATGACACTTTATATTCGTCGTG Reverse: <u>GTCGACT</u> CACGCGCCATTCATTGTG
IPCS 3	Forward: <u>GAATTC</u> ATGCCGGTTTACGTTGATCGCG Reverse: <u>GTCGACT</u> CAATGATCATCTGCTACATTG

3.1.2 Optimising Primers for Cloning Full Length IPCS Genes

A PCR using the standard method was carried out to clone full length IPCS genes from *A. thaliana* cDNA which was prepared from total leaf RNA by RT-PCR.

The annealing temperature was calculated using $\{2(A+T) + 4(G+C)\} - 5$. -5 was added as the annealing temperature was too high without it.

Using this formula, for full-length IPCS genes, an annealing temperature of 64°C was selected. PCR products were electrophoresised on a 0.8% agarose gel (Figure 6). For full length IPCS1 and 2, a band size of 918bp and for IPCS3, a PCR product of 870bp were expected, but no product or only a very faint band was observed, when analysed by agarose gel electrophoresis. This could be due to too high annealing temperature or sub-optimal MgCl₂ concentration. Therefore a PCR using the temperature gradient function of a robocycler gradient 96 (Stratagene) was carried out to optimise each of the pairs with respect to temperature and MgCl₂ concentrations.



Figure 6 Amplification of Full Length IPCS ORFs

PCR was carried out using IPCS full length primer pairs to amplify IPCS ORFs. Annealing temperature was set at 64°C and MgCl₂ was 1.5mM. Single primer controls showed no bands (figure not shown). Faint bands are found in 1 and 2, but further optimisation of primers were needed. Expected band size is IPCS1: 918bp, IPCS2: 918bp and IPCS3: 870bp. Large amounts of primer dimers were observed possibly due to primer complementarity and/or low template concentration.

A temperature gradient and MgCl₂ optimisation experiment was carried out using a robocycler with a range of annealing temperatures from 58 °C to 66 °C and MgCl₂ concentration of 1.5mM to 3mM. Single primer controls were carried out at 58°C with MgCl₂ of 3mM. From these results, an optimal temperature and MgCl₂ concentration were determined (Table 4).

Table 4 Optimal Primer Pair Conditions

	Temperature(°C)	MgCl ₂ (mM)
IPCS 1 Full Length Primer Pairs	64	2
IPCS 2 Full Length Primer Pairs	60	3
IPCS 3 Full Length Primer Pairs	54	3

To clone full length IPCS ORFs, a PCR using the PXE 0.5 thermal cycler (Thermo Electron Corporation) PCR machine was carried out under the above conditions, and 50 µl of PCR product was separated on 0.8% agarose gel.

The appropriate band sizes were cut out from the gel and DNA was purified using perfectprep gel cleanup kit (Eppendorf), following the manufacture protocol. The amount of DNA purified was measured using a NanoDrop ND-1000 Spectrophotometer (Table 5).

Table 5 Quantity of Purified IPCS

	Quantity (ng/µl)
IPCS1	31.2
IPCS2	31.5
IPCS3	13.2

3.1.3 Cloning Full Length IPCS cDNAs into pGEM-TEasy

Subsequently, the purified cDNA for IPCS genes 1-3 were ligated into T-vectors, and transformed into competent *E. coli* XL1-blue cells. Cells were plated on LB medium containing AIX (Ampicillin, IPTG and X-GAL). As these plasmid/host combination allowed for selection of recombinant plasmids, white colonies on the transformation plates were inoculated into ampicillin containing LB broth, and incubated overnight at 37°C with shaking.

Plasmid preparations and restriction enzyme digestion using *EcoRI* was carried out to confirm the presence of inserts. As the vector has two *EcoRI* sites, only a single digestion was carried out to confirm insertion. As an example, restriction digest of IPCS3 is shown in Figure 7. An insertion in 3.2 was confirmed.

IPCS1 and 2 were also successfully cloned into vectors (Figure 7).

After confirming an insertion from digestion, samples were sent for DNA sequencing. Results were analysed using NCBI-Blast, and results confirmed that each three IPCS genes were successfully cloned. By aligning the sequence, sequencing errors were corrected and the complete gene was identified.

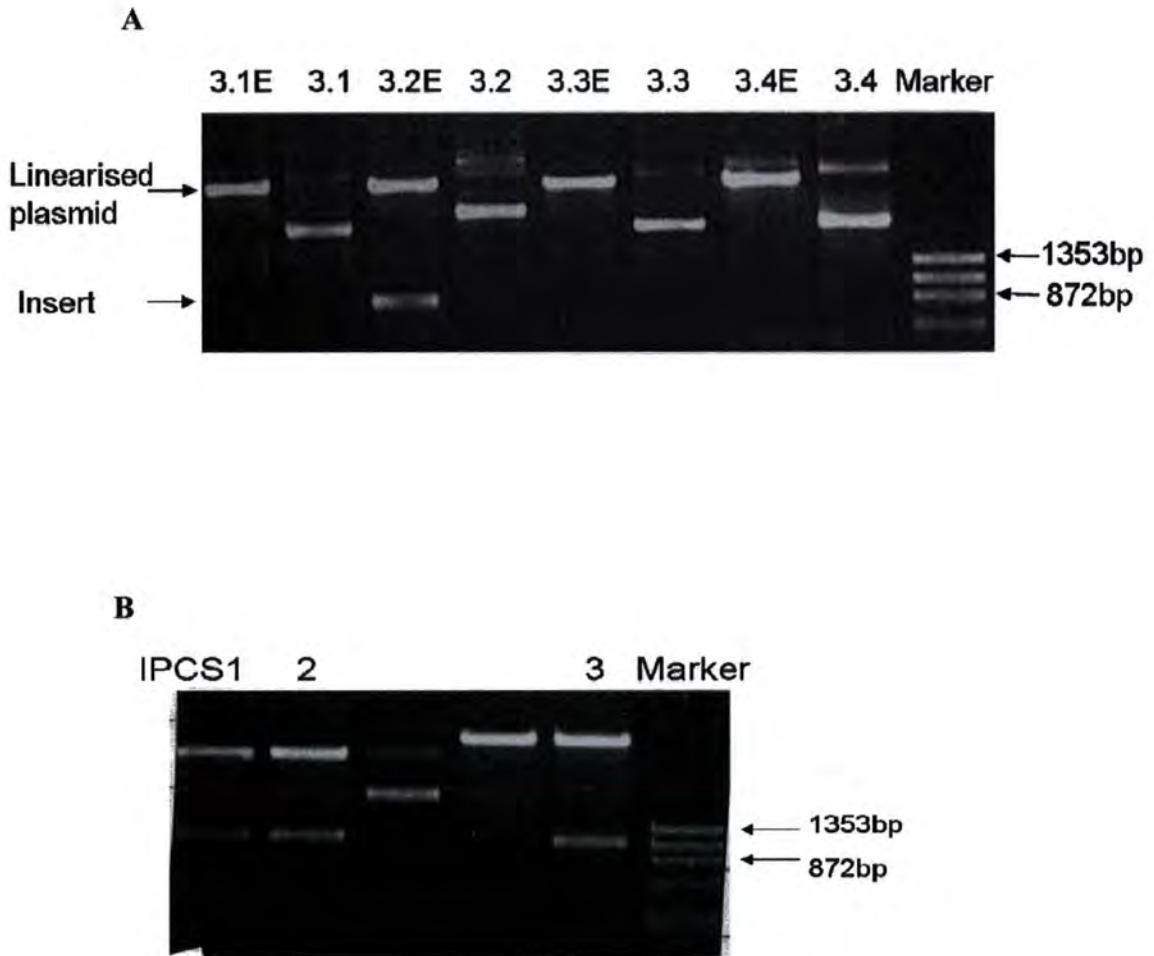


Figure 7 Restriction Digest of IPCS3

A) Enzyme digestion treated with (E) and without EcoR1 for 2-3 hours. Results show that 3.2 has IPCS3 insertion. B) Enzyme digestion with EcoR1 shows that IPCS1, 2 and 3 has insertion.

3.1.4 Cloning into pRS426 MET Plasmid

The IPCS 1-3 cDNAs were cloned into the yeast –*E. coli* shuttle vector pRS426 MET using *EcoRI* and *SalI* to release the cDNA from the T-vector and subsequent ligation into the same sites of the recipient plasmid.

Recombinant pRS426 MET plasmids were transformed into *E. coli* XL1-blue and colony PCR was carried out using full length IPCS primer pairs to check for the presence of inserts. Although there was an expected band size for the control, there were no bands in any colony PCR product. This would indicate that the ligation, transformation did not work. As there are *EcoRI* and *SalI* sites in the DNA and plasmid, it is doubtful to think the ligation did not work. Therefore the plasmid was checked to see if there was *EcoRI* and *SalI* site by carrying out a single enzyme digestion. From this result, it was concluded that *EcoRI* site was cut, but *SalI* site was not cut. As *XhoI* has a compatible ligation end to *SalI*, a restriction enzyme digestion with *XhoI* was carried out, and the plasmid was successfully cut (Figure 8).

Plasmid pRS426 MET was cut with *EcoRI* and *XhoI* and a ligation was set with the 3 IPCS DNA digested with *EcoRI-SalI*. Transformation was carried out and colony PCR was set to confirm the insertion. Results show that all 3 IPCS genes were successfully cloned into pRS426 MET (Figure 9). Plasmids were then sequenced to confirm the sequence which showed 100% similarity (Figure 10).

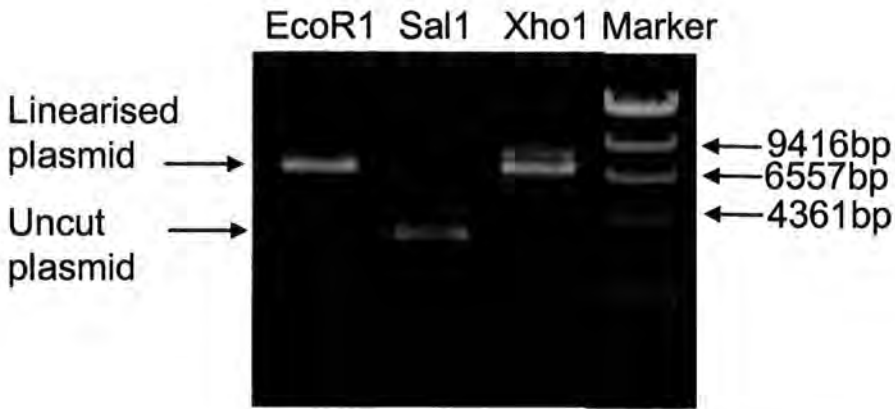


Figure 8 Restriction Enzyme of pRS426

pRS426 was cut with EcoR1, Sal1 and Xho1. From these results, it is clear that Sal1 does not cut the plasmid but EcoR1 and Xho1 does. Therefore for subsequent uses, EcoR1 and Xho1 were used to cut plasmid.

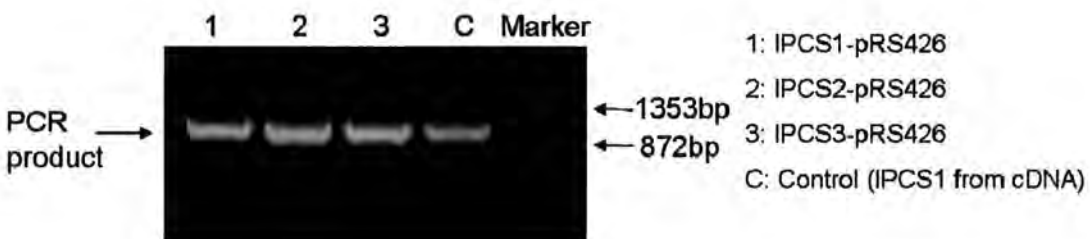


Figure 9 Colony PCR of IPCS-pRS426

A colony PCR was carried out from the colonies formed on LB medium containing AIX. A standard programme was run with an annealing temperature of 54°C. From these results, it was confirmed that all IPCS genes were transformed into plasmid pRS426. Sequencing was carried out with a specific primer.

A IPCS1 and At3g54020

```

IPCS1      ATGACNCTTTATATTCGCCGCGAAGCTTCCAAGCTATGGAGGAGATTTGTTCGGAAATA
At3g54020  ATGACGCTTTATATTCGCCGCGAAGCTTCCAAGCTATGGAGGAGATTTGTTCGGAAATA
*****

IPCS1      ACAACGGAGATTGGTCTCCTCGCTGAGAAGTGGAAATACCTTCTTGTGCTGGTCTTCTCTGT
At3g54020  ACAACGGAGATTGGTCTCCTCGCTGAGAAGTGGAAATACCTTCTTGTGCTGGTCTTCTCTGT
*****

IPCS1      CAGTATATTCATGGTTTAGCTGCCAGGGGAGTTCATATATATTCATCGCCAGGACCAACG
At3g54020  CAGTATATTCATGGTTTAGCTGCCAGGGGAGTTCATATATATTCATCGCCAGGACCAACG
*****

IPCS1      CTTCAAGATTCGGCTTTTTTGTCTTCCGGAGCTTGGTCAAGATAAAGGCTTCATAAGT
At3g54020  CTTCAAGATTCGGCTTTTTTGTCTTCCGGAGCTTGGTCAAGATAAAGGCTTCATAAGT
*****

IPCS1      GAAACTGTGTTCACTTGTGTATTTCTTTTCAATTTTCTGTGGACTTCCATCCTTTCATC
At3g54020  GAAACTGTGTTCACTTGTGTATTTCTTTTCAATTTTCTGTGGACTTCCATCCTTTCATC
*****

IPCS1      GTGAAAAGCAAGAAGATATACACTGTGTGATATGGTGCAGGGTTCGCGCTTCTTAGTT
At3g54020  GTGAAAAGCAAGAAGATATACACTGTGTGATATGGTGCAGGGTTCGCGCTTCTTAGTT
*****

IPCS1      GCTTGTGAGTTTCTCCGTGTTATAACATTCATTTCAACTCAGCTTCCGCGCCTAACATAT
At3g54020  GCTTGTGAGTTTCTCCGTGTTATAACATTCATTTCAACTCAGCTTCCGCGCCTAACATAT
*****

IPCS1      CACTGTCGAGAGGGTTCTGAGCTTGCCAGGTTGCCAAGGCCACATAACGTTCTTGAGGTT
At3g54020  CACTGTCGAGAGGGTTCTGAGCTTGCCAGGTTGCCAAGGCCACATAACGTTCTTGAGGTT
*****

IPCS1      CTCTTGCTCAACTTTCCTCGTGGTGTGATATACGGATGTGGAGACCTGATTTTCTCATCG
At3g54020  CTCTTGCTCAACTTTCCTCGTGGTGTGATATACGGATGTGGAGACCTGATTTTCTCATCG
*****

IPCS1      CACATGATATTCACATTAGTCTTTGTCCGCACCTACCAGAAATACGGTTCTAAAAGGTTTC
At3g54020  CACATGATATTCACATTAGTCTTTGTCCGCACCTACCAGAAATACGGTTCTAAAAGGTTTC
*****

IPCS1      ATAAAGCTGTTAGGTTGGGTGTCATTGCCATCTTGCAAAGCCTCTTGATTATGCGTCCCGT
At3g54020  ATAAAGCTGTTAGGTTGGGTGTCATTGCCATCTTGCAAAGCCTCTTGATTATGCGTCCCGT
*****

IPCS1      AAACATTACACTCTTGATGTGGTGTGCGTGGTATACTGTGAACCTGGTGTCTTCTTTC
At3g54020  AAACATTACACTCTTGATGTGGTGTGCGTGGTATACTGTGAACCTGGTGTCTTCTTTC
*****

IPCS1      CTCGACAAGAAATACCAGAATTGCCGTGATCGAACACGGCATTGCTCCCTGTGATCTCN
At3g54020  CTCGACAAGAAATACCAGAATTGCCGTGATCGAACACGGCATTGCTCCCTGTGATCTCA
*****

IPCS1      AAAAGACAGAACCAAGAAGAGAGTACNAAACCTTGAATGGGAACGGTGTGATCCTG
At3g54020  AAA-GACAGAACCAAGAAGAGAGTACAAA-CTCTTGAATGGGAACGGTGTGATCCTG
*** *****

IPCS1      CAGATCGGAGACCGAGGGCTCAAGTGAATGGCAA-ACAGCAATGGAGGTC-CACTGATA
At3g54020  CAGATCGGAGACCGAGGGCTCAAGTGAATGGCAAAGACAGCAATGGAGGTCACACTGATA
*****

IPCS1      ATGCTACTAATGGCACATGA
At3g54020  ATGCTACTAATGGCACATGA
*****

```

B IPCS2 and At2g37940

IPCS2 ATGACACTTTATATTTCGTCGTTGAATCTTCCAAGCTATGGAAGAGATTTTGCTCTGAGATA
 AT2G37940 ATGACACTTTATATTTCGTCGTTGAATCTTCCAAGCTATGGAAGAGATTTTGCTCTGAGATA

IPCS2 TCGACGGAGATTGGTCTTCTTGCTGAGAAGTGGAAATATCTTCGCTGGTCTTATCTGT
 AT2G37940 TCGACGGAGATTGGTCTTCTTGCTGAGAAGTGGAAATATCTTCGCTGGTCTTATCTGT

IPCS2 CAGTACATTCATGGTTTAGCTGCTAAAGGAGTTCATTTATATTTCATCGCCCGGGACCGACA
 AT2G37940 CAGTACATTCATGGTTTAGCTGCTAAAGGAGTTCATTTATATTTCATCGCCCGGGACCGACA

IPCS2 CTTTCAGGATCTTGGCTTCTTCTTCTTCCGGAGCTTGGTCAAGAGAGAAGCTACATAAGT
 AT2G37940 CTTTCAGGATCTTGGCTTCTTCTTCTTCCGGAGCTTGGTCAAGAGAGAAGCTACATAAGT

IPCS2 GAAACCGTGTTCAGTGTGTTTCTTTCGTTTTCCTGTGGACTTTCATCCATTCATT
 AT2G37940 GAAACCGTGTTCAGTGTGTTTCTTTCGTTTTCCTGTGGACTTTCATCCATTCATT

IPCS2 CTGAAAACCAAAAAGATATACACCGTTTGGATATGGTGCAGAGTTCATAGCATTCTTAGTT
 AT2G37940 CTGAAAACCAAAAAGATATACACCGTTTGGATATGGTGCAGAGTTCATAGCATTCTTAGTT

IPCS2 GCCTGCCAGTTTCTCCGTGTTATAACTTTCATTTCAACTCAGCTTCCGCGCCTAACAT
 AT2G37940 GCCTGCCAGTTTCTCCGTGTTATAACTTTCATTTCAACTCAGCTTCCGCGCCTAACAT

IPCS2 CACTGCCGTGAGGGCTCTAAAGTTTCTAGGTTGCCATGGCCCAAAGCGCTCTTGAGGTT
 AT2G37940 CACTGCCGTGAGGGCTCTAAAGTTTCTAGGTTGCCATGGCCCAAAGCGCTCTTGAGGTT

IPCS2 CTCGAGATTAACCCTCATGGGGTGATGTATGGATGCGGAGACCTGATTTTCTCATCGCAC
 AT2G37940 CTCGAGATTAACCCTCATGGGGTGATGTATGGATGCGGAGACCTGATTTTCTCATCGCAC

IPCS2 ATGATATTCACCTCTAGTCTTTGTCCGTAATTACCAGAAATATGGCACTAAAAGGTTTCATA
 AT2G37940 ATGATATTCACCTCTAGTCTTTGTCCGTAATTACCAGAAATATGGCACTAAAAGGTTTCATA

IPCS2 AAGCTGTTTGGGTGGCTCAGTGAATTTGTGCAGAGCCTCTTGATCATTCGCTCTCGTAAA
 AT2G37940 AAGCTGTTTGGGTGGCTCAGTGAATTTGTGCAGAGCCTCTTGATCATTCGCTCTCGTAAA

IPCS2 CATTACAGTGTGATGTAGTTGTTGCATGGTATACTGTGAATTTGGTGGTGTCTGTCTA
 AT2G37940 CATTACAGTGTGATGTAGTTGTTGCATGGTATACTGTGAATTTGGTGGTGTCTGTCTA

IPCS2 GACAAGAAATTACCAGAATTACCAGATCGGACTGCTGTGTTGCTCCAGTAATCTCAAAA
 AT2G37940 GACAAGAAATTACCAGAATTACCAGATCGGACTGCTGTGTTGCTCCAGTAATCTCAAAA

IPCS2 GACAGAACAAAAGAAGAGAACCACAAGCTGTTGAATGGAAACGGTGTGACCCTGCTGAT
 AT2G37940 GACAGAACAAAAGAAGAGAACCACAAGCTGTTGAATGGAAACGGTGTGACCCTGCTGAT

IPCS2 TGGAGACCGAGGGCTCAGGTGAACGGGAAGATTGACAGCAACGGAGTTCACACGGATAAC
 AT2G37940 TGGAGACCGAGGGCTCAGGTGAACGGGAAGATTGACAGCAACGGAGTTCACACGGATAAC

IPCS2 ACAATGAATGGCGCGTGA
 AT2G37940 ACAATGAATGGCGCGTGA

C IPCS3 and At2g29525

IPCS3	ATGCCGGTTTACGTTGATCGCGAAGCTCCTAAGCTATGGAGACGAATTTACTCAGAAGCG	60
At2g29525	ATGCCGGTTTACGTTGATCGCGAAGCTCCTAAGCTATGGAGACGAATTTACTCAGAAGCG	60

IPCS3	ACATTAGAAGCTTCTCTTCTTGCTGAAAAATGGAAGCTTGTTCCTGCTGGACTTGTATTT	120
At2g29525	ACATTAGAAGCTTCTCTTCTTGCTGAAAAATGGAAGCTTGTTCCTGCTGGACTTGTATTT	120

IPCS3	CAGTACATTCATGGACTTGCCTGCTCATGGAGTTCACTACTTACACCGACCTGGTCCCTACT	180
At2g29525	CAGTACATTCATGGACTTGCCTGCTCATGGAGTTCACTACTTACACCGACCTGGTCCCTACT	180

IPCS3	CTTCAAGATGCTGGTTTCTTTATCTTCCAGCACCTTGGGCAAGATAAAGCATTTTTCAGT	240
At2g29525	CTTCAAGATGCTGGTTTCTTTATCTTCCAGCACCTTGGGCAAGATAAAGCATTTTTCAGT	240

IPCS3	GAAACTGTGTTTGTCACTATCTTTGGATCATTATCTTGTGGACATTTTCATCCTTTTGT	300
At2g29525	GAAACTGTGTTTGTCACTATCTTTGGATCATTATCTTGTGGACATTTTCATCCTTTTGT	300

IPCS3	TCCCACAGTAAAAAGATTTGTACAGTTTTGATATGGTGCAGAGTTTTTGTATTATTAGCT	360
At2g29525	TCCCACAGTAAAAAGATTTGTACAGTTTTGATATGGTGCAGAGTTTTTGTATTATTAGCT	360

IPCS3	GCTTCTCAAAGTCTGAGGATCATAACATTCTTTGCAACACAGCTTCCCTGGGCCGAATTAT	420
At2g29525	GCTTCTCAAAGTCTGAGGATCATAACATTCTTTGCAACACAGCTTCCCTGGGCCGAATTAT	420

IPCS3	CATTGTCGAGAAGGCTCCAAGCTCGCCAAGATCCACCTCCAAGAATGTTCTTGAAGTA	480
At2g29525	CATTGTCGAGAAGGCTCCAAGCTCGCCAAGATCCACCTCCAAGAATGTTCTTGAAGTA	480

IPCS3	CTCTTGATTAACTTTCTTGATGGAGTTATATATGGTTGTGGAGATCTGATATTTTCATCA	540
At2g29525	CTCTTGATTAACTTTCTTGATGGAGTTATATATGGTTGTGGAGATCTGATATTTTCATCA	540

IPCS3	CATACGATATTCACCTTAGTCTTTGTACGCACATATCAAAGATACGGCACACGAAGGTGG	600
At2g29525	CATACGATATTCACCTTAGTCTTTGTACGCACATATCAAAGATACGGCACACGAAGGTGG	600

IPCS3	ATCAAGCACTTGGCTTGGCTTATGGCAGTAATACAGAGCATATTGATTATAGCATCAAGG	660
At2g29525	ATCAAGCACTTGGCTTGGCTTATGGCAGTAATACAGAGCATATTGATTATAGCATCAAGG	660

IPCS3	AAACATTACACAGTTGACATTGTTGTTGCATGGTATACTGTGAACCTTGTAAATGTTCTAC	720
At2g29525	AAACATTACACAGTTGACATTGTTGTTGCATGGTATACTGTGAACCTTGTAAATGTTCTAC	720

IPCS3	GTTGACAGTAACTGCCAGAAATGGCAGAACGTTCTAGTGGACCTTCTCCTACGCCTTTA	780
At2g29525	GTTGACAGTAACTGCCAGAAATGGCAGAACGTTCTAGTGGACCTTCTCCTACGCCTTTA	780

IPCS3	CTTCCACTGAGCACAAGGACAGTAAGAACAAGAGCAAAGAAGATCATCAGAGACTTCTA	840
At2g29525	CTTCCACTGAGCACAAGGACAGTAAGAACAAGAGCAAAGAAGATCATCAGAGACTTCTA	840

IPCS3	AACGAGAACAATGTAGCAGATGATCATTGA	870
At2g29525	AACGAGAACAATGTAGCAGATGATCATTGA	870

Figure 10 Alignment of Cloned IPCS Genes and Sequence of each Gene

The alignment of each IPCS genes cloned and each of the gene models are shown. The * shows the similarity of the sequences. From this alignment, all genes were confirmed to be successfully cloned. A:IPCS1, B:IPCS2 and C:IPCS3.

3.2 Characterizing the Function of IPCS

3.2.1 AUR1 Mutant Cells Complemented with *Arabidopsis thaliana* IPCS Genes

AUR1 is the gene which encodes the IPCS in fungi which was first discovered in *S. cerevisiae*. It is a vital gene, in which mutation will be lethal (Heidler and Radding 1995). The AUR1 mutant strain which was used for this experiment was YPH499-HIS-GAL-AUR1 *S. cerevisiae* strain. This was constructed in YPH499 (*Mat a; ura3-52; lys2-801amber; ade2-101ochre; trp1-63; his3-200; leu2-1*) (Stratagene). The AUR1 promoter in the yeast genome was exchanged by a HIS/GAL cassette which allowed the expression of the AUR1 gene under a strict control of the GAL1 promoter. The GAL1 promoter is repressed in the presence of Glu (Denny *et al.* 2006). Therefore, YPH499-HIS-GAL-AUR1 was maintained in minimal medium lacking His with Gal and Raf (See methods) to allow expression of the AUR1 gene.

Only when the *A. thaliana* IPCS gene was successfully transformed, and expressed the same characteristic as AUR1, the YPH499-HIS-GAL-AUR1 was able to grow in Glu containing medium.

3.2.1.1 Transforming pRS426 MET plasmids into AUR1 Yeast Cells

AUR1 mutant yeast cells were grown in YPGR medium overnight and the culture were diluted to an OD₆₀₀ of 0.4 in 50ml fresh YPGR medium and were grown for an additional 2 hours. Cells were made competent and the transformation was carried out following the small-scale yeast transformation protocol from Invitrogen. Cells were plated onto SD-His-Ura medium containing Gal Raf and incubated at 30°C for a week.

Colonies formed on the plates were sub-cultured onto SD-His-Ura with Gal Raf and SD-His-Ura with Glc and incubated at 30°C for a week. Also a colony PCR was carried out and PCR products were separated by agarose gel electrophoresis to confirm the presence of IPCS inserts (Figure 11).

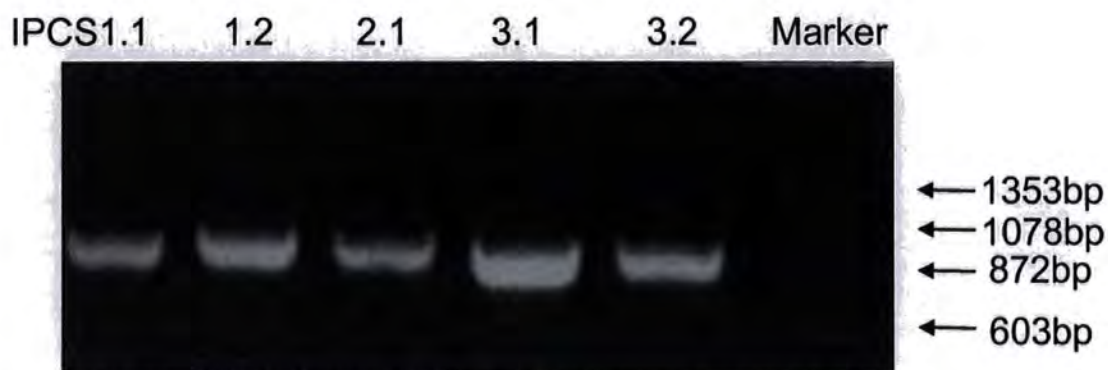


Figure 11 Results of Colony PCR of IPCS transformants to AUR1

Plasmids containing *At* IPCS genes were transformed into AUR1 mutant cells using the small-scale yeast transformation protocol from Invitrogen. Cells were plated onto SD-His-Ura with Glc and a colony PCR was carried out on the colonies that formed. From these results, all 3 IPCS genes have been transformed into AUR1 yeast cells. The expected band size is; IPCS1: 918bp, IPCS2: 918bp IPCS3: 870bp.

3.2.1.2 *In vitro* Complementation Assay / Functional Assay of IPCS Activity

Cells were grown in SD-His-Ura with Gal Raf for 3 days, their densities measured (OD₆₀₀) and adjusted where necessary to equivalent densities with 0.9% NaCl. Cultures were then spotted onto SD-His-Ura with Gal Raf plates and SD-His-Ura with Glc plates.

From these results, all AUR1 mutant yeast cells complemented by *At* IPCS grew on SD-His-Ura with Glc, which indicates that *At* IPCS complements the *Sc* AUR1 gene (Figure 13).

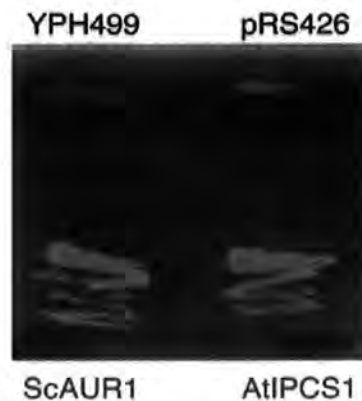


Figure 12 Functional Complementation of AUR1 Mutant Cells

Cells were grown on SD-His-Ura. YPH499, AUR1 mutant cells do not grow under the presence of Glc. *S. cerevisiae* and *A. thaliana* IPCS complement AUR1. Data from J. G. Mina Unpublished.

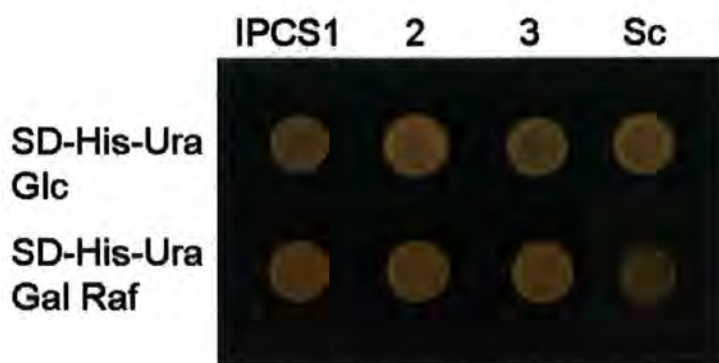


Figure 13 Functional Complementation of AUR1 Mutant Cells

At IPCS transformant cells were grown in SD-His-Ura with Gal Raf at 30 °C overnight. Density was adjusted and 10µl of sample was spotted on to SD-His-Ura with Glc and SD-His-Ura with Gal Raf.

From these results, it is concluded that *At* IPCS genes function as AUR1.

3.2.1.3 Biochemical Assay of Metabolic Labelling

Further biochemical tests were carried out to confirm the *in vitro* results of the AUR1. Metabolic labelling was carried out to confirm the complementation of *A. thaliana* IPCS genes in AUR1 mutant cells.

AUR1 mutant cells were grown in SD-His-Ura with Gal Raf, mutant cells complemented with *S. cerevisiae* IPCS and *A. thaliana* IPCS genes were grown in SD-His-Ura with Glc. For negative control, mutant cells were grown in SD-His-Ura with Glc. From this experiment, mutant cells grown in SD-His-Ura with Gal Raf, and mutant cells complemented with *S. cerevisiae* IPCS were expected to show a band with the same mobility as IPC. As Glu represses the GAL promoter, mutant cells grown in SD-His-Ura with Glc were expected to show no IPC product. From previous experiments by J. G. Mina Unpublished and *in vitro* complementation assay, mutant cells complemented with *A. thaliana* IPCS genes were expected to show a band with the same mobility as IPC. Lipids were separated by TLC chloroform/ methanol/ 0.25% KCl: 55: 45: 10 (v/v/v) (Figure 14). The *R_f* values for the excess NBD-C₆-ceramide and NBD-C₆-IPC were taken from J. G. Mina Unpublished, and were 0.96, 0.57 respectively.

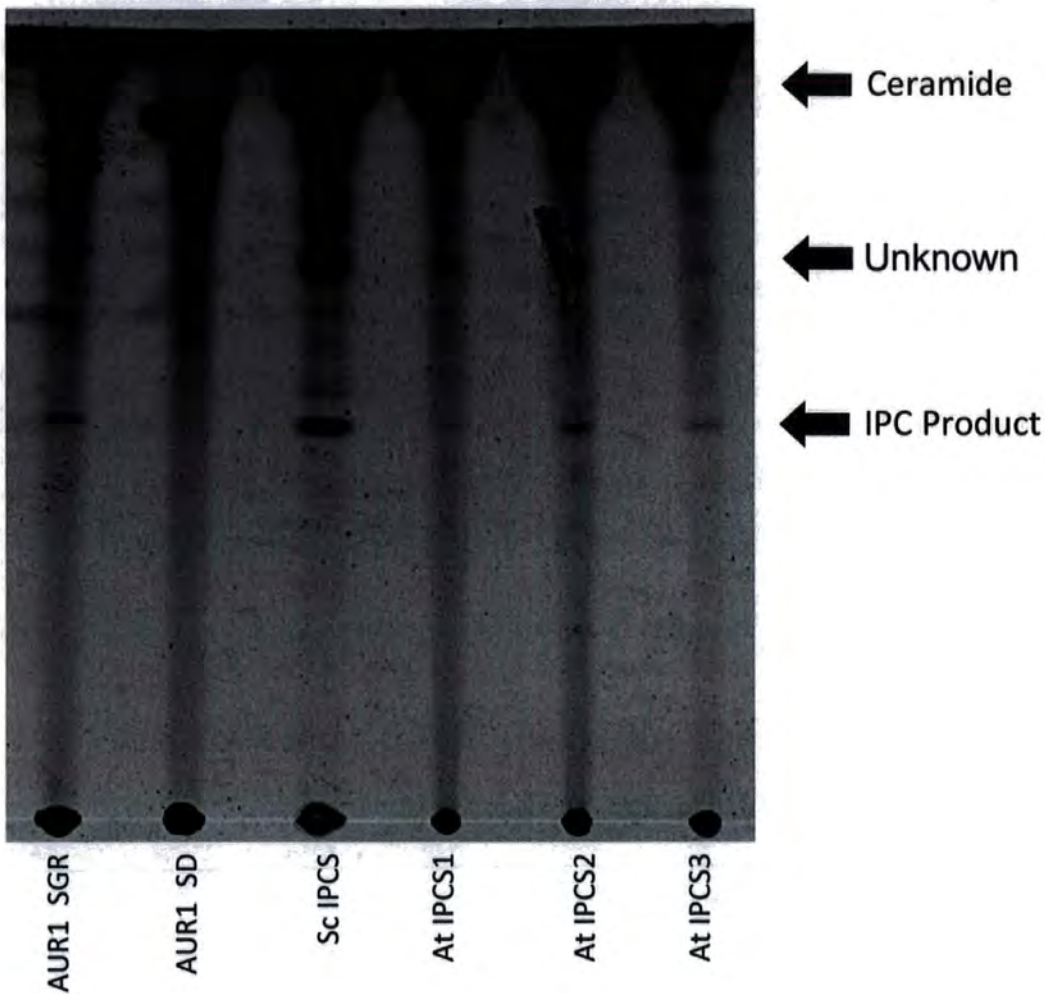


Figure 14 *At* IPCS genes complement AUR1

The fluorescent image of TLC separation is shown. All AUR1 cells were grown in SD-His-Ura with Glc media expect for the positive control which was grown in SD-His-Ura with Gal Raf. Cells were labelled with NBD-C₆-ceramide and lipids were extracted with 10:10:3 C: M: W and separated by TLC (chloroform/ methanol/ 0.25% KCl: 55: 45: 10). In the positive control lane (AUR1 SGR), IPC product is observed. In the negative control (SUR1 SD), no IPC product is found. ScIPCS has a high IPC product, AtIPCS1 is faint but can observe IPC product, At IPCS2 produces as much IPC as the positive control and IPC product is found in AtIPCS3 as well.

The positive control; *S. cerevisiae* AUR1 grown in SD-His-Ura with Gal Raf, and AUR1 complemented with *S. cerevisiae* AUR1 grown in SD-His-Ura with Glc, gives a *Rf* value of which represents the IPC product and these were used as the positive control. AUR1 complemented with *S. cerevisiae* gives a stronger band. When the AUR1 mutant was grown in SD-His-Ura with Glc no band of IPC product was produced and this is the negative control, AUR1. Complementation of the mutant with *A. thaliana* IPCS gives an *Rf* value of the same mobility as IPC which indicates that the *A. thaliana* cDNA encodes an IPCS activity. Among three IPCS genes, IPCS2 appears to have the strongest band then IPCS3 and then IPCS1.

3.2.1.4 Sensitivity of *At* IPCS to Aureobasidin A

An agar diffusion assay was carried out to test the sensitivity of *Arabidopsis* IPCS to a known inhibitor of the fungal enzyme; AbA. The *S. cerevisiae* IPCS and *A. thaliana* IPCS complemented AUR1 mutant yeast were imbedded into SD-His-Ura with Glc medium and volumes of 1, 2, and 3 μ l of 25 μ M AbA, 1mM MYR, and a control of DMSO were spotted onto the surface of the plates. The plates were incubated for 3 to 4 days at 30°C and inhibition was determined by lack of growth at the site of application of inhibitor.

From Figure 15, *S. cerevisiae* IPCS complemented AUR1 mutant yeast cells were sensitive to AbA, and MYR, but not DMSO. *A. thaliana* IPCS1, 2 and 3 complemented AUR1 mutant yeast cells were resistant to AbA but sensitive to MYR. MYR is known to inhibit SPT and this characteristic has not changed in *At* IPCS complemented cells. Although AbA is known to inhibit IPCS, *At* IPCS complemented cells are resistant to AbA.

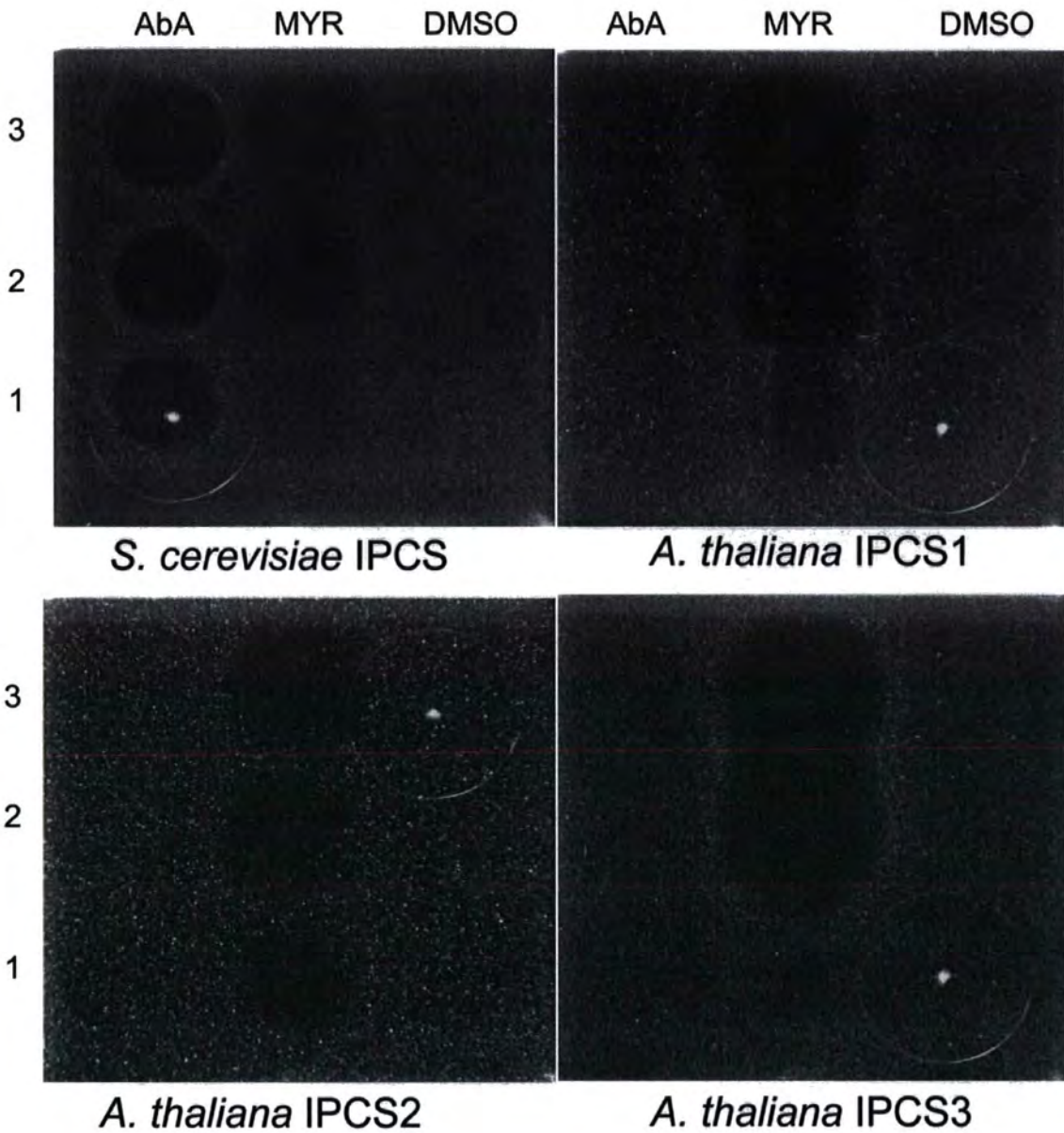


Figure 15 *At* IPCS is resistant to AbA

YPH499-HIS-GAL-AURI complemented with pRS426 *Sc* IPCS, *At* IPCS1, 2 and 3. *At* IPCS is specifically resistant to the fungal inhibitor AbA. Volumes of 1, 2, and 3 μ l of 25 μ M AbA, 1mM MYR and DMSO (control) spotted onto each yeast plates.

3.2.2 Testing Phospholipase Activity in *Arabidopsis thaliana* IPCS Genes

ISC1 (YER019w) is a gene which has been identified to encode inositol phosphosphingolipid phospholipase C (IPS-PLC) in *S. cerevisiae* (Sawai *et al.* 2000a). Cells deleted in ISC1 have demonstrated negligible neutral SMase activity (Sawai *et al.* 2000a). Though SM does not exist in *S. cerevisiae*, the existence of N-SMase has been reported (Ella K 1997).

This raised the possibility that N-SMase activity may be an *in vitro* activity of yeast IPS phospholipase C (IPS-PLC) (Sawai *et al.* 2000a).

Studies from Hirofumi Sawai *et al.*, show that overexpression of ISC1 in *S. cerevisiae* dramatically increased PLC activities on IPS. And the deletion of ISC1 completely eliminated all IPS-PLC activities Sawai *et al.* 2000a.

Therefore by complementing *At* IPCS genes into ISC1 cells, it is possible to test whether *At* IPCS contain an IPC-PLC activity.

3.2.2.1 Transforming pRS426 MET plasmids into ISC1 Yeast Cells

A transformation was carried out using wild type (JS91) yeast cells and ISC1 (DZY1) yeast cells using empty pRS426 plasmid and *A. thaliana* IPCS 1-3 recombinant pRS426 plasmids. Transformed cells with empty plasmids in wild type was called J426 and in mutant cells were called D426, transformed cells with IPCS genes in mutant cells were called D1, D2 and D3.

3.2.2.2 *In vivo* Complementation of ISC1 - Salt Tolerance Test

In *S. cerevisiae*, toxic concentrations of Na⁺ or Li⁺ ions induce the expression of the cation-extrusion ATPase gene, *ENA1* (Haro *et al.* 1991). *ISC1* is involved in stimulation of *ENA1* expression and, consequently, in mediating Na⁺ and Li⁺ tolerance in yeast (Betz *et al.* 2002). Deletion of *ISC1* decreased cellular Na⁺ and Li⁺ tolerance and growth was severely impaired (Betz *et al.* 2002). Therefore, if *At* IPCS functioned as IPC-PLC, *ISC1*, the mutant cells (DZY1) will recover its tolerance to salt and should grow to the same density as wild type. Therefore, ISC1 mutant cells complemented with *At* IPCS genes were grown on various concentrations of NaCl and LiCl to test the sensitivity.

Wild type and mutant cells were grown in YPD media and cells with plasmid were grown in SD-Ura media overnight. Their densities were measured (OD₆₀₀) and adjusted where

necessary to equivalent densities with 0.9% NaCl. Cultures were then spotted onto SD-His, various YPD (Figure 16) and SD-Met plates (Figure 17) incubated at 30°C overnight.

On SD-His plates, wild type (J) and wild type with an empty plasmid (J426) did not grow but mutant cells (D) and mutant cells with an empty plasmid (D426) grew. This is because the ISC1 gene is knocked out by a His cassette and therefore can produce His on its own without it being added to the media. Mutant cells with *A. thaliana* IPCS 1-3 genes (D1-D3) also grew on SD-His plates due to the His cassette.

On YPD plates containing various concentrations of salts, J grew to a high density except on high salt plates, 0.8M NaCl and 0.25M LiCl. J426 grew to the same density as J, D and D426 cells which would confirm there was no effect of pRS426 on growth. Both cell types were sensitive to salt as the growth on all NaCl and LiCl plates were low. J grows on 0.4M and 0.5M NaCl and 0.01M LiCl, but D does not. Therefore this is the minimum complementation that would be expected if the *At* IPCS functions as ISC1. For all *At* IPCS transformants, D1, D2 and D3, are sensitive to salt as D cells. From Betz *et al.* 2002, *isc1*Δ cells are sensitive to salt. If *At* IPCS functioned as ISC1, cells would have grown as wild type, tolerant to salt. As the transformed cells were sensitive to salt, it would suggest that *At* IPCS does not have the function of ISC1.

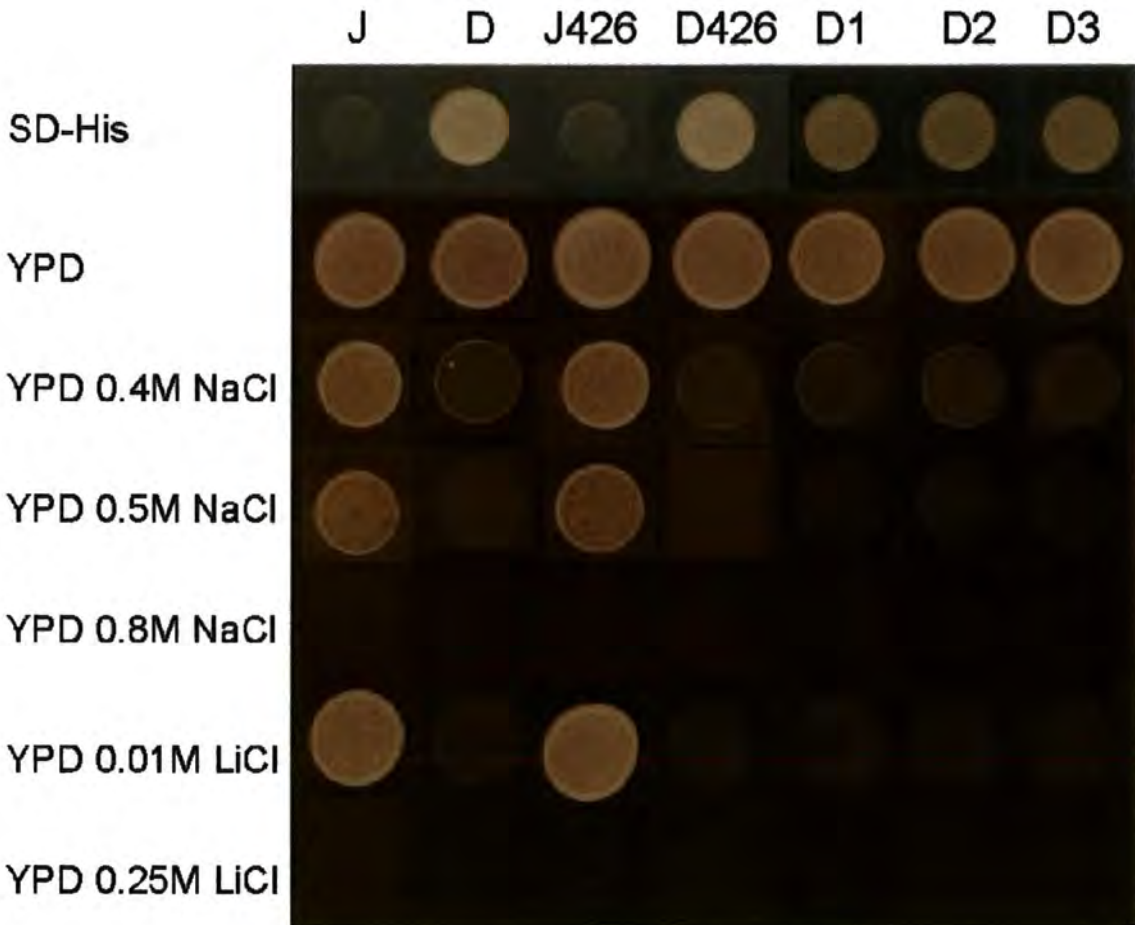


Figure 16 *In vivo* Complementation Assay of ISC1 on YPD Media

J and D were grown in YPD, all other samples were grown in SD-Ura overnight. Sample's density were adjusted and spotted on to various YPD plates.

From various YPD plates, the plasmid has no effect on the growth, and mutant cells are sensitive to salt which support previous results (Betz *et al.* 2002). If *At* IPCS functioned as ISC1, the reverse reaction of IPCS, the *At* IPCS transformed cells would be salt tolerant. As these results show the transformed cells are salt sensitive, suggesting that *At* IPCS does not act as ISC1. Experiment was repeated three times.

As plasmid pRS426 MET is known to be suppressed by the existence of Met (Schwank *et al.* 1997), plates with SD-Met containing various salt concentrations were prepared and yeast cells were spotted as YPD plates.

This was conducted to eliminate the possibility of the transformed cells being sensitive to salt due to the promoter being suppressed by Met and not allowing *At* IPCS genes to be expressed. As all cells grew to a similar density on YPD, it would be expected that Met will not have a massive effect on suppressing the promoter of pRS426.

As cells were grown on minimal media, the density was not as high of that of YPD. J and J426 show growth in the presence of 0.4M, 0.5M and 0.8M NaCl and 0.01M LiCl, but D and D426 do not. There is no difference in the growth of D and D1, D2, D3 which confirm the results on YPD plates that *At* IPCS does not have the function of ISC1.

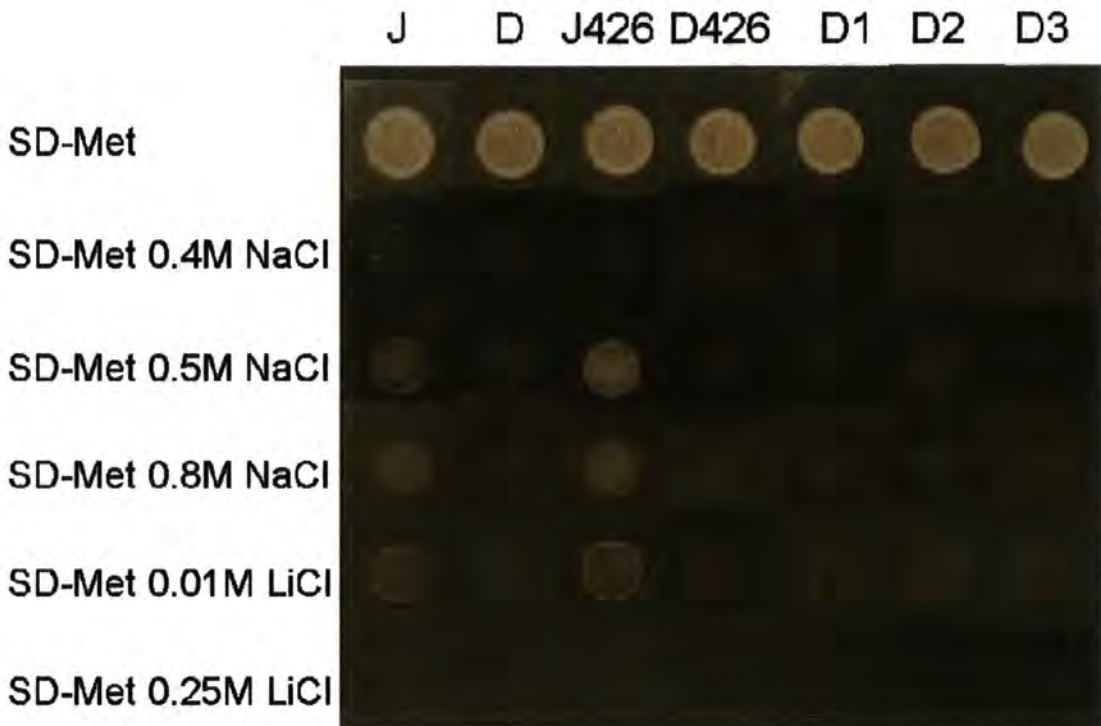


Figure 17 *In vivo* Complementation Assay of ISC1

J and D were grown in YPD, all other samples were grown in SD-Ura overnight. Sample's density were adjusted and spotted onto various SD-Met plates. This was to confirm the effect of Met on pRS426 as it is known to suppress the promoter.

Comparing the growth of cells with plasmid and without, there is no difference in the density. This would suggest that Met had no major effect on pRS426 and the *At* IPCS genes were expressed, and the various YPD media results are reliable.

As results from YPD media, IPCS complemented mutant cells are sensitive to salt, which would suggest that *At* IPCS does not function as ISC1. Experiment was repeated three times.

3.2.2.3 Biochemical Assay of IPC-PLC Activity by Metabolic Labelling

Further biochemical tests were carried out to confirm the *in vivo* complementation results of ISC1. Metabolic labelling was carried out to confirm the non complementation of *A. thaliana* IPCS genes in ISC1 mutant cells by testing an increase in N-SMase activity in *At* IPCS containing ISC1 mutant cells.

All cells J426, D426, D1, D2 and D3 were grown in SD-Ura. 2×10^7 cells were labelled with $2.5\mu\text{M}$ NBD- C_6 -SM and incubated for 1 hour. Following lipid extraction, equal amounts of fluorescence were spotted and lipids were separated by TLC with a solvent of chloroform/methanol/ 15mM CaCl_2 60:35:8 (v/v/v) (Figure 18).

The positive control, J426 gives an *Rf* value of which represents ceramide (0.93). The negative control D426, gives no band of ceramide, and the complementation of mutant with *A. thaliana* IPCS does not give a band size of ceramide.

From these results, ceramide was detected only in wild type (J426). All mutant types, D426, D1, D2 and D3, did not give a *Rf* value of ceramide. This would support the salt tolerance test that *At* IPCS does not function as ISC1. The *Rf* value calculated was, ceramide 0.92 and NBD- C_6 -SM 0.37.

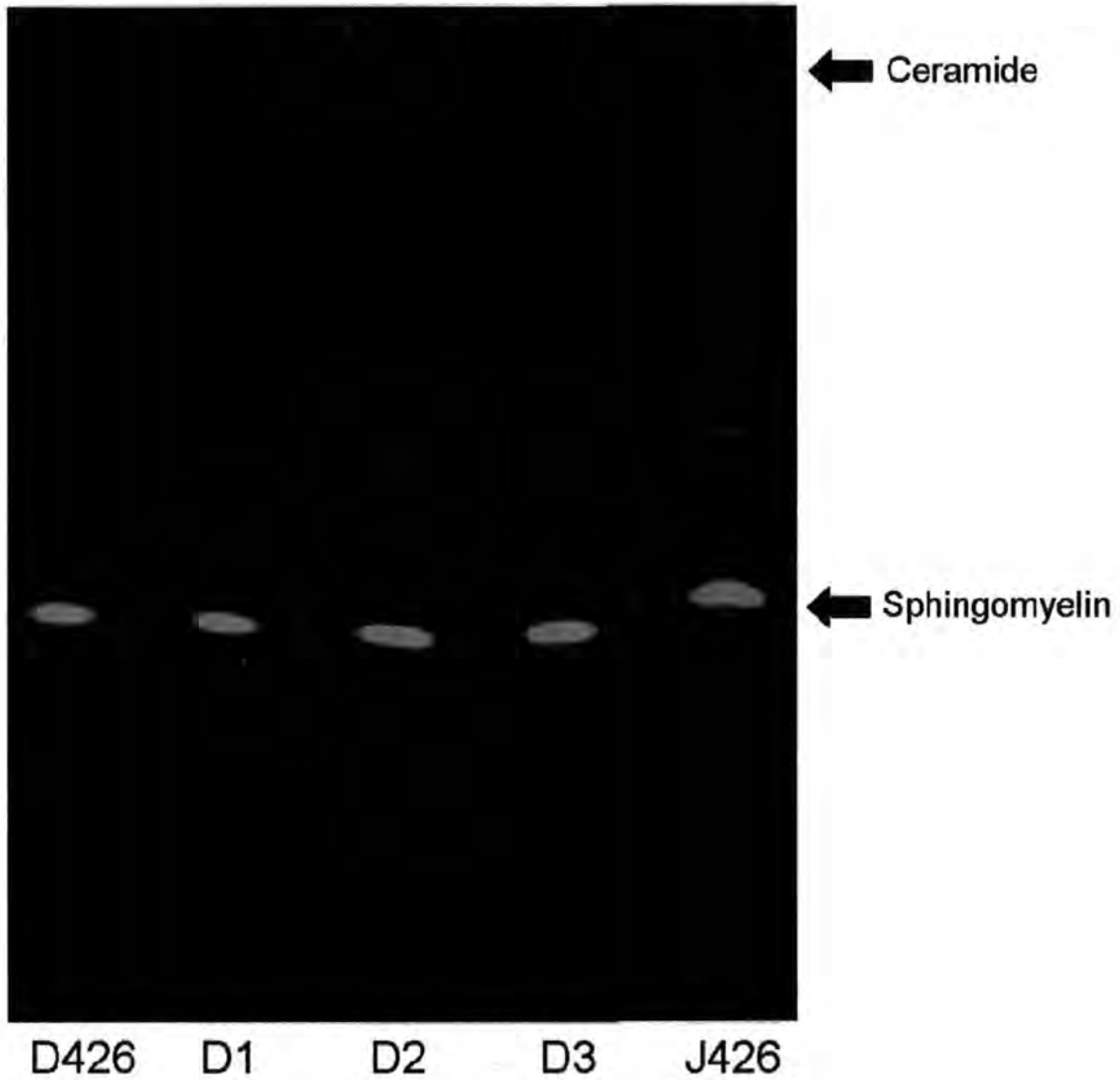


Figure 18 TLC of ISC1 complemented by *At* IPCS genes - Metabolic labelling

The ISC1 mutant DZY containing *At* IPCS 1, 2, and 3 were metabolic labelled with NBD- C_6 -SM. All cells were grown in SD-Ura. 2×10^7 cells were labelled with $2.5 \mu\text{M}$ NBD- C_6 -SM for 1 hour. Lipids were extracted with C/M/W and separated by TLC (chloroform/ methanol/ 15mM CaCl_2 : 60: 35: 8). The R_f values for ceramide and NBD- C_6 -SM were 0.92 and 0.37 respectively

4. Results - Expression of IPCS Genes in *Arabidopsis thaliana*

The expression level of these *A. thaliana* IPCS genes have never been quantified before. Only one gene type, At2g37940 (IPCS2), can be found at genevestigator (<https://www.genevestigator.ethz.ch/>) for microarray data. The signal intensity values have arbitrary units that are scaled to the total abundance of transcripts within a sample. The mean signal value is set as 1000, and the background range is 0-100. From this data, IPCS2 was found to be expressed highly in senescent leaf of approximately 4,200. Expression of cauline leaf, rosette leaf and roots was approximately 2,400, and stem, flower, and siliques were approximately 1,000. Also from genevestigator data, mutation in fls2-17 resulted in a four times lower expression of IPCS2. This value is also calculated when the mean signal value is set as 1,000. FLS2 is a flagellin receptor gene and fls2-17 is a flagellin-insensitive mutant. A mutation in cpr5:scv1 (cpr5, constitutive expressers of pathogenesis-related gene, encodes a novel transmembrane protein which is involved in cell proliferation and cell death control and scv1 is *S. cerevisiae* virus 1) increased the expression three times. Treatment with anoxia(+), UV filtered WG327 and heat decreased the expression twice. Whereas chitin (+) and ozone increased the expression three times, and cycloheximide (+) and syringolin (+) increased the expression four times. Other various chemicals and stress do not have a severe impact on the expression of IPCS but, a few do and by identifying the effect of these stimulants, can lead to further understanding of these genes.

To understand the expression of all three IPCS genes in various plant tissues, a Q-PCR was carried out with various *A. thaliana* plant material.

To be able to compare the expression of gene in each material, standard curves were created. Also each primer sets were optimised to its highest efficiency to compare the expression level of different genes within the sample.

4.1 Gene Specific Primers for Real Time PCR

For real time PCR, primer sets which amplify approximately 150 bp were designed. These primers were designed to amplify each specific gene to allow gene-specific characterisation of transcripts.

As the figure below shows (Figure 19), there is a high homology between these three genes, therefore primer sets were carefully designed so that the targeted gene would be specifically amplified.


```

At3g54020      AAACATTACACTGTTGATGTGGTTGTTGCGTGGTATACTGTGAACCTGGTTGCTTCTTC 720
At2g37940      AAACATTACAGTGTTCGATGTAGTTGTTGCATGGTATACTGTGAATTTGGTGGTGTCTGT 717
At2g29525.1    AAACATTACACAGTTGACATGTTGTTGCATGGTATACTGTGAACCTGTAATGTTCTAC 720
                ***** ** * * ***** ***** * * * * *
At3g54020      CTCGACAAGAAATTACCAGAATTGCCTGATCGACAAACGGCATTGCTCCCTGTGATCTCA 780
At2g37940      CTAGACAAGAAATTACCAGAATTACCAGATCGGACTGCTGTGTTGCTCCAGTAATCTCA 777
At2g29525.1    GTTGACAGTAAACTGCTGCAATGCTCAAGGCTGAGTGGACCTTCTCCTACGCCTTTA 780
                * **** * * * * * * * * * * *
At3g54020      AAAGACAGAACCAAAGAAGAGAGTCAAAACTCTTGAATGGGAACGGTGTGATCCTGCA 840
At2g37940      AAAGACAGAACCAAAGAAGAGAACCACAAGCTGTTGAATGGAAACGGTGTGACCCTGCT 837
At2g29525.1    CTTCCACTGAGCACAAAGGACAGTAAGAACAAGAGCAAAGAAGATCATCAGAGACTTCTA 840

At3g54020      GATCGGAGACCGAGGGCTCAAGTGAATGGCAA--GACAGCAATGGAGGTCACACTGAT 897
At2g37940      GATTGGAGACCGAGGGCTCAGGTGAACGGGAAGATTGACAGCAACGGAGTTCACACGGAT 897
At2g29525.1    AAC--GAGAACAATGTAGCAGATGATCATTGA----- 870

At3g54020      AATGCTACTAATGGCACATGA 918
At2g37940      AACACAATGAATGGCGCGTGA 918
At2g29525.1    -----

```

Figure 19 Alignment of IPCS Genes and Designed Primer Pairs

Alignment was carried out using Clustal W, and primer sets were designed to amplify the specific gene, approximately 20bp, with no four identical bases and preferably with a G or C at the end to strength the binding. Expected product size was, IPCS1 135bp, IPCS2 135bp and IPCS3 141bp.

Table 6 Gene Specific Primer Pairs

IPCS 1	Forward: AGCCTCTTGATTATTGCGTC Reverse: AACAAACGGCATTGCTCCCT
IPCS 2	Forward: AGCCTCTTGATCATTGCCTC Reverse: GACTGCTGTGTTGCTCCCA
IPCS 3	Forward: TGGCTTATGGCAGTAATACAG Reverse: GCCAGAAATGGCAGAACGTTCT

4.2 Optimising Primers for 150bp IPCS Amplicons

A PCR using the standard method was carried out to confirm the specificity of these primer sets.

The annealing temperature was calculated using $\{2(A+T) + 4(G+C)\}-5$.

From this formula, an annealing temperature of 56 °C was selected, which would cover all three primer sets. PCR products were electrophoresed on a 1.5% agarose gel to separate the bands as the amplicon size was small (Figure 20). 1.5% agarose gel was sufficient to resolve these bands as the minimum difference in PCR product size is 100 – 200bp (www.gel-electrophoresis.com/gels/articles/agarose-gel-electrophoresis/).

Only a faint band and some non-specific bands were found. These non-specific bands were confirmed as genomic DNA contamination as calculating the base pairs of gDNA gave the band size of the product. The band size of gDNA is IPCS1: 208bp, IPCS2: 331bp and IPCS3: 228bp. For cDNA the expected band size was IPCS1: 145bp, IPCS2: 145bp and IPCS3: 141bp.

Following this conclusion, a DNase treatment was carried out on the RNA according to methods and another RT-reaction followed by PCR was carried out to compare the results.

The RT-PCR using both DNase treated RNA, and a non treated RNA was carried out using 3 mM of MgCl₂ at 52°C (Figure 21). Temperature was lowered as the bands were faint at 56°C.

From this result, it was clear that the RNA preparation was contaminated with gDNA, and for subsequent procedures, an on-column DNase digest was carried out to remove gDNA contamination.

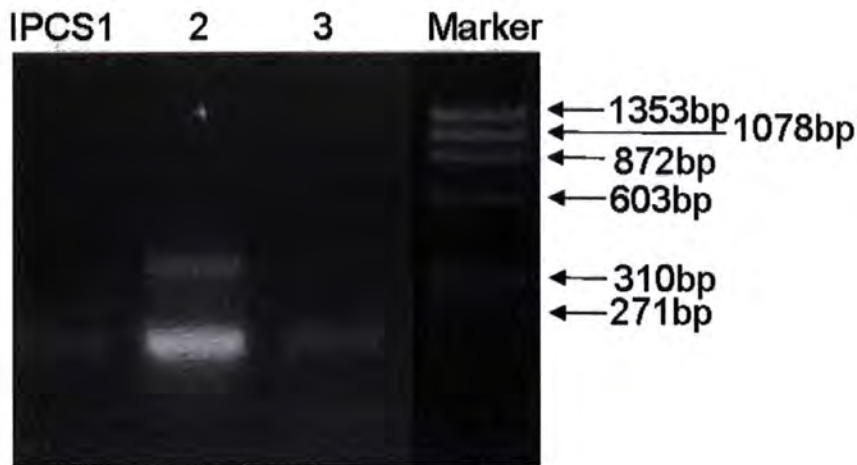


Figure 20 PCR Product of IPCS Amplicons from *A. thaliana* cDNA

PCR with 1.5mM MgCl₂ and an annealing temperature at 56 °C was carried out to amplify IPCS amplicons for Real Time PCR. cDNA was used from *A. thaliana* total RNA as template. Bands are faint and contamination of genomic DNA was observed.

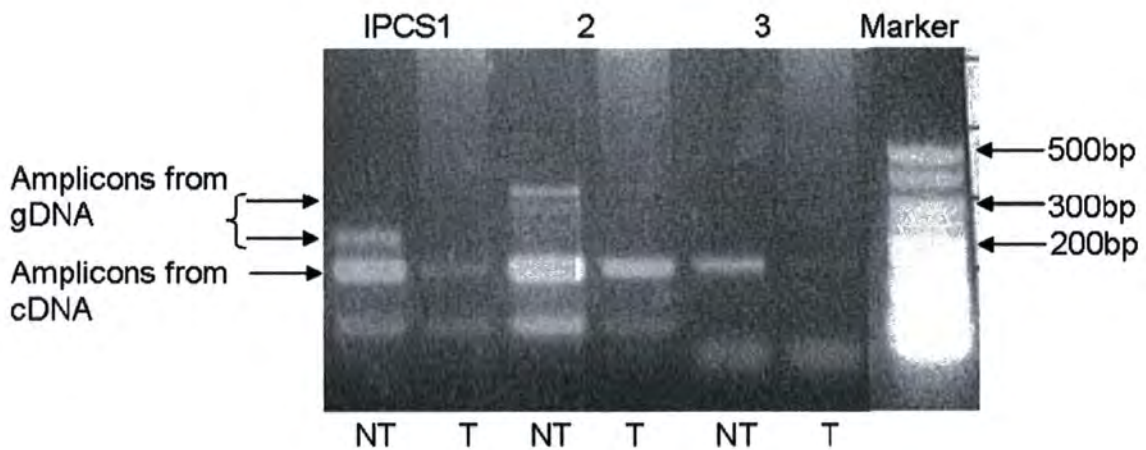


Figure 21 PCR Results of IPCS Amplicons - RNA with and without DNase Treatment

PCR products of IPCS amplicons with RNA being treated with DNase and without. NT: not treated, T: treated. From these results, the larger bands were confirmed as gDNA. The expected band size of gDNA was; IPCS1: 208bp, IPCS2: 331bp and IPCS3: 228bp. Annealing temperature of PCR was 52°C and 3mM of MgCl₂.

Further to obtain a stronger band, a robocycler was carried out to optimise the temperature and MgCl₂ concentrations for each primer pair. The optimal temperature and MgCl₂ concentration for each primer sets were determined as below Table 7.

Table 7 Optimised Primer Set Conditions

	Temperature(°C)	MgCl ₂ (mM)
IPCS1 150bp Primer Sets	52	3
IPCS2 150bp Primer Sets	52	3
IPCS3 150bp Primer Sets	52	4

No bands were observed with single primer controls or no target controls.

4.3 Confirming specificity of 150bp Primers

To confirm these primer pairs specifically amplified the specific IPCS gene, a PCR was carried out using the three cloned full length IPCS cDNAs as templates with all three primer pairs. The results confirmed that these primers are gene specific (Figure 22). The expected band size of the PCR products were IPCS1: 145bp, IPCS2: 145bp and IPCS3: 141bp.

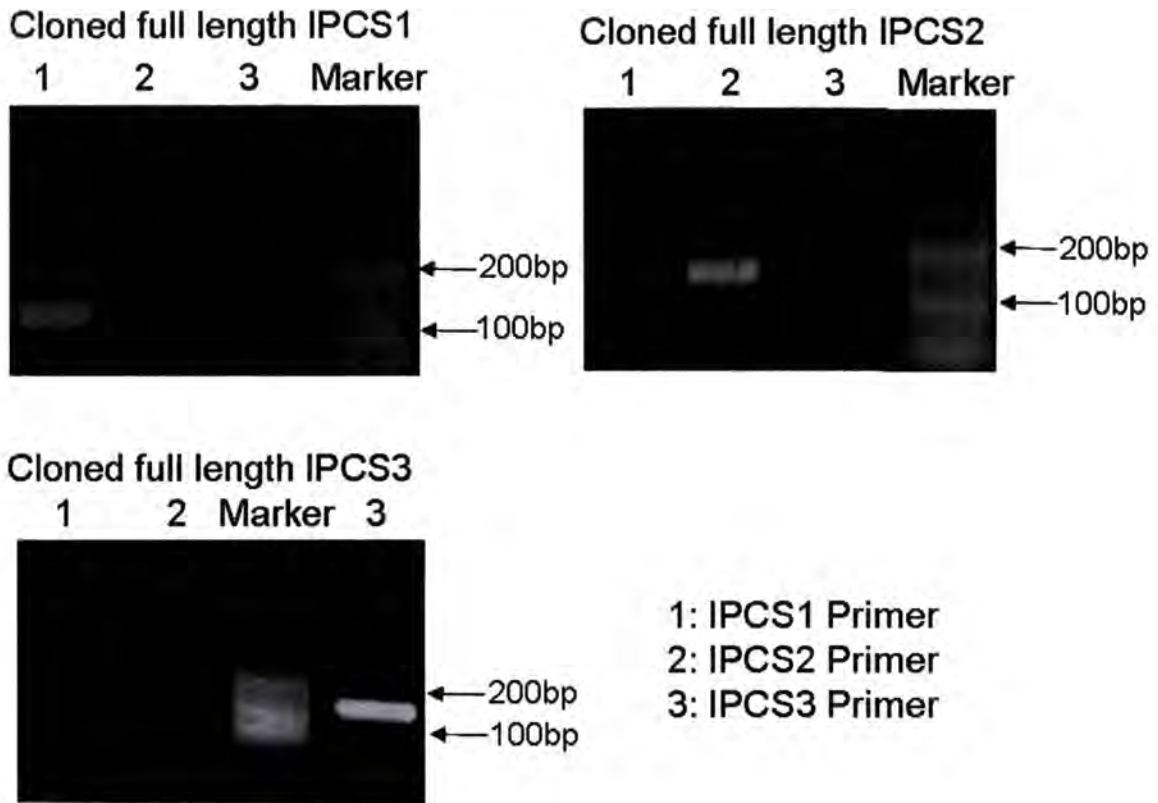


Figure 22 Confirming Specificity of IPCS Primer Sets

A PCR was set up with previously cloned IPCS genes to confirm the specificity of IPCS 150bp primer sets. The PCR programme was run at the optimised conditions (see table). From these results, it was confirmed that IPCS primers only amplify the targeted genes. Expected band size of the PCR was IPCS1: 145bp, IPCS2: 145bp and IPCS3: 141bp.

4.4 Expression of IPCS genes in Arabidopsis tissues (QPCR)

After optimizing the primer pairs for the targeted gene, Q-PCR was conducted to quantify the expression of each gene in various plant tissues.

4.5 Preparing Samples

Samples of plant tissues from root, rosette leaf, cauline leaf, stem, flower, seed siliques and senescing leaf were collected at each development stage. These target points were determined using (Boyes *et al.* 2001). Rosette leaves were collected at stage 3.90, cauline leaves and stem were collected at stage 5.10, roots and flowers were collected at stage 6.50, siliques were collected at stage 8.00, and senescing leaves were collected when a quarter of the leaf was starting to senesce. From these samples, RNA was isolated according to manufacturer protocol (QIAGEN). As it was demonstrated that gDNA would be carried over, an on-column DNase step was included into the RNA extraction procedure.

The quality and quantity of RNA are described in Table 8. The A260/280 shows the purity of the RNA and when between 1.7 and 2.0 it is considered good RNA. A260/230 shows polysaccharide contamination and between 2.0 and 2.3 indicates good RNA (Agilent Fluorescent Direct Label Kit Protocol). From this, it was considered the quality of RNA was sufficient enough to carry out subsequent experiments.

Table 8 Extracted RNA Samples

Sample	ng/μl	$\frac{260}{230}$	$\frac{260}{280}$
Roots	230	2.34	2.13
Rosette Leaves	203	2.36	2.14
Cauline Leaves	502	2.35	2.08
Stem	907	2.44	2.14
Flower Buds	711	2.35	2.14
Siliques	169	1.84	2.08
Senescing Leaf	311	2.17	1.66

The RNA yield of senescing leaf was extremely low. Several RNA extractions were carried out and RNA was precipitated using LiCl. Sample was re-suspended in 10 μ l of MQ

and the quantity shown in Table 8 is after precipitation. Using 2 μ g of total RNA, a RT-Reaction was carried out and cDNA were prepared.

4.6 RT-PCR

To quantify the expression of each RNA in the tissue, real-time PCR was carried out.

4.7 Primer Optimization

Prior to this, the primer concentrations were optimised to the optimum sensitivity for each primer template concentration. This is due to the fact that primers have different binding efficiency depending on their sequence. As optimization of real-time PCR is crucial for reliable and reproducible results, it is important to optimise primer and sample concentrations as well as temperatures and times (Chini *et al.* 2007).

It is known that by changing a single nucleotide in the primer can change the C_T value (Werbrouck *et al.* 2007). For end-point PCR, primer optimization is not a crucial step, but for real-time PCR, it can have a big effect on the C_T value. If each primer was not optimised to its most sensitive concentration, the amplification efficiency would be variable and therefore the results between different genes will not be comparable.

Various primer concentrations were prepared as described in methods, and a RT-PCR was carried out to find the optimal primer concentrations using each cloned plasmid DNA as the template.

From these results, it was confirmed that the highest primer concentration combinations (6 μ M of forward and reverse primer) gave the lowest C_T values (Figure 23). Therefore, subsequently higher primer concentrations were carried out (Figure 24).

Results of the C_T value and the efficiency suggested that for IPCS1, 10 μ M of forward and 10 μ M of reverse primer, for IPCS2, 8 μ M of forward and 8 μ M of reverse and for IPCS3, 8 μ M of forward and 10 μ M of reverse primers were the optimal primer concentrations.

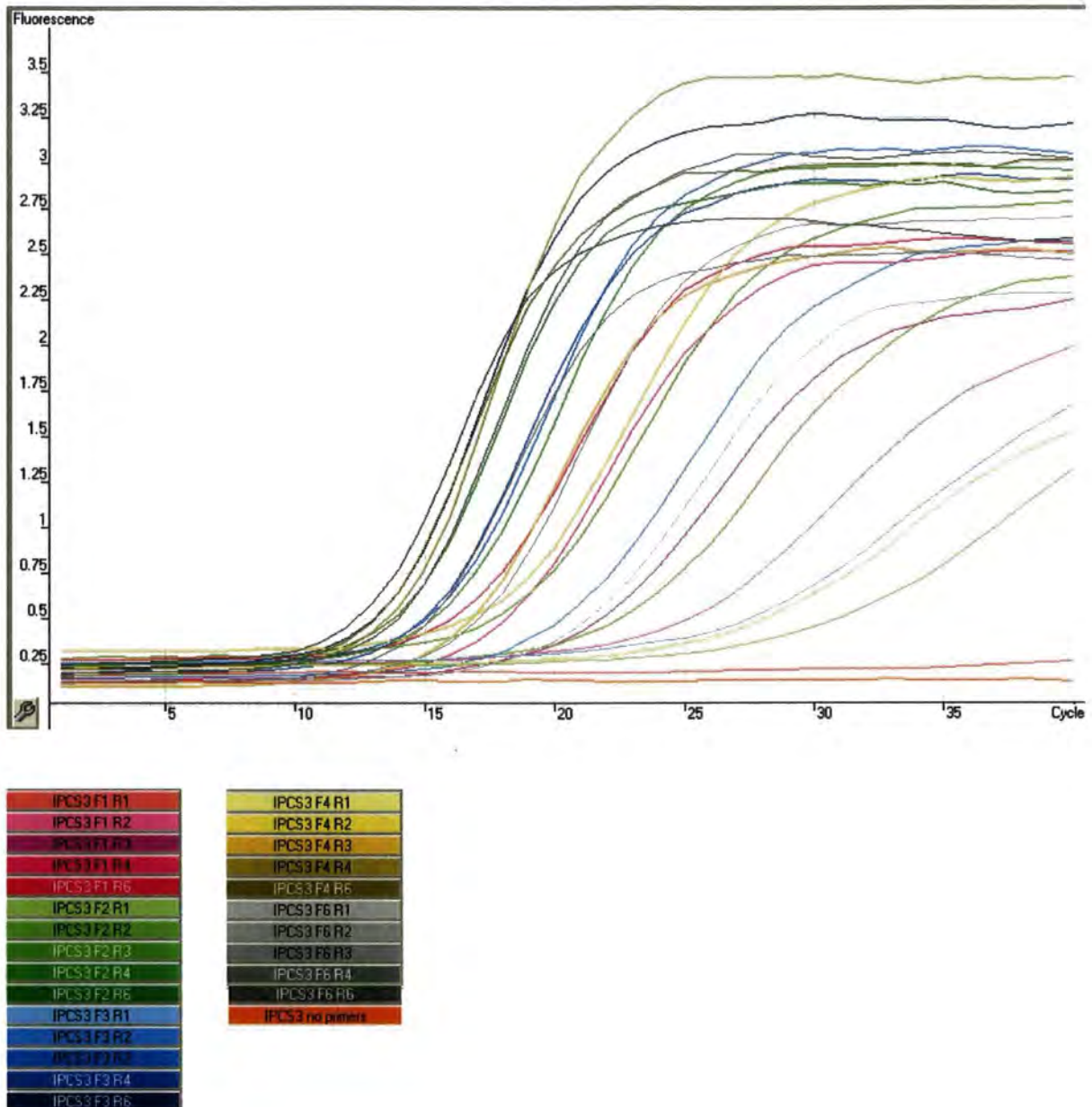


Figure 23 Primer Optimization

Real time PCR was carried out to optimise primers. Depending on primer concentrations, the take off value varies. The lower the primer concentration, the later the take off value is. Also in lower forward primer concentration, the take off value is earlier when reverse primer concentrations are higher. This indicates that depending on both forward and reverse primer concentrations, the efficiency of the PCR will change. From these results, 6 μ M of forward and reverse primer gave the lowest C_T value. Therefore, higher primer concentrations may give lower C_T values.

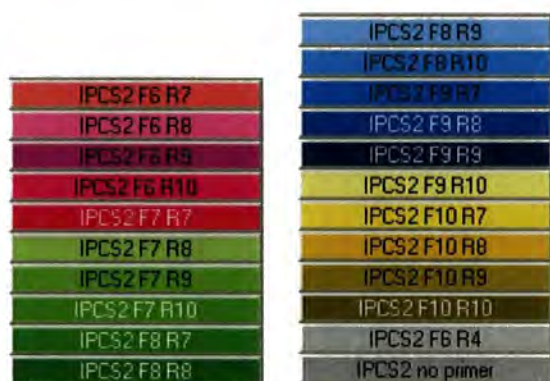
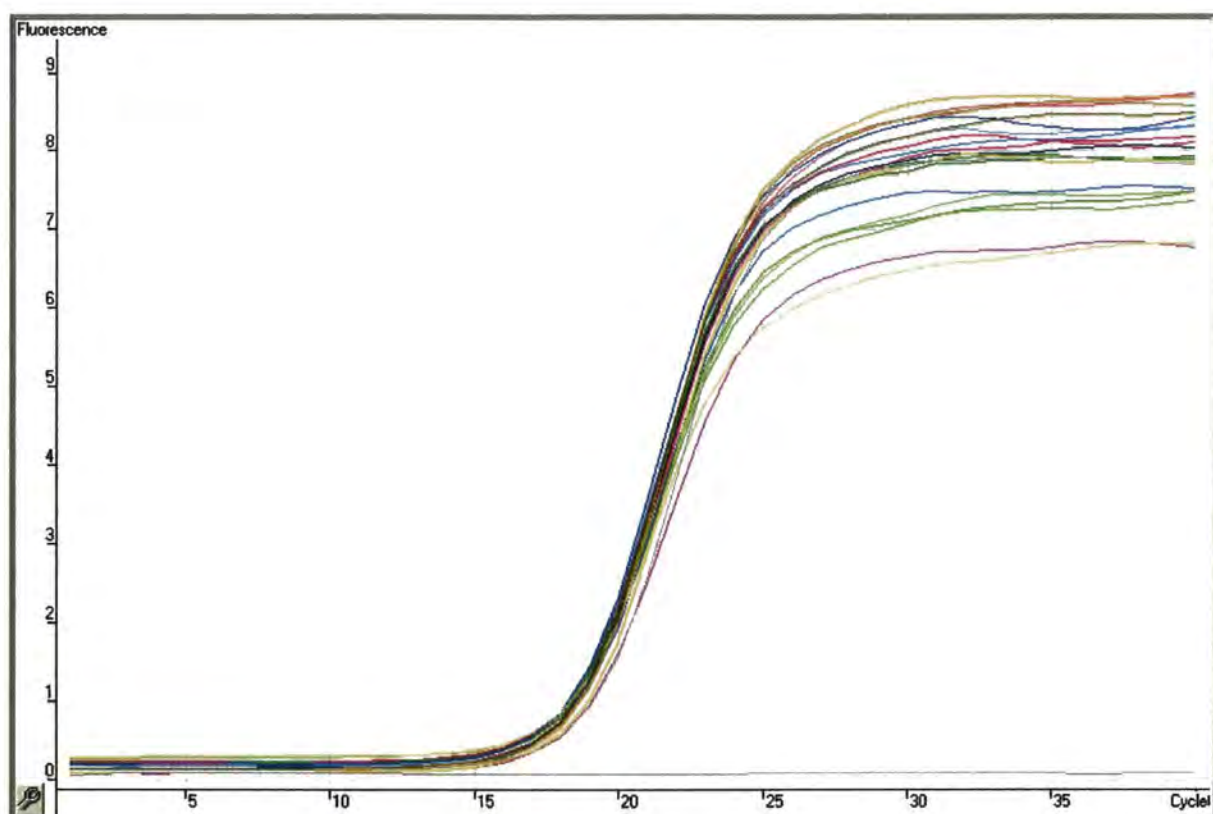


Figure 24 Further Primer Optimization

Further primer optimization was carried out to find optimal concentrations. From these results, when primer concentrations are over a certain point, it does not change the efficiency of the amplification. From this, it was concluded that for IPCS1, 10 μ M of forward and 10 μ M of reverse primer, for IPCS2, 8 μ M of forward and 8 μ M of reverse, and for IPCS3, 8 μ M of forward and 10 μ M of reverse primers are the optimal primer concentrations.

4.8 Creating Standard Curve

After the optimal primer concentrations were determined, a standard curve was created for each IPCS gene.

A serial dilution of each gene specific plasmid DNA were prepared from 10^{-2} to 10^{-9} . As the amount of each RNA added to the reaction is known, by making a serial dilution, a standard curve can be created. Once a standard curve is created, by comparing the fluorescence produced, the amount of sample can be determined.

A result of the IPCS3 standard curve is shown in Figure 25.

The values of each standard curve are shown below (Table 9).

Table 9 Values of Standard Curve

	IPCS1	IPCS2	IPCS3
R	0.99	0.99	0.99
R ²	0.99	0.99	0.99
M	-3.12	-2.79	-3.19
Efficiency	1.09	1.28	1.06

The optimal value for M and R² are -3.322 and 0.99 respectively. This is the slope of the formula which represents the efficiency of the amplification. When the M value is higher than -3.322, primers and probe concentrations, MgCl₂ or SYBR-Green I concentrations should be optimized. When the M value is lower than -3.322, it suggests that there is a disproportionate digestion of probe compared to the amplicon produced (Operator Manual Rotor-GeneTM 3000 Real Time Thermal Cycler). Although for IPCS2, the M value is low, as the R value is close to optimal, the standard curve was used to quantify the samples.

These standard curves were imported into the sample run to quantify each gene expressed in samples.

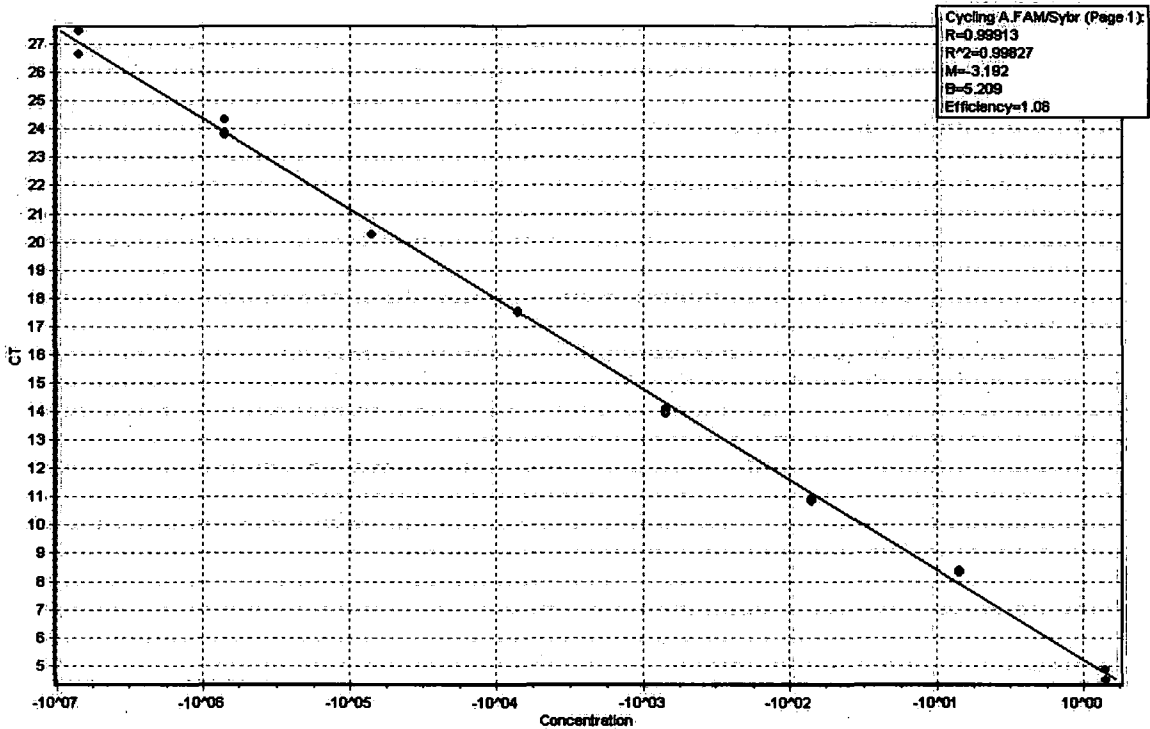


Figure 25 Standard Curve

A standard curve was created by a serial dilution of gene specific plasmid DNA. As the amount of DNA in the plasmid is known, the number of target molecules can be calculated to quantify the samples. As the details of the standard curve are given in table 9, only the graph of IPCS3 is given. Both IPCS1 and 2 show similar results to IPCS3.

4.9 Quantitative PCR

After optimising the primers and creating a standard curve, a quantitative PCR (Q-PCR) was carried out to quantify the IPCS expressed in each tissue.

cDNA synthesized from 0.4 μ g total RNA was added to each sample. As not enough material was collected for triplicate results on senescing leaves, only one Q-PCR was carried out. Triplicates were carried out for other material.

4.10 Quantification of IPCS Gene Expressed

The expression levels of each IPCS gene in different plant materials were calculated by importing the standard curves. The moles of each cDNA was calculated from the fact that 1 μ g of 1Kb DNA is 1.5pmol. By using the avogadro numbers, the copy number of each gene was calculated.

Although an absolute quantification can be calculated by importing standard curves, as the amplification efficiency and the efficiency of the reverse transcript for each gene is different, it is extremely difficult to carry out absolute quantification among other genes.

Although, for the reverse transcript, as the three genes have highly similar sequences, it could be assumed that the efficiency of the reaction is similar. For the amplification efficiency, although the M value for IPCS2 is lower, as each primer sets were optimised, and the R² value is 0.99, it could be assumed that the efficiency of the amplification of these genes were similar.

Another thing to consider when importing a standard curve is that the variations of reagents, primers, and probe (sequence alterations and fluorescence intensity), day-to-day or sample-to-sample variations will not be covered (Pfaffl 2004).

Under the understanding of the possible efficiency differences, all expressed genes were quantified and compared (Figure 26). It should be noted that the (Y) axis is in logarithmic scale. From these results, IPCS2 is the most expressed gene among the three. In root, IPCS1 is expressed only 1% of IPCS2. IPCS2 is highly expressed in root, cauline leaf and rosette leaf. Although IPCS2 is the most abundant gene, for stem and flower, IPCS3 is expressed as much as IPCS2.

EST and cDNA data of these genes from TAIR support these results where IPCS2 is the predominant gene and then IPCS1 and IPCS3 (Table 10). In IPCS1, cDNA was found using whole plants (2). In IPCS2, cDNA was found using whole plant (4), flower & buds (1) and when a callus was treated with hormone. In IPCS3, cDNA was found using whole

plant (4) and flower & buds (3). The EST in IPCS1 comes from, whole plant (58%) and rosette leaf (42%). For IPCS2, whole plant (65%), rosette leaf (26%), seedlings (5%) and senescence leaf (3%). For IPCS3, whole plant (44%), floral buds and roots (44%) and rosette leaf (12%).

Table 10 EST and cDNA in each IPCS Gene

	EST	cDNA
IPCS1	32	2
IPCS2	57	6
IPCS3	25	7

Microarray data is only available for IPCS2 in genevestigator. The data for each tissue is shown in Table 11. The signal intensity values have arbitrary units that are scaled to the total abundance of transcripts within a sample. The mean signal value is set as 1000, and the background range is 0-100.

Table 11 Microarray Data for IPCS2

Root	Rosette Leaf	Cauline Leaf	Stem	Flower	Siliques	Senescing Leaf
2383	2135	2509	1167	998	705	4236

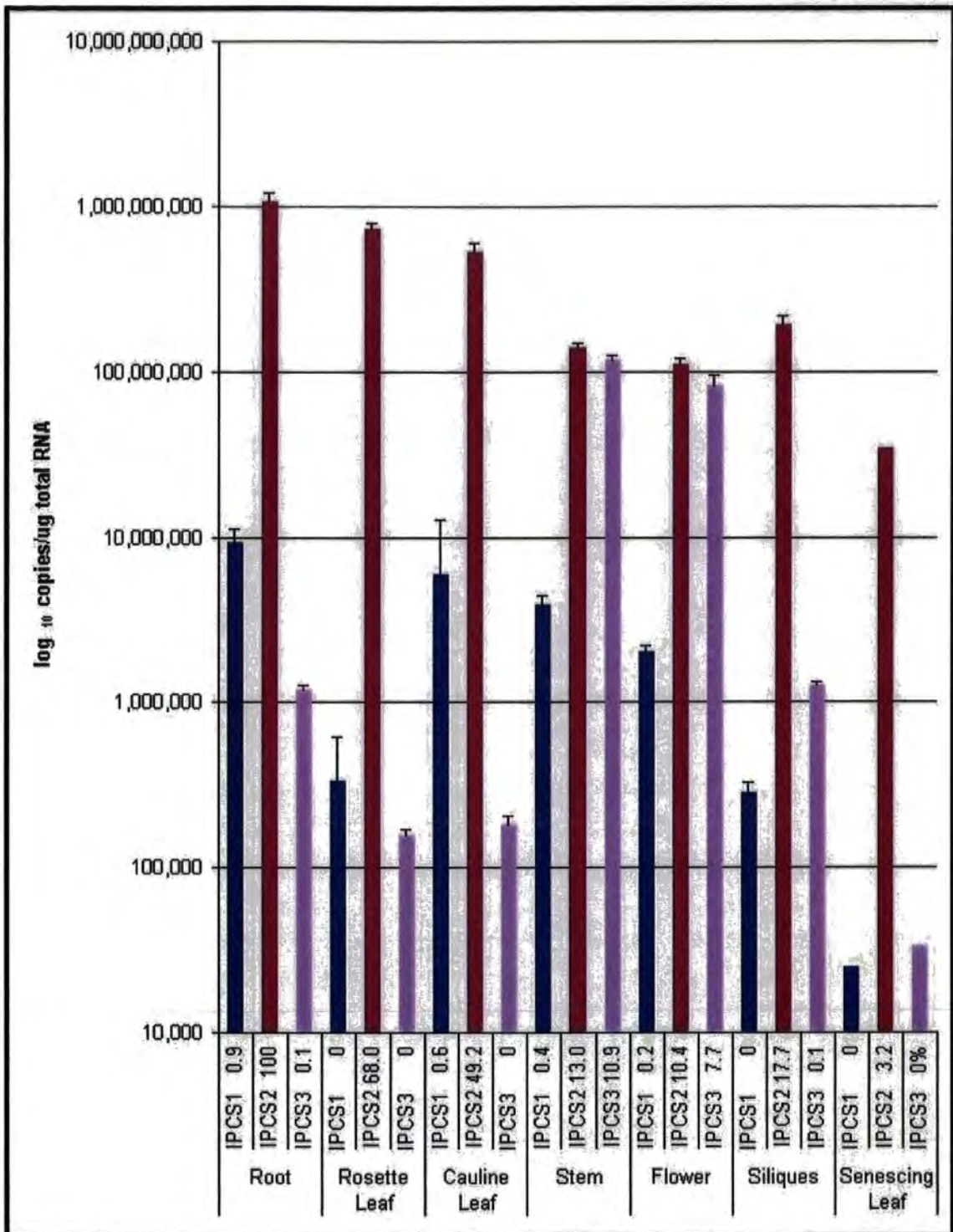


Figure 26 Quantification of IPCS transcripts per microgram of total RNA

Comparing the expression of IPCS genes in various plant tissues, IPCS2 is expressed the most among all genes. It is particularly highly expressed in root, rosette leaf and cauline leaf. In stem and flower, IPCS3 is expressed as much as IPCS2. From these results, IPCS2 is the predominant gene, and the genes are expressed in a tissue dependent manner. It should be noted that the (Y) axis is in logarithmic scale. Therefore the expression of IPCS1 in root is only 1% of the expression in IPCS2. The relative expressions of the samples are expressed in percentage. Triplicate assays were carried out except for senescing leaf.

Although the results here are not a perfect match to the data obtained, the general trend appears to be similar. Where root, rosette leaf and cauline leaf are expressed most and then stem, flower and siliques. In microarray data cauline leaf is expressed higher than root, but as the assay is only done three times, the results are not as reliable. Also as the expression level varies depending on the development stage of the tissue, if the data collected for the microarray was a different developmental stage to the samples which were been tested, this would have affected the results. For seeds, results obtained in Q-PCR are higher than stem and flower, but in microarray data it is lower. This may also be due to different developmental stages. For senescing leaf, in microarray data, it is expressed the most where as in Q-PCR it was the lowest. This could be due to the difficulty in collecting the samples and due to low quality RNA. As mentioned in 4.2, extraction of RNA from senescing leaf was extremely difficult and only low amount and low quality RNA was obtained. As only single experiments were carried out for senescing leaf, further experiments are needed to test and confirm the expression level.

Comparing the data to the cDNA obtained from genevestigator, the high expression of IPCS3 in flower matches the data for cDNA in IPCS3 as three cDNAs were found in flower. This could suggest that IPCS3 is predominately expressed in flower tissue. Also the higher cDNA found in IPCS2 compared to IPCS1 matches the QPCR results where IPCS2 is constantly highly expressed compared to IPCS1.

5. Discussion

In recent years, many sphingolipids have been discovered, and their importance has been understood using mutant yeast cells to identify and characterize plant sphingolipids. Recently plant IPCS activity has been measured in plant extracts (Bromley *et al.* 2003), but no plant orthologue of the yeast gene encoding this activity was visible in databases (Lynch and Dunn 2004). Identification of an IPCS in *Leishmania* (Denny *et al.* 2006) has subsequently allowed orthologous IPCS genes to be identified in *A. thaliana* (J. G. Mina Unpublished).

The three highly related IPCS sequence orthologues were cloned from *A. thaliana* cDNA and transformed into the yeast-*E. coli* shuttle vector pRS426 MET as a basis for investigating the encoded activity.

5.1 Function of *At* IPCS

Results from rescuing YPH499-HIS-GAL-AUR1 *S. cerevisiae* with *At* IPCS-pRS426 indicate that the three *At* IPCS sequences complement the function of AUR1, which is the IPCS that catalyzes the transfer of inositolphosphate from phosphatidylinositol to ceramide producing diacylglycerol and IPC. Also further studies in *in vitro* metabolic labelling supported the results that *At* IPCS functionally complement AUR1. As there is no functional equivalent of IPCS in animals, this raises the possibility of developing specific inhibitors that do not affect mammals which will act as an herbicide.

As the mammalian sphingomyelin synthase equivalent to IPCS, carries out the (reverse) phospholipase reaction, the function of reverse reaction of IPCS, inositol phosphoshingolipid phospholipase C (IPS-PLC), was tested for further characterization of *At* IPCS. As *isc1Δ*; *isc1* deletion mutant has been shown to be sensitive to salt (Betz *et al.* 2002), a salt tolerance test was carried out and these results suggests that *At* IPCS does not have IPS-PLC function; *in vitro* metabolic labelling also supports these results. This would suggest that, like yeast, plants possess a different enzyme for phospholipase activity (Sawai *et al.* 2000b). However, this enzyme has yet to be identified. From anionic phospholipid-selective binding study of *ISC1* in yeast demonstrated that the interaction of the N-terminus and the C-terminus is required for activity of *Isc1p*, and the second transmembrane domain (TM2) and the C terminus are required for phosphatidylserine (PS) binding (Okamoto *et al.* 2002). *Isc1p* was found to interact specifically and directly with PS/ cardiolipin / phosphatidylglycerol by lipid-protein overlay assays (Sawai *et al.* 2000b), which suggests

that the catalytic domain in the N terminus of Isc1p is pulled to the membrane to interact with substrate in the presence of PS/ CI/ PG (Okamoto *et al.* 2002). By looking at the sequence of the TM2, C terminus and N terminus, it might be possible to identify *ISC1* in plants. As *IPCS* was identified in plants by aligning many species, employing the same method might also facilitate in identifying *ISC1* in plants.

Results from experiments with an inhibitor of yeast AUR1 activity (Figure 15) showed that *At* *IPCS* is resistant to the fungal inhibitor. This will potentially allow the development of fungal pathogen inhibitors that will have no plant toxicity. However, *IPCS* activity in golden butter wax bean seed microsomes demonstrate sensitivity to AbA (Bromley *et al.* 2003). As the wax bean *IPCS* sequence is as yet unknown, the reason for this difference in sensitivity is unclear, but as the bean assay was carried out using microsomal membranes rather than by *in vivo*, the difference between the experimental methods may have caused the different results.

The amino acid sequences of these *IPCS* enzymes were compared, but no conserved homology was found between *At* *IPCS* and *Sc* *IPCS* (Figure 27). This is why the plant *IPCS* has never been identified using yeast sequences to interrogate plant databases.

```

IPCS1  ---MTLYIRREASKLWRRFCSEITTEIG---LLAENWKYLLAGLLCQYIHGLAARGVHY 53
IPCS2  ---MTLYIRRESSKLWKRFCSEISTEIG---LLAENWKYLLAGLICQYIHGLAAKGVHY 53
IPCS3  ---MPVYVDREAPKLWRRIYSEATLEAS---LLAEKWKLVLAGLVFQYIHGLAAHGVHY 53
ScAUR1  MANPFSRWFLSERPPNCHVADLETSLDPHQTLLKVQKYKPALS-DWVHYIFLGSIMLFVF 59
      :. :. * . : * : : * . : : * : : * : : * : : * : : * : : * : :
      :. :. * . : * : : * . : : * : : * : : * : : * : : * : :

IPCS1  IHRPGPTLQDSGFFVLP-----ELGQDKGFISETVFTCVFLSFFLWTFHP----- 98
IPCS2  IHRPGPTLQDLGFFLLP-----ELGQERSYISETVFTSVFLSFFLWTFHP----- 98
IPCS3  LHRPGPTLQDAGFFILP-----ALGQDKAFFSETVFTVIFGSFILWTFHP----- 98
ScAUR1  ITNPAPWIFKILFYCFLGTLFIIPATSQFFFNALPILTWVALYFTSSYFPDDRRPPITVK 119
      : . * . * : . * : : : . . : : : . : . : : : *

IPCS1  -----FIVKSKKIYTVLIWCRVLAFLVACQFLRVITFYST----- 133
IPCS2  -----FILKTKKIYTVLIWCRVLAFLVACQFLRVITFYST----- 133
IPCS3  -----FVSHSKKICTVLIWCRVVFVYLAASQSLRIITFFAT----- 133
ScAUR1  VLPVAVETILYGDNLSDILATSTNSFLDILAWLPYGLFHFAGPFVVAAILFVFGPPTVLQG 179
      : : : : : * * : . . : : :

IPCS1  -----QLPGPNYHCREGSE-LARLPRPHNVLEVLL 162
IPCS2  -----QLPGPNYHCREGSK-VSRLPWPKSALEVLE 162
IPCS3  -----QLPGPNYHCREGSK-LAKIPPPKNVLEVLL 162
ScAUR1  YAFAFGYMNLFGVIMQNVFPAAPPWYKILYGLQSANYDMHGSPGGLARIDKLLGINMYTT 239
      * . . * . : . . : : :

      D3
IPCS1  LNFPRGVIYGCCGDLIFSSHMIFTLVFVRTYQKYGSKRFIKLLGWVIAILQSL-----L 215
IPCS2  IN-PHGVMYGCCGDLIFSSHMIFTLVFVRTYQKYGTKRFIKLFGWLTAIVQSL-----L 214
IPCS3  INFDPGVIYGCCGDLIFSSHTIFTLVFVRTYQRYGTRRWIKHLAWLMAVIQSI-----L 215
ScAUR1  AFSNSSVIFGAFPSLHSGCATMEALFFCYCFPKLKPLFIAYVCWLWWSTMYLTHHYFVDL 299
      * : : * . : * . : : * . : * : : * : : *

      D4
IPCS1  IIASRKHYTVDVVVAWYTVNLVVFFLDKKLPELDPRT-----TALLEVISKD---RTKEE 267
IPCS2  IIASRKHYSVDVVVAWYTVNLVVFCLDKKLPELDPRT-----AVLLEVISKD---RTKEE 266
IPCS3  IIASRKHYTVDIVVAWYTVNLVMFYVDSKLPEMAERSSGSPPTPLPLSTKDSKNKSKED 275
ScAUR1  MAGSVLSYVIFQYTKYTHLPIVDTSLFCRWSYTSIEKYDISKSDPLAADSNDIESVPLSN 359
      : . * * : . : : : * : : . . . : * . : : * . . .

IPCS1  SHKLLNGNGVDPADRRPRAQVNGK-DSNGGHTDNATNGT--- 305
IPCS2  NHKLLNGNGVDPADWRPRAQVNGKIDSNVHTDNTMNGA--- 305
IPCS3  HQRLLENENVADDH----- 289
ScAUR1  LELDFDLNMTDEPSVSPSLFDGSTSISRSSATSITSLGVKRA 401
      . : : * .

```

Figure 27 Alignment of *A. thaliana* IPCS and *S. cerevisiae* IPCS (AUR1)

An alignment was carried out with ClustalW2, but only some homology was found between *At* IPCS and *Sc* IPCS. Sequences with boxes are motif D3 and D4 (Figure 29).

Red: small (small + hydrophobic (incl. aromatic –Y)), Blue: acidic, Pink: basic, Green: hydroxyl + amine + basic – Q), "*" : residues in this column are identical in all sequences in the alignment. ":" : conserved substitutions have been observed according to colour. "." : semi-conserved substitutions are observed.

As no significant homology was found in the amino acid level, further analysis on motif scan (<http://scansite.mit.edu/>) was carried out (Figure 28).

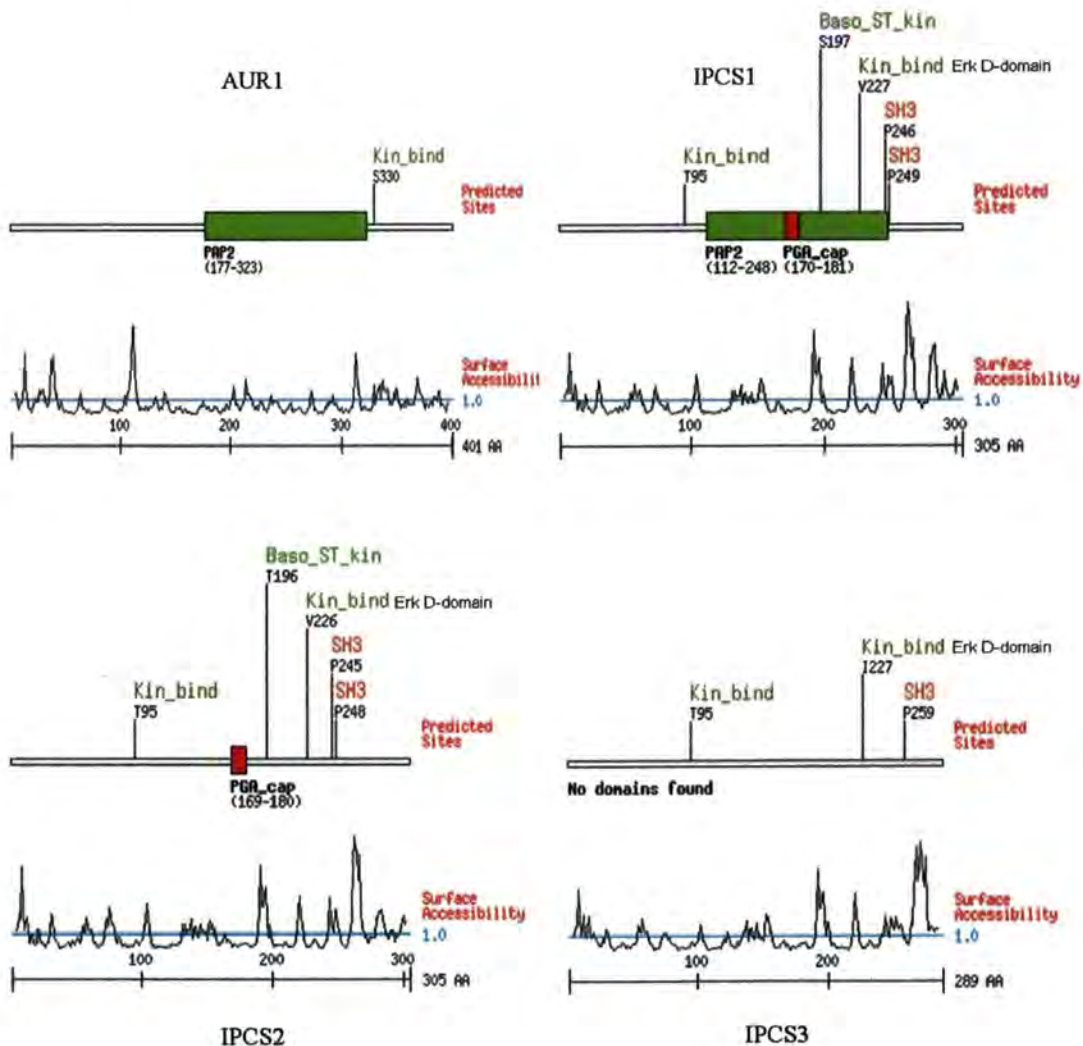


Figure 28 Motif Scan of IPCS Genes

Motif scan was carried out using (<http://scansite.mit.edu/>), and domains were predicted. Although not found in all IPCS genes, PAP2, a phosphatidic acid phosphatase family which is involved in signal transduction was predicted on AUR1 and IPCS1. The only common domain found in all three *At* IPCS genes was Erk D-domain, a kinase binding site group.

All of the *At* IPCS genes were shown to have a kinase binding site Erk D-domain, whereas AUR1 did not. Erk is an extracellular signal-regulated kinase involved in functions including the regulation of meiosis, mitosis, and postmitotic functions in differentiated cells. Looking at the predicted domains in *At* IPCS, PAP2 and PGA_cap domains were found in IPCS1, PGA_cap domain was identified in IPCS2 and no domains were predicted in IPCS3. The PAP2 superfamily includes the enzyme type 2 phosphatidic acid phosphatase (PAP2), Glu-6-phosphatase, phosphatidylglycerophosphatase B and bacterial acid phosphatase, and this superfamily has been identified as a lipid phosphatase in yeast (Stukey and Carman 1997). PGA_cap is a putative poly-gamma-glutamate capsule biosynthesis protein found in bacteria. It is a surface-associated protein and may be involved in virulence and be associated with bacterial survival in high salt concentrations (Candela and Fouet 2006). As IPCS is thought to be located in the golgi, it is unlikely that these domains cause the resistance to AbA.

Although the sequence of *At* IPCS is dissimilar to that of AUR1, when aligned with various other species, the conserved areas D3 and D4 were found (J. G. Mina Unpublished). These motifs D3 and D4 are shown in boxes in Figure 27. When only *A. thaliana* and *S. cerevisiae* are aligned, these domains do not match. Motifs D3 and D4 are highly conserved throughout the sphingomyelin synthases (Huitema *et al.* 2004), and are part of the catalytic site in SM synthesis responsible for liberating cholinephosphate from phosphatidylcholine. These motifs are similar to the C2 and C3 motifs in lipid phosphate phosphatase (LPP) (Huitema *et al.* 2004). LPP possesses a three-domain lipid phosphatase motif that is localized to the hydrophilic surface of the membrane (Han *et al.* 2004). The conserved motifs D3 and D4 in *Homo sapiens*, *A. thaliana*, *S. cerevisiae* and the LPP motifs C2 and C3 are shown in Figure 29.

	D3		D4
<i>Hs</i> SMS1	CGDYLYSGHT		HYTVDVVVAYYYITTFLEFWWVHT
<i>Hs</i> SMS2	CGDFLESGHT		HYTIIDVYIIAYYITTRLEFWWYHS
<i>At</i> IPCS1	CGDLIFSSHM		HYTVDVVVAVWYTVNLLVVFFLDK
<i>At</i> IPCS2	CGDLIFSSHM		HYSVDVVVAVWYTVNLLVVFCLDK
<i>At</i> IPCS3	CGDLIFSSST		HYTVDIVVAVWYTVNLLVVFYVDS
<i>Sc</i> IPCS	IFGAFPGLHS		HYFVDLMAGSVLSYVIFQYTR
LPD	nxP[red]SGE	hxxnxxnRbxxxxx[red]	xxD[red]bxxnxxxn
	C2		C3

Figure 29 Alignment of Motif D3 and D4

At IPCS consists of highly similar SMS motifs D3 and D4, while although less homologous, *Sc* IPCS also has these motifs. Also shown are LPDs (lipid phosphatase domain) and the conserved histidine and aspartate residues that form the catalytic triad. LPD C2 and C3 are localized to the hydrophilic surface of the membrane.

All these motifs, D3, D4 and C2, C3 include aspartate and histidine residues which form a catalytic triad mediating the nucleophilic attack on the lipid phosphate ester bond (Neuwald 1997). The histidine and aspartate residues are conserved between species. From previous research by Hashida-Okado *et al.*, has shown that a mutation in the first conserved domain (146-161bp) produces mutant colonies resistant to AbA (HashidaOkado *et al.* 1996). The research showed that by replacing the 158 position Phe with Tyr gave resistances to AbA. However, changing this amino acid did not give any difference in motif prediction but, looking at the amino acid property, it was found that only Phe was hydrophobic whereas Tyr, the amino acid sequence in *A. thaliana*, Lys (IPCS1 and 2) and His (IPCS3) were all hydrophilic (Figure 30) and (Table 12). The hydropathy index in protein structure is important as hydrophobic amino acids tend to be internal whereas hydrophilic amino acids are more commonly found in the protein surface. AbA is suggested to bind to a distinct hydrophobic site on IPCS that is conserved among various fungal species (Zhong *et al.* 1999). Further research would be necessary but this may well be the key point for AbA resistance.

AtIPCS1	FLWTFHPPFIVKSKKIYTVLIWCR-----VLAFLVACQFLRVITFYSTQLPGPNYHC	142
AtIPCS2	FLWTFHPPFILTKKIYTVLIWCR-----VLAFLVACQFLRVITFYSTQLPGPNYHC	142
OsIPCS1	LLWSFHPPFIYHSKR FYTVLLWRR-----VLAFLVASQFLRIITFYSTQLPGPNYHC	142
OsIPCS2	VLWTFHPPFIYHSKR FYTVLIWRR-----VLAFLVASQVLR IITFYSTQLPGPNYHC	142
OsIPCS3	VLWTFHPPFILQTKR FYTVLIWRR-----VLAFLCASQFLRIVTFYSTQLPGPNYHC	143
AtIPCS3	ILWTFHPPFVSKKICTVLIWCR-----VFVYLAASQSLRIITFFATQLPGPNYHC	142
HsSMS1	MILVGLWLIQWLLLKYKSIISR-----FFCIVGTLYLYRCITMYVTTLVPVGMHF	248
MmSMS1	MILVGLWLFQWLLLKYKSIISR-----FFCIVGTLYLYRCITMYVTTLVPVGMHF	248
HsSMS2	IILVGLWITQWFLFLRYKSIVGRR-----FCFIIGTLYLYRCITMYVTTLVPVGMHF	186
MmSMS2	MVLVGLWITQWFLFLRYKSIVGRR-----FFFIMGTLYLYRCITMYVTTLVPVGMHF	186
ScAUR1	LAWLPYGLFHGAPFVVAAILFVFGPPTVLQGYAFAFGYMNLFVIMQNVFPAAPPWYKI	207
CaIPCS	LAWLPYGIHFSFPFVLA AIIIFLFGPPTALRSFGFAFGYMNLLGVLIQMAFPAAPPWYKN	220
SjIPCS	IAWLPYGVIIHYGAPFIVSFVLFVFPPTLPVWARSFGYMNLIQVLIQIFFPCSPWYEN	209
SpIPCS	LAWVPYGVMHYSAPFIISFILFIFAPPPTLPVWARTFGYMNLFVLIQMAFPCSPWYEN	207
AfIPCS	LAWLPYGICHYGAPFVCSAIMFIFGPPGTVPLFARTFGYISMAAVTIQLFFPCSPWYEN	242
PcAUR1	LAWIPYGIHFGAPFITAIIVIYLSPPPTLPVFAKCFGYLNLIGVIIQLVFPSPWYES	225
CeSMS1	IGSFVSLLVLILFHRHRWIVLRR-----LCFIGSILYGMRCITMMVTPVPKADEF	289
CeSMS2	TVSSVVAFTIIFLHHQRWIVLRR-----TFLLGAIMYGLRAVILGVTFLPPSFHNR	162
CeSMS3	ALCIVMLGALLVIHQHRGTILKR-----VVFCAGTLYAMRSVTLAATQLPSGYTDN	139
LmIPCS	LDSGRRPFPLNVFPIMAIRFLT-----SYAVVMVFRFVIMGTSYPATDNHC	185

Figure 30 Alignment with Various Species

Alignment of various species was carried out to identify conserved motifs. Section of *Sc* 158 was extracted. The conserved area is shown in Figure 29. Using this alignment the sequence at *Sc* position 158 was compared with various other species. When the F at *Sc* 158 was replaced by Y, the cells became resistant to AbA. Both *At* IPCS and *Lm* IPCS are known to be AbA resistant and both have a K (*At*IPCS1, 2 and *Lm*IPCS) or H (*At*IPCS3). *At*: *A. thaliana*, *Os*: *Oryza sativa*, *Hs*: *Homo sapiens*, *Mm*: *Mus musculus*, *Sc*: *S. cerevisiae*, *Ca*: *Candida albicans*, *Sj*: *Schizosaccharomyces japonicus*, *Sp*: *Schizosaccharomyces pombe*, *Af*: *Aspergillus fumigatus*, *Pc*: *Pneumocystis carinii*, *Ce*: *Caenorhabditis elegans*, *Lm*: *L. major*

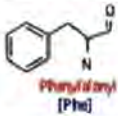
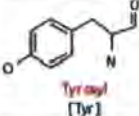
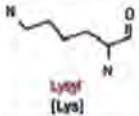
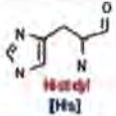
Amino Acid	F (Phe)	Y (Tyr)	K (Lys)	H (His)
Structure	 Phenylalanyl [Phe]	 Tyrosyl [Tyr]	 Lysyl [Lys]	 Histidyl [His]
Side Chain Polarity	nonpolar	polar	polar	polar
Side Chain Acidity/ Basicity	neutral	neutral	basic	basic (weakly)
Hydropathy Index	2.8	-1.3	-3.9	-3.2
Aureobasidin A	sensitive	resistant	resistant	resistant

Table 12 Properties of Amino Acids Found at the *Sc* 158bp Position

Only Phe is shown to be hydrophobic and Tyr, Lys and His are hydrophilic. AbA resistance may be due to this as the hydropathy index affects the protein structure.

Although all three *At* IPCS genes have been predicted to have different domains, from the metabolic labelling of *At* IPCS complemented AUR1 (Figure 14), all *At* IPCS produced IPC although in a different degree. From the TLC results, where equal amounts of cells were incubated with NBD- C_6 -Ceramide, IPCS2 had the strongest band. This would suggest that the IPCS2 enzyme is most active. Interestingly, for expression, IPCS2 was also the most highly expressed gene in all tissues. Which would suggest that mRNA for IPCS2 is produced the most. Therefore the amount of IPCS activity and the expression of IPCS genes appear to be correlated.

5.2 Expression of *At* IPCS

Results from Q-PCR have been presented for the expression of each *At* IPCS gene in various plant tissues. From these results, IPCS2 was the predominantly expressed gene, being highly expressed in root, rosette leaf and cauline leaf. Publicly available microarray data (<https://www.genevestigator.ethz.ch/>) also support these tissue level expression results.

Results of IPCS1 and IPCS3 are completely new data, as no microarray data for these genes are currently available. From the results of Q-PCR experiments, the expression of IPCS1 and IPCS3 are more than 10-times less than that of IPCS2 in root, rosette leaf, cauline leaf and siliques. Although in stem and flower, IPCS3 is expressed as much as IPCS2. Comparing the expression levels of IPCS1 and IPCS3, IPCS1 appears to be more active in the early development stages 1 to 5 and IPCS3 is more active in the later development stages 6 to 9. Stages were taken from as described in Boyes *et al.* 2001. These results suggest that these IPCS genes are expressed in a tissue dependent manner.

Activity measurements carried out on bean extracts (Bromley *et al.* 2003) suggest that light has no effect on IPCS activity, while data from microarray suggest that UV light decreases the expression level of IPCS2. Although the light used in the experiments was natural light (Bromley *et al.* 2003), this may suggest that depending on the environment conditions and different stress conditions, the expressed IPCS genes maybe selected or affected. Also, since plants have three functional IPCS genes, it seems highly likely that IPCS is an important activity enabling them to deal with various environmental conditions.

Further experiments would be needed to confirm the selection of these genes, but it can be conjectured that these IPCS genes are expressed in a tissue dependent manner and that the surrounding environment may also have an effect on how the genes are expressed.

Finally, identification of the gene sequence of IPCS in *A. thaliana* will facilitate identifying other IPCS genes in other plant species. Also the function and expression of IPCS in *A. thaliana* will facilitate the understanding of the role played by this protein, such as in secondary signalling molecules and lipid rafts. The expression level will give insight into how the gene responds to various stresses. Furthermore as *A. thaliana* IPCS was found to be insensitive to the anti-fungal agent AbA, understanding the mechanism of this will become a key in managing fungal diseases in plants in future.

6. Future Work

Further work should be carried out to understand the expression levels of these IPCS genes under various stress conditions. As IPCS is a vital gene, the gene will have to be able to bear stress for the plant to survive. By doing this, the importance of this gene in plants can be identified and the selection of the three genes under various stress conditions can be determined. As this is the first time a plant IPCS gene has been identified, using its orthologue other IPCS genes in various plants can also be identified. Also as plant IPCS does not code for IPS-PLC, it will be important to identify the gene coding for IPS-PC.

As *A. thaliana* IPCS was resistant to AbA, further study should be conducted to identify the mechanism of this. As described in discussion, the hydropathy index appears to be important in AbA resistance. Therefore by carrying out an agar diffusion assay with various species that are hydrophobic and hydrophilic at the Sc 158 position may give insight to AbA resistance.

As plant IPCS has only been identified recently, further study of this gene can be conducted to analyze the function and importance of sphingolipids in plants.

7. References

- A. H. Jr. Merrill, C. C. S. (1996). Sphingolipids: metabolism and cell signalling. *New comprehensive biochemistry: biochemistry of lipids, lipoproteins and membranes*. J. E. V. D. E. Vance. Amsterdam, the Netherlands, Elsevier.
- Aerts, A. M., Francois, I., Bammens, L., Cammue, B. P. A., Smets, B., Winderickx, J., Accardo, S., De Vos, D. E. and Thevissen, K. (2006). "Level of M(IP)(2)C sphingolipid affects plant defensin sensitivity, oxidative stress resistance and chronological life-span in yeast." *Febs Letters* **580**(7): 1903-1907.
- Beeler, T., Bacikova, D., Gable, K., Hopkins, L., Johnson, C., Slife, H. and Dunn, T. (1998). "The *Saccharomyces cerevisiae* TSC10/YBR265w gene encoding 3-ketosphinganine reductase is identified in a screen for temperature-sensitive suppressors of the Ca²⁺-sensitive *csg2* Delta mutant." *Journal of Biological Chemistry* **273**(46): 30688-30694.
- Betz, C., Zajonc, D., Moll, M. and Schweizer, E. (2002). "ISC1-encoded inositol phosphosphingolipid phospholipase C is involved in Na⁺/Li⁺ halotolerance of *Saccharomyces cerevisiae*." *European Journal of Biochemistry* **269**(16): 4033-4039.
- Bille, J., Weiser, T. and Bentrup, F. W. (1992). "The lysolipid sphingosine modulates pyrophosphatase activity in tonoplast vesicles and isolated vacuoles from a heterophic cell-suspension culture of *chenopodium-rubrum*." *Physiologia Plantarum* **84**(2): 250-254.
- Birch, P. R. J., Avrova, A. O., Duncan, J. M., Lyon, G. D. and Toth, R. L. (1999). "Isolation of potato genes that are induced during an early stage of the hypersensitive response to *Phytophthora infestans*." *Molecular Plant-Microbe Interactions* **12**(4): 356-361.
- Borner, G. H. H., Sherrier, D. J., Stevens, T. J., Arkin, I. T. and Dupree, P. (2002). "Prediction of glycosylphosphatidylinositol-anchored proteins in arabidopsis. A genomic analysis." *Plant Physiology* **129**(2): 486-499.
- Borner, G. H. H., Sherrier, D. J., Weimar, T., Michaelson, L. V., Hawkins, N. D., MacAskill, A., Napier, J. A., Beale, M. H., Lilley, K. S. and Dupree, P. (2005). "Analysis of detergent-resistant membranes in Arabidopsis. Evidence for plasma membrane lipid rafts." *Plant Physiology* **137**(1): 104-116.
- Boyes, D. C., Zayed, A. M., Ascenzi, R., McCaskill, A. J., Hoffman, N. E., Davis, K. R. and Goriach, J. (2001). "Growth stage-based phenotypic analysis of arabidopsis: A model for high throughput functional genomics in plants." *Plant Cell* **13**(7): 1499-1510.
- Brandwagt, B. F., Mesbah, L. A., Takken, F. L. W., Laurent, P. L., Kneppers, T. J. A., Hille, J. and Nijkamp, H. J. J. (2000). "A longevity assurance gene homolog of tomato mediates resistance to *Alternaria alternata* f. sp *lycopersici* toxins and fumonisin B-1." *Proceedings of the National Academy of Sciences of the United States of America* **97**(9): 4961-4966.
- Brodersen, P., Petersen, M., Pike, H. M., Olszak, B., Skov, S., Odum, N., Jorgensen, L. B., Brown, R. E. and Mundy, J. (2002). "Knockout of Arabidopsis ACCELERATED-CELL-DEATH11 encoding a sphingosine transfer protein causes activation of programmed cell death and defense." *Genes & Development* **16**(4): 490-502.
- Bromley, P. E., Li, Y. N. O., Murphy, S. M., Sumner, C. M. and Lynch, D. V. (2003). "Complex sphingolipid synthesis in plants: characterization of inositolphosphorylceramide synthase activity in bean microsomes." *Archives of Biochemistry & Biophysics* **417**(2): 219-226.

- Candela, T. and Fouet, A. (2006). "Poly-gamma-glutamate in bacteria." *Molecular Microbiology* 60(5): 1091-1098.
- Chen, M., Han, G. S., Dietrich, C. R., Dunn, T. M. and Cahoon, E. B. (2006). "The essential nature of sphingolipids in plants as revealed by the functional identification and characterization of the Arabidopsis LCB1 subunit of serine palmitoyltransferase." *Plant Cell* 18(12): 3576-3593.
- Cheng, J. J., Park, T. S., Fischl, A. S. and Ye, X. S. (2001). "Cell cycle progression and cell polarity require sphingolipid biosynthesis in *Aspergillus nidulans*." *Molecular & Cellular Biology* 21(18): 6198-6209.
- Chini, V., Foka, A., Dimitracopoulos, G. and Spiliopoulou, I. (2007). "Absolute and relative real-time PCR in the quantification of *tst* gene expression among methicillin-resistant *Staphylococcus aureus*: evaluation by two mathematical models." *Letters in Applied Microbiology* 45(5): 479-484.
- Chung, N. J., Mao, C. G., Heitman, J., Hannun, Y. A. and Obeid, L. M. (2001). "Phytosphingosine as a specific inhibitor of growth and nutrient import in *Saccharomyces cerevisiae*." *Journal of Biological Chemistry* 276(38): 35614-35621.
- Clementi, E., Borgese, N. and Meldolesi, J. (2003). "Interactions between nitric oxide and sphingolipids and the potential consequences in physiology and pathology." *Trends in Pharmacological Sciences* 24(10): 518-523.
- Coursol, S., Fan, L. M., Le Stunff, H., Spiegel, S., Gilroy, S. and Assmann, S. M. (2003). "Sphingolipid signalling in Arabidopsis guard cells involves heterotrimeric G proteins." *Nature* 423(6940): 651-654.
- Denny, P. W., Shams-Eldin, H., Price, H. P., Smith, D. F. and Schwarz, R. T. (2006). "The protozoan inositol phosphorylceramide synthase - A novel drug target that defines a new class of sphingolipid synthase." *Journal of Biological Chemistry* 281(38): 28200-28209.
- Dickson, R. C. and Lester, R. L. (1999). "Yeast sphingolipids." *Biochimica Et Biophysica Acta-General Subjects* 1426(2): 347-357.
- Dunn, T. M., Lynch, D. V., Michaelson, L. V. and Napier, J. A. (2004). "A post-genomic approach to understanding sphingolipid metabolism in *Arabidopsis thaliana*." *Annals of Botany* 93(5): 483-497.
- Futerman, A. H. (2005). "Defective calcium homeostasis in sphingolipid storage diseases." *Journal of Neurochemistry* 94: 5-5.
- Gable, K., Slife, H., Bacikova, D., Monaghan, E. and Dunn, T. M. (2000). "Tsc3p is an 80-amino acid protein associated with serine palmitoyltransferase and required for optimal enzyme activity." *Journal of Biological Chemistry* 275(11): 7597-7603.
- Grilley, M. M., Stock, S. D., Dickson, R. C., Lester, R. L. and Takemoto, J. Y. (1998). "Syringomycin action gene SYR2 is essential for sphingolipid 4-hydroxylation in *Saccharomyces cerevisiae*." *Journal of Biological Chemistry* 273(18): 11062-11068.
- Guillas, I., Kirchman, P. A., Chuard, R., Pfefferli, M., Jiang, J. C., Jazwinski, S. M. and Conzelmann, A. (2001). "C26-CoA-dependent ceramide synthesis of *Saccharomyces cerevisiae* is operated by Lag1p and Lac1p." *Embo Journal* 20(11): 2655-2665.
- Haak, D., Gable, K., Beeler, T. and Dunn, T. (1997). "Hydroxylation of *Saccharomyces cerevisiae* ceramides requires Sur2p and Scs7p." *Journal of Biological Chemistry* 272(47): 29704-29710.
- Hakomori, S. (1983). Chemistry of glycosphingolipids. *Handbook of lipid research, vol. 3, sphingolipid biochemistry*. J. N. Kanfer, and Hakomori, S., New York, NY, USA, Plenum Press: 1-164.

- Han, G. S., Johnston, C. N. and Carman, G. M. (2004). "Vacuole membrane topography of the DPP1-encoded diacylglycerol pyrophosphate phosphatase catalytic site from *Saccharomyces cerevisiae*." *Journal of Biological Chemistry* **279**(7): 5338-5345.
- Hanahan, D. (1983). "Studies on transformation of *Escherichia coli* with plasmids " *Journal of Molecular Biology* **166**(4): 557-580.
- Hannun, Y. A., Loomis, C. R., Merrill, A. H. and Bell, R. M. (1986). "Sphingosine Inhibition of Protein-Kinase-C Activity and of Phorbol Dibutyrate Binding *In Vitro* and in Human-Platelets." *Journal of Biological Chemistry* **261**(27): 2604-2609.
- Haro, R., Garciadeblas, B. and Rodrigueznavarro, A. (1991). "A novel P-type ATPase from yeast involved in sodium-transport." *FEBS Letters* **291**(2): 189-191.
- HashidaOkado, T., Ogawa, A., Endo, M., Yasumoto, R., Takesako, K. and Kato, I. (1996). "AUR1, a novel gene conferring aureobasidin resistance on *Saccharomyces cerevisiae*: A study of defective morphologies in Aur1p-depleted cells." *Molecular & General Genetics* **251**(2): 236-244.
- Hearn, J. D., Lester, R. L. and Dickson, R. C. (2003). "The uracil transporter Fur4p associates with lipid rafts." *Journal of Biological Chemistry* **278**(6): 3679-3686.
- Heidler, S. A. and Radding, J. A. (1995). "The AUR1 gene in *Saccharomyces cerevisiae* encodes dominant resistance to the antifungal agent aureobasidin A (LY295337)." *Antimicrobial Agents & Chemotherapy* **39**(12): 2765-2769.
- Hetherington, A. M. and Drobak, B. K. (1992). "Inositol-containing lipids in higher plants." *Progress in Lipid Research* **31**(1): 53-63.
- Huitema, K., van den Dikkenberg, J., Brouwers, J. and Holthuis, J. C. M. (2004). "Identification of a family of animal sphingomyelin synthases." *EMBO Journal* **23**(1): 33-44.
- Huwiler, A., Kolter, T., Pfeilschifter, J. and Sandhoff, K. (2000a). "Physiology and pathophysiology of sphingolipid metabolism and signaling." *Biochimica Et Biophysica Acta-Molecular and Cell Biology of Lipids* **1485**(2-3): 63-99.
- Huwiler, A., Kolter, T., Pfeilschifter, J. and Sandhoff, K. (2000b). "Physiology and pathophysiology of sphingolipid metabolism and signaling." *Biochimica et Biophysica Acta-Molecular & Cell Biology of Lipids* **1485**(2-3): 63-99.
- J. G. Mina, S. P., Hosam Shams-Eldin, Patrick G. Steel, Palph T. Schwarz, Tony Fawcett and Paul W. Denny (Unpublished). "Inositol phosphorylceramide synthase: A missing link in plant sphingolipid biosynthesis."
- Jiang, J. C., Kirchman, P. A., Allen, M. and Jazwinski, S. M. (2004). "Suppressor analysis points to the subtle role of the LAG1 ceramide synthase gene in determining yeast longevity." *Experimental Gerontology* **39**(7): 999-1009.
- Karlsson, K. A. (1970). "Chemistry and Occurrence of Sphingolipid Long-Chain Bases." *Chemistry and Physics of Lipids* **5**(1): 6-&.
- Kester, M. and Kolesnick, R. (2003). "Sphingolipids as therapeutics." *Pharmacological Research* **47**(5): 365-371.
- Khurana, S. M. P., Pandey, S. K., Sarkar, D. and Chanemougasoundharam, A. (2005). "Apoptosis in plant disease response: A close encounter of the pathogen kind." *Current Science* **88**(5): 740-752.
- Kihara, A. and Igarashi, Y. (2004). "Cross talk between sphingolipids and glycerophospholipids in the establishment of plasma membrane asymmetry." *Molecular Biology of the Cell* **15**(11): 4949-4959.
- Kinney, H. C., Karthigasan, J., Borenshteyn, N. I., Flax, J. D. and Kirschner, D. A. (1994). "Myelination in the developing human brain - Biochemical correlates." *Neurochemical Research* **19**(8): 983-996.

- Kluk, M. J. and Hla, T. (2001). "Role of the sphingosine 1-phosphate receptor EDG-1 in vascular smooth muscle cell proliferation and migration." *Circulation Research* **89**(6): 496-502.
- Kondo, Y. and Nakano, M. (1987). "Sphingolipid-saccharide complex from black gram sprouts." *Biochimica et Biophysica Acta-Molecular & Cell Biology of Lipids* **919**(2): 156-163.
- Lester, R. L. and Dickson, R. C. (1993). Sphingolipids with Inositolphosphate-Containing Head Groups. *Advances in Lipid Research, Vol 26*. **26**: 253-274.
- Liang, H., Yao, N., Song, L. T., Luo, S., Lu, H. and Greenberg, L. T. (2003). "Ceramide modulate programmed cell death in plants." *Genes & Development* **17**(21): 2636-2641.
- Lynch, D. V. and Dunn, T. M. (2004). "An introduction to plant sphingolipids and a review of recent advances in understanding their metabolism and function." *New Phytologist* **161**(3): 677-702.
- Maceyka, M., Payne, S. G., Milstien, S. and Spiegel, S. (2002). "Sphingosine kinase, sphingosine-1-phosphate, and apoptosis." *Biochimica et Biophysica Acta-Molecular & Cell Biology of Lipids* **1585**(2-3): 193-201.
- Mandala, S. M., Thornton, R. A., Milligan, J., Rosenbach, M., Garcia-Calvo, M., Bull, H. G., Harris, G., Abruzzo, G. K., Flattery, A. M., Gill, C. J., Bartizal, K., Dreikorn, S. and Kurtz, M. B. (1998). "Rustmicin, a potent antifungal agent, inhibits sphingolipid synthesis at inositol phosphoceramide synthase." *Journal of Biological Chemistry* **273**(24): 14942-14949.
- Markham, J. E. and Jaworski, J. G. (2007). "Rapid measurement of sphingolipids from *Arabidopsis thaliana* by reversed-phase high-performance liquid chromatography coupled to electrospray ionization tandem mass spectrometry." *Rapid Communications in Mass Spectrometry* **21**(7): 1304-1314.
- Markham, J. E., Li, J., Cahoon, E. B. and Jaworski, J. G. (2006). "Separation and identification of major plant sphingolipid classes from leaves." *Journal of Biological Chemistry* **281**(32): 22684-22694.
- Milstien, S., Gude, D. and Spiegel, S. (2007). "Sphingosine 1-phosphate in neural signalling and function." *Acta Paediatrica* **96**: 40-43.
- Mitsuo, K., Kobayashi, T., Shinnoh, N. and Goto, I. (1989). "Metabolism of exogenous galactosylceramide in the twitcher mouse brain." *Neurochemical Research* **14**(12): 1191-1194.
- Moore, T., Martineau, B., Bostock, R. M., Lincoln, J. E. and Gilchrist, D. G. (1999). "Molecular and genetic characterization of ethylene involvement in mycotoxin-induced plant cell death." *Physiological & Molecular Plant Pathology* **54**(3-4): 73-85.
- Mumberg, D., Muller, R. and Funk, M. (1994). "Regulatable promoters of *Saccharomyces cerevisiae* - comparison of transcriptional activity and their use for heterologous expression." *Nucleic Acids Research* **22**(25): 5767-5768.
- Nagiec, M. M., Baltisberger, J. A., Wells, G. B., Lester, R. L. and Dickson, R. C. (1994). "The LCB2 Gene of *Saccharomyces* and the Related LCB1 Gene Encode Subunits of Serine Palmitoyltransferase, the Initial Enzyme in Sphingolipid Synthesis." *Proceedings of the National Academy of Sciences* **91**(17): 7899-7902.
- Nagiec, M. M., Nagiec, E. E., Baltisberger, J. A., Wells, G. B., Lester, R. L. and Dickson, R. C. (1997). "Sphingolipid synthesis as a target for antifungal drugs - Complementation of the inositol phosphorylceramide synthase defect in strain of *Saccharomyces cerevisiae* by the AUR1 gene." *Journal of Biological Chemistry* **272**(15): 9809-9817.

- Nagiec, M. M., Young, C. L., Zaworski, P. G. and Kobayashi, S. D. (2003a). "Yeast sphingolipid bypass mutants as indicators of antifungal agents selectively targeting sphingolipid synthesis." *Biochemical and Biophysical Research Communications* **307**(2): 369-374.
- Nagiec, M. M., Young, C. L., Zaworski, P. G. and Kobayashi, S. D. (2003b). "Yeast sphingolipid bypass mutants as indicators of antifungal agents selectively targeting sphingolipid synthesis." *Biochemical & Biophysical Research Communications* **307**(2): 369-374.
- Neuwald, A. F. (1997). "An unexpected structural relationship between integral membrane phosphatases and soluble haloperoxidases." *Protein Science* **6**(8): 1764-1767.
- Ng, C. K. Y., McAinsh, M. R., Gray, J. E., Hunt, L., Leckie, C. P., Mills, L. and Hetherington, A. M. (2001). "Calcium-based signalling systems in guard cells." *New Phytologist* **151**(1): 109-120.
- Obeid, L. A., Okamoto, Y. and Mao, C. G. (2002a). "Yeast sphingolipids: metabolism and biology." *Biochimica et Biophysica Acta-Molecular & Cell Biology of Lipids* **1585**(2-3): 163-171.
- Obeid, L. M., Okamoto, Y. and Mao, C. (2002b). "Yeast sphingolipids: metabolism and biology." *Biochimica et Biophysica Acta (BBA) - Molecular and Cell Biology of Lipids* **1585**(2-3): 163-171.
- Okamoto, Y., de Avalos, S. V. and Hannun, Y. A. (2002). "Structural requirements for selective binding of ISC1 to anionic phospholipids." *Journal of Biological Chemistry* **277**(48): 46470-46477.
- Ono, A. and Freed, E. O. (2001). "Plasma membrane rafts play a critical role in HIV-1 assembly and release." *Proceedings of the National Academy of Sciences of the United States of America* **98**(24): 13925-13930.
- Peskan, T., Westermann, M. and Oelmüller, R. (2000). "Identification of low-density Triton X-100-insoluble plasma membrane microdomains in higher plants." *European Journal of Biochemistry* **267**(24): 6989-6995.
- Pfaffl, M. W. (2004). Quantification strategies in real-time PCR. *A-Z of Quantitative PCR*. S. A. Bustin. La Jolla, International University Line: 89-113.
- Sakaki, T., Zahringer, U., Warnecke, D. C., Fahl, A., Knogge, W. and Heinz, E. (2001). "Sterol glycosides and cerebrosides accumulate in *Pichia pastoris*, *Rhynchosporium secalis* and other fungi under normal conditions or under heat shock and ethanol stress." *Yeast* **18**(8): 679-695.
- Sawai, H., Okamoto, Y., Luberto, C., Mao, C., Bielawska, A., Domae, N. and Hannun, Y. A. (2000a). "Identification of ISC1 (YER019w) as Inositol Phosphosphingolipid Phospholipase C in *Saccharomyces cerevisiae*." *J. Biol. Chem.* **275**(50): 39793-39798.
- Sawai, H., Okamoto, Y., Luberto, C., Mao, C. G., Bielawska, A., Domae, N. and Hannun, Y. A. (2000b). "Identification of ISC1 (YER019w) as inositol phosphosphingolipid phospholipase C in *Saccharomyces cerevisiae*." *Journal of Biological Chemistry* **275**(50): 39793-39798.
- Schmelzle, T., Helliwell, S. B. and Hall, M. N. (2002). "Yeast protein kinases and the RHO1 exchange factor TUS1 are novel components of the cell integrity pathway in yeast." *Molecular & Cellular Biology* **22**(5): 1329-1339.
- Schwank, S., Hoffmann, B. and Schuller, H. J. (1997). "Influence of gene dosage and autoregulation of the regulatory genes INO2 and INO4 on inositol/choline-repressible gene transcription in the yeast *Saccharomyces cerevisiae*." *Current Genetics* **31**(6): 462-468.

- Sessler, J. L., Sibert, J. W. and Lynch, V. (1993). "Synthesis and crystal-structure of the 1/1 PD(II) complex of 1,4,7,10-tetraoxa-13,16,19,22-tetraazacyclotetracosane." *Inorganica Chimica Acta* 206(1): 63-67.
- Skrzypek, M., Lester, R. L. and Dickson, R. C. (1997). "Suppressor gene analysis reveals an essential role for sphingolipids in transport of glycosylphosphatidylinositol-anchored proteins in *Saccharomyces cerevisiae*." *Journal of Bacteriology* 179(5): 1513-1520.
- Spassieva, S. D., Markham, J. E. and Hille, J. (2002). "The plant disease resistance gene Asc-1 prevents disruption of sphingolipid metabolism during AAL-toxin-induced programmed cell death." *Plant Journal* 32(4): 561-572.
- Stukey, J. and Carman, G. M. (1997). "Identification of a novel phosphatase sequence motif." *Protein Science* 6(2): 469-472.
- Sun, Y. D., Taniguchi, R., Tanoue, D., Yamaji, T., Takematsu, H., Mori, K., Fujita, T., Kawasaki, T. and Kozutsumi, Y. (2000). "Sli2 (Ypk1), a homologue of mammalian protein kinase SGK, is a downstream kinase in the sphingolipid-mediated signaling pathway of yeast." *Molecular & Cellular Biology* 20(12): 4411-4419.
- Suzuki, K. (1998). "Twenty five years of the "psychosine hypothesis": A personal perspective of its history and present status." *Neurochemical Research* 23(3): 251-259.
- van Meer, G. and Lisman, Q. (2002). "Sphingolipid transport: Rafts and translocators." *Journal of Biological Chemistry* 277(29): 25855-25858.
- Vesper, H., Schmelz, E. M., Nikolova-Karakashian, M. N., Dillehay, D. L., Lynch, D. V. and Merrill, A. H. (1999). "Sphingolipids in food and the emerging importance of sphingolipids to nutrition." *Journal of Nutrition* 129(7): 1239-1250.
- Wang, H., Li, J., Bostock, R. M. and Gilchrist, D. G. (1996). "Apoptosis: A functional paradigm for programmed plant cell death induced by a host-selective phytotoxin and invoked during development." *Plant Cell* 8(3): 375-391.
- Warnecke, D. and Heinz, E. (2003). "Recently discovered functions of glucosylceramides in plants and fungi." *Cellular and Molecular Life Sciences* 60(5): 919-941.
- Werbrouck, H., Botteldoorn, N., Uyttendaele, M., Herman, L. and Van Coillie, E. (2007). "Quantification of gene expression of *Listeria monocytogenes* by real-time reverse transcription PCR: Optimization, evaluation and pitfalls." *Journal of Microbiological Methods* 69(2): 306-314.
- Worrall, D., Ng, C. K. Y. and Hetherington, A. M. (2003). "Sphingolipids, new players in plant signaling." *Trends in Plant Science* 8(7): 317-320.
- Xu, X. L., Bittman, R., Dupontail, G., Heissler, D., Vilcheze, C. and London, E. (2001). "Effect of the structure of natural sterols and sphingolipids on the formation of ordered sphingolipid/sterol domains (rafts)." *Journal of Biological Chemistry* 276(36): 33540-33546.
- Zhong, W., Jeffries, M. W. and Georgopapadakou, N. H. (2000). "Inhibition of Inositol Phosphorylceramide Synthase by Aureobasidin A in *Candida* and *Aspergillus* Species." *Antimicrobial Agents and Chemotherapy* 44(3): 651-653.
- Zhong, W. Y., Murphy, D. J. and Georgopapadakou, N. H. (1999). "Inhibition of yeast inositol phosphorylceramide synthase by aureobasidin A measured by a fluorometric assay." *Febs Letters* 463(3): 241-244.

Appendix I - Preparation of Media

½ MS (Murashige and Skoog Basal Salt Mixture) 10 Media for Plants

½ MS 10 plates were prepared for *Arabidopsis* growth media. 2.2g of MS salts, 9.5g of LP0011 Agar Bacteriological (Agar No.1) (OXOID) and 10g of sucrose were added to 1 litre of distilled water. The pH was adjusted to 5.6.

The media was autoclaved at 121°C for 20mins. Once the media had cooled to 60°C, media were poured into standard petri dishes (Bibby Sterilin) in the flow cabinet. Plates were left with the lid off in the flow cabinet until set.

Plates could be stored in a 4°C room for a month before use; any condensation that occurred during storage was dried out in the flow cabinet before use.

LB (Luria-Bertani Broth) Media and Plates

LB plates were prepared for transformation. 1L of LB broth was prepared with 10g Bactotrypton, 5g Bacto-Yeast Extract and 10g NaCl. pH was adjusted to 7.5 with NaOH, which was approximately 0.2 ml of 5N. When agar was needed, it was added to 1.5% (w/v). Both LB media and agar were autoclaved at 151lb/in². Plates were stored at 4°C.

YPD (Yeast Peptone Dextrose) Media and Plates

For 1 litre of YPD plates, 10g LP0021 Yeast Extract (OXOID), 20g BBL™ Trypticase™ peptone (BD), 20g D-(+)-Glucose (SIGMA) and 20g LP0011 Agar Bacteriological (Agar No.1) (OXOID) was used. YPD Media was prepared without agar. Solutions were autoclaved at 121 for 15 min and were stored at 4°C.

For checking the IPCS reverse reaction, YPD plates with various salt concentrations were prepared. These plates were prepared the same as YPD plates with the addition of appropriate salts, 0.4M NaCl, 0.5M NaCl, 0.8M NaCl, 0.01M LiCl and 0.25M LiCl.

YPGR (Yeast Peptone Galactose and Raffinose) Media and Plates

To cultivate AUR1 yeast strains, YPGR media was made. For 1 litre of YPGR, A: 10g LP0021 Yeast Extract (OXOID), 20g BBL™ Trypticase™ peptone (BD), B: 40g D-(+)-Galactose (Fluka) and 20g D-(+)-Raffinose pentahydrate (Fluka) was used. A and B were autoclaved separately and mixed after. For plates, 20g LP0011 Agar Bacteriological (Agar

No.1) (OXOID) was added to solution A. Solutions were autoclaved at 121°C for 15 min and were stored at 4°C.

Scientifically Defined (SD) Media and Plates

SD-His and SD-Met plates were prepared for analysing the IPC-PLC activity.

1 litre of SD-His plates were made by 20g D-(+)-Glucose (SIGMA) and 20g LP0011 Agar Bacteriological (Agar No.1) (OXOID), 1.7g Difco™ Yeast Nitrogen Base w/o amino Acids (BD), 5.0g NH₄SO₄ (SIGMA) and appropriate amino acid stocks (10mL adenine sulphate, 10mL uracil, 2mL L-tryptophan, 4mL L-arginine, 2mL L-methionine, 25mL L-tyrosine, 6mL L-leucine, 6mL L-isoleucine, 5mL L-lycine, 5mL L-phenylalanine, 10mL L-aspartic, 10mL L-glutamic acid, 5mL L-valine, 5mL L-threonine and 5mL L-serine) were added to the media. SD-Met plates were made as above with the deletion of 2mL L-methionine but with 2mL L-histidine.

SD-His-Ura plates with Glu and SD-His-Ura plates with Gal and Raf were made to test the *Arabidopsis* IPCS complementation of yeast AUR1 genes. 1 litre of SD-His-Ura with Glu was made as above by not adding His and Ura. SD-His-Ura with Gal and Raf were prepared by adding 40g D-(+)-Galactose (Fluka) and 20g D-(+)-Raffinose pentahydrate (Fluka) instead of Glu. Solutions were autoclaved at 121°C for 15 min and were stored at 4°C.

The concentration of the stock amino acids were, 2mg/mL adenine sulphate, 2mg/mL uracil, 10mg/mL L-tryptophan, 10mg/mL L-arginine, 10mg/mL L-methionine, 2mg/mL L-tyrosine, 10mg/mL L-leucine, 10mg/mL L-isoleucine, 10mg/mL L-lycine, 10mg/mL L-phenylalanine, 0.01mg/mL L-aspartic, 10mg/mL L-glutamic acid, 30mg/mL L-valine, 40mg/mL L-threonine and 80mg/mL L-serine)

